



---

Faculty of Engineering and Technology  
Department of Electrical, Computer and Telecommunications Engineering

## **DESIGN AND SIMULATION OF A PHASED ARRAY ANTENNA FOR 5G WIRELESS APPLICATIONS**

by

**REUBEN RAMOGOMANA**

Student ID number: 13001133

MEng Computer & Telecommunications

A Thesis Submitted to the Faculty of Engineering and Technology in Partial Fulfilment of the  
Requirements for the Award of the Degree of Master of Engineering in Computer and  
Telecommunications Engineering of BIUST

**Supervisor: Dr. Bokamoso Basutli**

Department of Electrical, Computer and  
Telecommunications Engineering  
Faculty of Engineering and Technology,  
BIUST  
basutlib@biust.ac.bw

**Co-Supervisor: Prof. Abid Yahya**

Department of Electrical, Computer and  
Telecommunications Engineering  
Faculty of Engineering and Technology,  
BIUST  
yahyaa@biust.ac.bw

September, 2022

---

**DECLARATION REGARDING THE WORK AND COPYRIGHT**

**Candidate** (please write in caps or type): REUBEN RAMOGOMANA

**Student ID:** 13001133

**Thesis Titled:** Design and Simulation of a Phased Array Antenna for 5G Wireless Applications

I, **Reuben Ramogomana**, certify that the Thesis is all my own original work and that I have not obtained a degree in this University or elsewhere on the basis of any of this work.


*(If the thesis is based on a group project, then the student must indicate the extent of her / his contribution, with reference to any other theses submitted or published by each collaborator in the project, and a declaration to this effect must be included in the thesis)*

This thesis is copyright material protected under the Berne Convention, the Copyright and Neighbouring Rights Act, Act. No. 8 of 2000 and other international and national enactments, in that behalf, on intellectual property. It must not be reproduced by any means, in full or in part, except for short extracts in fair dealing; for researcher private study, critical scholarly review or discourse with an acknowledgement, without the written permission of the office of the Postgraduate School, on behalf of both the author and the BIUST.

Signed:  Date: 09/09/2022

**Primary Supervisor** (please write in caps or type): DR BOKAMOSO BASUTLI

I, Dr. Bokamoso Basutli, hereby confirm that I have inspected the above titled thesis and, to the best of my knowledge, it is based on the original work of the candidate.

Signed:  Date: 09 September /2022

*“Life balance is a myth. It’s an illusion and the very pursuit of it is driving us crazy. For me it’s about proportion - it’s really a work hard/play hard equation.”*

-Danielle LaPorte

## *Abstract*

Amidst escalating data traffic demands, the fifth generation (5G) of mobile communication has been launched to curb these demands by providing high data rates, decreased latency, increased network capacity and large bandwidth. The ambitious performance expected from the 5G cellular communication network is enabled by different key technologies including shifting towards the millimeter wave frequency band. However, the millimeter wave band is accompanied by limitations of signal path loss and propagation loss due to small wavelengths. As a result, antenna arrays with high antenna gain are used to mitigate these signal path and propagation losses without consuming more power and at a low cost. Antenna arrays have a shortfall of having a limited angular coverage due to narrow beams. As such, phased array antennas are adopted to provide electronic beam steering in desirable directions.

This thesis proposes an eight element phased array antenna for 5G wireless applications. The proposed antenna is designed to operate in the millimeter wave band specifically at 28 GHz. Antenna element or radiating element is an important aspect in designing a phased array antenna, in this thesis a single rectangular patch antenna is used as a radiating element. Three single patch antennas are designed using three dielectric substrates. After antenna performance comparison, the single patch antenna designed using RT 5880 dielectric substrate was chosen as the radiating element for the proposed eight element phased array antenna. The proposed phased array antenna is composed of two  $1 \times 4$  array antenna which are fed by two excitation ports and phase shifting is introduced at these ports to achieve beam steering.

From the simulation results, the proposed phased array antenna achieved reflection coefficient of -40.19 dB, bandwidth of 1.51 GHz, antenna gain of 15.92 dBi, scan angle of  $\pm 41^\circ$  and mutual coupling effect in the array is -27.97 dB. To reduce mutual coupling, a dumbbell shaped defected ground structure (DGS) is inserted in the array and a mutual coupling reduction of 6.27 dB is achieved. In conclusion, the proposed phased array antenna has a limited scan angle and the insertion a dumbbell shaped DGS in the array reduced mutual coupling and increased the bandwidth of the antenna. However, the insertion of DGS did not improve antenna parameters related to radiation pattern as there is a decrease in antenna gain and directivity.

## *Acknowledgements*

First and foremost, I am grateful to the Almighty God for showering me with all the grace and strength throughout my research journey to completing it successfully. I express my deep thanks and sincere appreciation to my supervisors, Dr. Bokamoso BASUTLI and Prof. Abid YAHYA . To Dr. BASUTLI, I sincerely thank you for introducing me to the field of antenna design. I am grateful for the motivation, criticism and patience you have always afforded me during my research journey. Without your guidance and support, this work would not have been possible. To Prof. YAHYA, I am grateful for your inspiring guidance, encouragement, and valuable discussions during need.

I thank my family for their encouragement and endless support during my highs and lows in my research journey and my life as a whole. To my mother, I am grateful for your encouragement and all the sacrifices that you have made for me to get this far in life. For that, I will forever be grateful. My beautiful sisters, Dimpho and Bonno, I am grateful for your presence in my life, your love and prayers for me have led me this far.

I convey many thanks to all my friends, who are an integral part of my life through their criticism, love and advice. To Bokamoso K. Ledimo, I thank you for the insightful lessons you have always given me with regarding CST microwave studio suite, a software which is used as electromagnetic simulator in antenna design. Thank you for the amazing times we always have in and out of academia.

Last but not least, I would like to thank BotswanaSat-1 team for giving me an opportunity to learn and develop under their prestigious project. I express my gratitude to you all.

# Contents

<b>Declaration of Authorship and Copyright</b>	<b>i</b>
<b>Certification</b>	<b>ii</b>
<b>Abstract</b>	<b>iv</b>
<b>Acknowledgements</b>	<b>v</b>
<b>List of Figures</b>	<b>ix</b>
<b>List of Tables</b>	<b>x</b>
<b>List of Abbreviations</b>	<b>xi</b>
<b>List of Symbols</b>	<b>xiii</b>
<b>1 Introduction</b>	<b>1</b>
1.1 A Brief History on Generations of Mobile Network Communication . . . . .	1
1.2 Fifth Generation of Mobile Communication . . . . .	2
1.3 Motivation . . . . .	5
1.4 Problem Statement . . . . .	6
1.5 Research Aim and Objectives . . . . .	6
1.6 Research Publications . . . . .	7
1.7 Thesis Outline . . . . .	7
<b>2 Background on Antenna Arrays</b>	<b>9</b>
2.1 Introduction to Antenna Arrays . . . . .	9
2.1.1 Linear Antenna Array . . . . .	10
2.1.2 Planar Antenna Array . . . . .	11
2.1.3 Circular Antenna Arrays . . . . .	13
2.2 Feed Networks for Array Antennas . . . . .	14
2.2.1 Series Feed Network . . . . .	14
2.2.2 Corporate Feed Network . . . . .	15
2.3 Phased Array Antenna . . . . .	15
2.4 Mutual Coupling in Phased Array Antennas . . . . .	18
2.5 Microstrip Patch Antenna . . . . .	22
2.5.1 Basic characteristics of Microstrip Patch Antenna . . . . .	23
2.5.2 Feeding Methods of Microstrip Patch Antennas . . . . .	25
Microstrip feed line . . . . .	25
Coaxial Probe feeding . . . . .	26
Aperture Coupling . . . . .	26
Proximity Coupling . . . . .	26
2.6 Antenna Parameters . . . . .	26

2.6.1	Radiation Pattern . . . . .	26
2.6.2	Beamwidth . . . . .	27
2.6.3	Directivity . . . . .	28
2.6.4	Gain and Realized Gain . . . . .	28
2.6.5	Bandwidth . . . . .	29
2.6.6	Active Reflection Coefficient . . . . .	29
2.6.7	Beam Scanning . . . . .	29
2.7	Transmission Line Parameters . . . . .	30
2.7.1	Voltage Standing Wave Ratio . . . . .	30
2.7.2	Impedance Matching . . . . .	30
2.7.3	Return Loss . . . . .	30
2.8	Conclusion . . . . .	31
<b>3</b>	<b>Microstrip Patch Antenna Design</b>	<b>32</b>
3.1	Introduction . . . . .	32
3.1.1	Related Works . . . . .	33
3.1.2	Contributions . . . . .	34
3.2	Design Model . . . . .	34
3.2.1	Design Process . . . . .	35
	Design using RT/Duroid 5880 Substrate . . . . .	36
	Summary on the designs using FR-4 and RO3003 substrates . . . . .	39
3.3	Simulation Results of the Single Patch Antenna . . . . .	39
3.3.1	Reflection Coefficient . . . . .	39
3.3.2	Voltage Standing Wave Ratio . . . . .	41
3.3.3	Far Field Pattern . . . . .	42
3.4	Conclusion . . . . .	46
<b>4</b>	<b>Phased Array Antenna Design</b>	<b>47</b>
4.1	Introduction . . . . .	47
4.1.1	Related Works . . . . .	48
4.1.2	Contributions . . . . .	49
4.2	Four Elements Array Design . . . . .	50
4.2.1	Simulation Results of Four Elements Array Antenna . . . . .	51
	Reflection Coefficient . . . . .	51
	VSWR . . . . .	53
	FarField . . . . .	54
4.3	Eight Elements Phased Array Antenna Design . . . . .	56
4.3.1	Results Analysis of the Designed Antenna . . . . .	56
	Reflection Coefficient . . . . .	57
	VSWR . . . . .	57
	FarField . . . . .	58
	Beam Steering . . . . .	60
4.3.2	Mutual Coupling Reduction . . . . .	61
4.3.3	Simulation of Phased Array Antenna with DGS. . . . .	63
	Reflection Coefficient . . . . .	63
	VSWR . . . . .	64
	FarField . . . . .	64
	Beam Steering . . . . .	65
4.4	Conclusion . . . . .	69

<b>5 Conclusions</b>	<b>70</b>
5.1 Conclusion . . . . .	70
5.2 Future Works . . . . .	71
<b>References</b>	<b>72</b>



# List of Figures

1.1	Expected performance of 5G networks [12]. . . . .	3
2.1	Linear array configuration with dots denoting the antenna elements [57] . . . .	11
2.2	Planar array configuration with antenna elements in both x and y directions [46]. . . . .	12
2.3	Circular array configuration with antenna elements [59]. . . . .	13
2.4	Series feed network. . . . .	14
2.5	corporate feed network . . . . .	15
2.6	Phased array antenna in transmit mode [66] . . . . .	16
2.7	Mutual Coupling in transmit and reception mode. . . . .	19
2.8	Microstrip patch antenna [91] . . . . .	23
2.9	various geometry for patch antenna . . . . .	24
2.10	Radiation pattern of an antenna [46] . . . . .	27
3.1	The proposed single element antenna. . . . .	35
3.2	Comparison of reflection coefficient for antennas designed with different dielectric substrates. . . . .	40
3.3	Comparison of VSWR for antennas designed with different dielectric substrates. . . . .	41
3.4	Far field plots of a single patch antenna using RT/Duroid 5880. . . . .	43
3.5	Far field plots of a single patch antenna using R0 3003 substrate. . . . .	44
3.6	Far field plots of a single patch antenna using FR-4 substrate. . . . .	45
4.1	The designed $4 \times 1$ array antenna. . . . .	51
4.2	Reflection coefficient of the four element array antenna. . . . .	52
4.3	VSWR of the four element array antenna. . . . .	53
4.4	Directivity of the antenna array in 1D. . . . .	54
4.5	Far field plots of $1 \times 4$ array antenna. . . . .	55
4.6	The simulated eight element phased array antenna in a CST software layout. . . . .	56
4.7	Reflection coefficient and mutual coupling of the proposed antenna. . . . .	57
4.8	VSWR of the phased array antenna. . . . .	58
4.9	Far field plots of the phased array antenna before beam steering. . . . .	59
4.10	Directivity of the phased antenna array in 3D. . . . .	60
4.11	Beam steering performance of the antenna without DGS. . . . .	61
4.12	Dumbbell shaped DGS. . . . .	62
4.13	Reflection coefficient and mutual coupling of the phased array antenna with dumbbell DGS. . . . .	63
4.14	VSWR of the phased array antenna with dumbbell shaped DGS. . . . .	64
4.15	Far field plots of the phased array antenna before beam steering. . . . .	66
4.16	Directivity of the phased antenna array in 3D. . . . .	67
4.17	Beam steering performance of the phased array antenna with DGS. . . . .	67

# List of Tables

1.1	A brief summary of existing generations of mobile communications [1,3,6,10]	2
3.1	Dimensions of the single patch antenna using RT/Duroid 5880 substrate. . .	38
3.2	Dimensions of the single patch antenna using RT Duroid and FR-4 substrates. . . . .	39
3.3	Performance comparison for the three different dielectric substrates. . . . .	46
3.4	Comparison between the proposed single patch antenna with existing literature. . . . .	46
4.1	Dimensions of the $1 \times 4$ array antenna. . . . .	51
4.2	Performance comparison of the phased array antenna with and without DGS. . . . .	68
4.3	Comparison of the designed phased array antenna with existing works. . . . .	68

# List of Abbreviations

<b>1D</b>	<b>One Dimensional</b>
<b>1G</b>	<b>First-Generation</b>
<b>2D</b>	<b>Two Dimensional</b>
<b>2G</b>	<b>Second-Generation</b>
<b>3D</b>	<b>Three Dimensional</b>
<b>3G</b>	<b>Third-Generation</b>
<b>4G</b>	<b>Fourth-Generation</b>
<b>5G</b>	<b>Fifth-Generation</b>
<b>6G</b>	<b>Sixth-Generation</b>
<b>ADC</b>	<b>Analog-to-Digital Converter</b>
<b>CDMA</b>	<b>Code Division Multiple Access</b>
<b>CST</b>	<b>Computer Simulation Technology</b>
<b>DAC</b>	<b>Digital-to-Analog Converter</b>
<b>DGS</b>	<b>Defected Ground Structures</b>
<b>DOA</b>	<b>Direction Of Arrival</b>
<b>EM</b>	<b>Electro-Magnetic</b>
<b>EBG</b>	<b>Electromagnetic Band Gap</b>
<b>EDGE</b>	<b>Enhanced Data Rates for GSM Evolution</b>
<b>eMBB</b>	<b>Enhanced Mobile Broadband</b>
<b>FDMA</b>	<b>Frequency Division Multiple Access</b>
<b>FNBW</b>	<b>First Null Beamwidth</b>
<b>GPS</b>	<b>Global Position System</b>
<b>GSM</b>	<b>Global System for Mobile Communications</b>
<b>HPBW</b>	<b>Half Power Beamwidth</b>
<b>ITU</b>	<b>International Telecommunication Union</b>
<b>IoT</b>	<b>Internet of Things</b>
<b>LTE</b>	<b>Long Term Evolution</b>
<b>LMPs</b>	<b>Link Management Protocols</b>
<b>M2M</b>	<b>Machine to Machine Communications</b>
<b>mMTC</b>	<b>Massive Machine Type Communications</b>
<b>MIMO</b>	<b>Multiple-Input Multiple-Output</b>
<b>MC-CDMA</b>	<b>Multi Carrier- Code Division Multiple Access</b>
<b>OFDMA</b>	<b>Orthogonal Frequency Division Multiple Access</b>
<b>PAA</b>	<b>Phased Array Antenna</b>
<b>PCB</b>	<b>Printed Circuit Board</b>
<b>PIEA</b>	<b>Planar Inverted- E Antenna</b>
<b>TDMA</b>	<b>Time Division Multiple Access</b>
<b>TD-SCDMA</b>	<b>Time Division-Synchronous Code Division Multiple Access</b>
<b>QoS</b>	<b>Quality-of-Service</b>

<b>RF</b>	<b>Radio Frequency</b>
<b>SINR</b>	<b>Signal-to-Interference-plus-Noise Ratio</b>
<b>SLL</b>	<b>Side Lobe Level</b>
<b>SKA</b>	<b>Square Kilometer Array</b>
<b>UHD</b>	<b>Ultra High Definition</b>
<b>uRLLC</b>	<b>ultra Reliable Low Latency Communication</b>
<b>VSWR</b>	<b>Voltage Standing Wave Ratio</b>
<b>WIMAX</b>	<b>Worldwide Interoperability for Microwave Access</b>
<b>WLAN(s)</b>	<b>Wireless Local Area Network</b>

# List of Symbols

Symbol	Name
MHz	Megahertz
GHz	Gigahertz
$AF$	array factor
$d$	distance
$E_t$	total electric field
$E_r$	electric field of a single antenna
$N$	number of the antenna elements
$N_y$	antenna elements placed next to one another linearly in the $y$ direction
$N_x$	antenna elements placed next to one another linearly in the $x$ direction
$I_m$	excitation amplitude of $M$ antenna elements
$I_n$	current magnitude of the $n$ th element
$I_0$	indicates amplitude excitation at the origin
$L$	Length of the patch
$W$	Width of the patch
$L_g$	Length of the ground plane
$W_g$	Width of the ground plane
$C$	speed of light
$h$	height of the substrate
$f_r$	resonant frequency
$dB$	decibel
$L_{eff}$	effective length
$S_{mn}$	transmission coefficient
$P_r$	reflected power
$P_{in}$	incident power
$\alpha$	progressive phase factor
$\beta$	phase difference between antenna elements
$\omega$	angular frequency
$\theta$	bore sight angle
$\lambda$	wavelength
$\Gamma$	reflection magnitude
$\Delta L$	extension length
$\epsilon_r$	dielectric constant
$\epsilon_{reff}$	effective dielectric constant

*I dedicate this work to my graceful mother, Masego, whom through this journey, she offered unconditional love and a great support for me. Thank you very much.*

# Chapter 1

## Introduction

### 1.1 A Brief History on Generations of Mobile Network Communication

Since 1980, almost every decade marks the deployment of a new generation of mobile communication. The first generation (1G) used analog radio systems, frequency division multiple access (FDMA) for the division of available bandwidths into specific frequency channels, circuit switched networks and supported only voice transmission [1, 2]. However, this network generation was characterized by issues of limited network capacity, low security and poor hand-off. Due to the limitations of 1G and the increased need for greater cellular capacity, second generation (2G) was developed and deployed in 1991 [3]. This generation used digital system technology for voice and used time division multiple access (TDMA) scheme [4]. Under 2G, different technologies were introduced and these are, global system for mobile communications (GSM), general packet radio service (GPRS) also known as 2.5G and enhanced data rates for GSM evolution (EDGE) also known as enhanced GPRS (EGPRS) [3]. 2G networks used circuit switched and packet switched domains for the purpose of voice transmission and; data transmission and reception, respectively [5]. In 2000, the third generation (3G) of mobile networks was deployed and was also termed IMT-2000. This technology enabled mobile telephony. The technology standards under 3G were, code division multiple access (CDMA)-2000, wide CDMA, universal mobile telecommunications system (UMTS) and time-division synchronous code-division multiple access (TD-SCDMA) [6]. This generation provided services such as improved internet speed, digital broadband, global roaming and high quality of service (QoS). In 2010, fourth generation (4G) of mobile

communication was launched and as compared to its predecessors it is an internet based technology [7]. 4G networks use a new access technique called orthogonal frequency division multiple access (OFDMA) and technology standards introduced under this generation are long term evolution (LTE), worldwide interoperability for microwave access (WIMAX), multi-carrier code-division multiple access (MC-CDMA) and network link management protocols (LMPs) [8, 9]. Today's LTE advanced systems are approaching their practical limits and falling short to meet increasing demands of modern wireless communications. Hence the fifth generation (5G) of mobile networks is upon us. Table 1.1 summarizes the comparison between the four generations of mobile communications.

Table 1.1: A brief summary of existing generations of mobile communications [1, 3, 6, 10]

Generation	1G	2G	3G	4G
Time Period	1980	1991	2000	2010-now
Data rate	2 kbps	64 -144 kbps	2 Mbps	More than 200 Mbps
Technology	Analog	digital, GSM, GPRS, EDGE	Broadband data	LTE
Multiple access	FDMA	TDMA, CDMA	CDMA	OFDMA
Service	voice, sms, data	voice, data, high quality audio	dynamic information access	dynamic information access
Switching	Circuit	Packet, Circuit	Packet	Packet

## 1.2 Fifth Generation of Mobile Communication

In the modern days, there is an exponential proliferation in wireless data traffic and mobile users demand for improved broadband wireless technology to support services such as ultra high definition (UHD) video streaming. Moreover, emerging applications such as internet-of-things (IoT) and machine to machine communications (M2M) demands for high data rates, enormous bandwidth and increased network capacity. These demands of modern wireless communication impose a challenge on the current cellular networks such as 4G and LTE advanced. As such, fifth generation (5G) of mobile communication has been launched to meet these demands of modern wireless by providing services such as efficient energy, high network capacity, low latency, high data rates, increased bandwidth and a great number of connected devices [11]. The main of 5G is to curb the impediments of the previous cellular networks at a low cost. Challenging specifications for 5G networks has been



set by International Telecommunication Union (ITU) to meet the practical limits of current wireless networks, as illustrated in Fig. 1.1, 5G networks are envisaged to provide latency less than 1 ms, cell spectral efficiency of 10 bits/s/Hz, up to 1 Gbps of peak data rate, 10x cost efficiency as compared to 4G, mobility up to 500 km/h and more than 1 million simultaneous connections per km<sup>2</sup>.

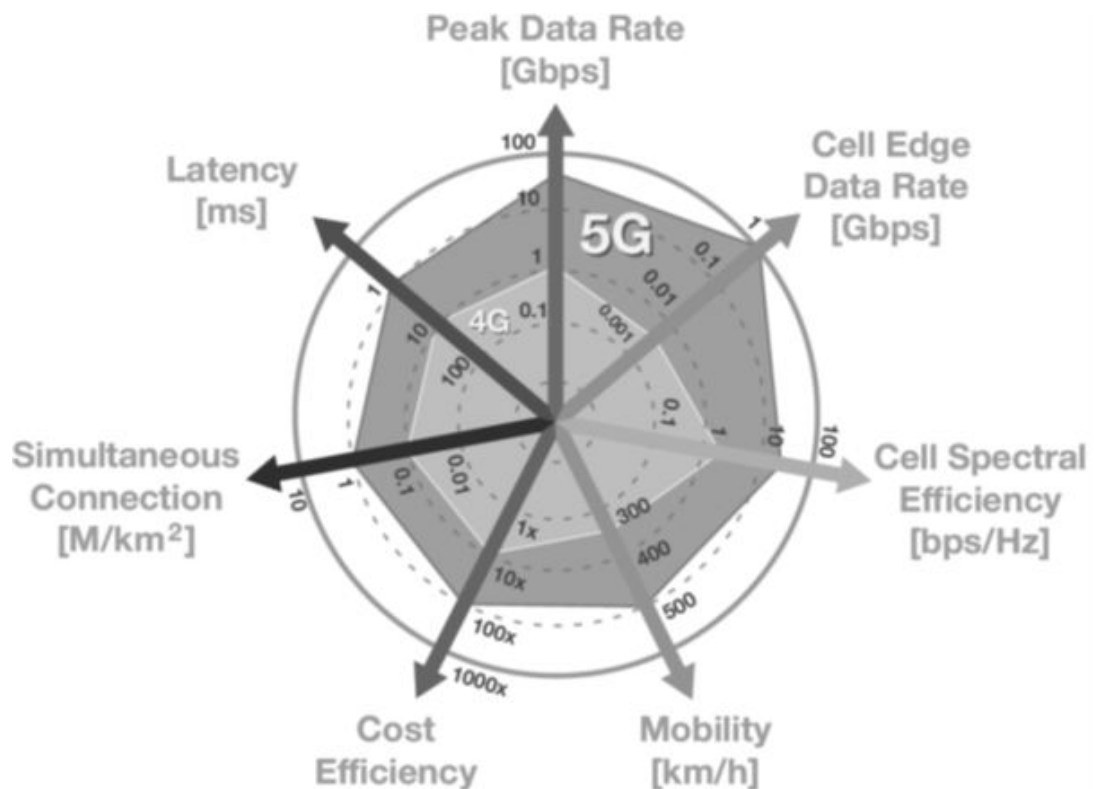


FIGURE 1.1: Expected performance of 5G networks [12].

5G networks have been designed to meet specifications of three usage scenarios, namely, enhanced mobile broadband (eMBB), massive machine type communication (mMTC) and ultra-realibe low latency communication (URLLC) [13]. The eMBB usage scenario describes the network capacity enhancements. Due to the ever-increasing requirements for higher data transfer rates, the eMBB application deals with data transfers that are in magnitudes of multiple gigabytes for the end-users. Example sub-use cases of eMBB include hot spots in densely populated areas for both indoor and outdoor coverage and broadband everywhere. URLLC use case describes ultra-responsive connections with extremely low latency and high reliability. Furthermore, this use case introduces support for the requirements of mission critical applications in relatively new industries. These applications include industrial automation, autonomous driving, eHealth and smart energy and grids. The mMTC use case describes the communication between interconnected machines

over a wired or wireless networks where data generation, information exchange and actuation takes place with minimal or no intervention from humans. In particular, mMTC involves wireless connectivity and networking between massive quantities of machines (billions), and is considered a key point in the progress from IoT to Internet of Everything.

The ambitious performance expected from 5G cellular communication network in order to accommodate variety of applications is enabled by different key technologies and these include millimeter wave band, massive multiple input multiple out (MIMO), ultra dense networks, green communication, full or flexible duplex communication, antenna array beamforming etc [14]. To meet the challenging specifications for 5G networks, the use of new frequencies is required. 5G networks operates on two sets of frequency ranges. The first range is from 450 MHz to 6 GHz (sub 6 GHz) and the second range from 24 GHz to 52 GHz (millimeter wave band). Millimeter wave frequency band is a band in the electromagnetic spectrum covering a range of 30 GHz to 300 GHz and wavelength range of 10 - 1 mm [15–18]. This band is also referred to as extremely high frequency (EHF). MmWave band is a less congested part of the spectrum and can be used in mobile and wireless networks for the provision of high data rates and increased network capacity. Benefits of using mmWave band include large bandwidth for high data rate transmission, implementation of large number of antennas due small wavelengths which gives high antenna gain, wideband spread spectrum which yields a reduction in multipath fading, high antenna directivity and low power transmission as a result of high antenna gain [19, 20]. However, millimeter wave is accompanied by limitations of signal path loss and propagation challenges [15, 21, 22]. Fortunately, small wavelengths of millimeter wave band enable the implementation of large number of antennas which provide high directive gain and beamforming abilities [15]. Beamforming antenna arrays provide high spatial gain which compensate for losses in the the millimeter wave band. Also the small wavelengths aid array architectures to be inserted into portable devices, thus making beamforming an appealing prospect. The combination of beamforming antenna arrays and millimeter wave communications is a key enabler in the implementation of 5G. In the development of 5G technology, which presently is being commercialized around the world [23, 24], different advanced antenna array architectures are used. This includes phased arrays, massive MIMO and beamforming arrays [25–30]. In millimeter wave communication systems, the antenna architectures of base and mobile stations are affected by random movement of mobile devices, outdoor and indoor propagation in urban environment and user mobility [28, 31]. As such, electronic beam steering provided by phased arrays

should be present in both mobile and base stations to archive a link with a good quality. [15,32,33].

### 1.3 Motivation

Over the years there has been proliferation of data traffic in wireless communications due to applications such as IoT, mobile cloud computing, ultra high definition videos and vehicle communications [34,35]. According to recent studies, wireless data traffic is expected to experience 1000 fold capacity increase in the foreseeable future [36,37]. These applications demand wireless networks to have services such as high data rate transmission, low latency, large bandwidth and high capacity channels. However, these demands bring challenges to the current wireless network architectures, bringing them to reach their practical performance limits. In that regard, 5G mobile communication has been launched to meet these demands. 5G networks operate in millimeter wave frequency band to provide enormous bandwidths however this frequency bands is characterized by propagation challenges due to small wavelengths. Phased array antennas are broadly deployed in 5G networks to compensate for losses in the millimeter wave band by providing high spatial gain and beamforming capabilities. These advantages of phased arrays include electronic steering of beams in the desired direction, high antenna gain with reduced side lobes, beamforming capabilities and miniaturized antenna elements [38]. Nonetheless, phased array antennas have an undesirable problem of mutual coupling effect between radiating elements which limits the overall performance of the array. Over the years, a lot of research has been undertaken to mitigate mutual coupling effect associated with phased array antennas. Some of the popular techniques or methods proposed by researchers to mitigate mutual coupling are; use of electromagnetic band gap (EBG) structures [39,40], use of defected ground structures (DGS) [41,42] and metamaterials [43–45].

In this thesis, a microstrip patch antenna is used as a radiating element of the proposed phased array antenna. Microstrip patch antennas have advantages such as low fabrication cost, low weight, easy to feeding process and miniaturized size [46]. Mutual coupling in phased array antennas which are designed with patch antennas as radiating elements is enhanced by the existence of space coupling and surface wave coupling between the patches. Furthermore, the overall radiation pattern of a phased antenna is determined by the product of the electric field of a single antenna located at the origin and the array factor. Array factor is a function that describes the position of the antenna elements in the array and the weights used. This factor

differs for each antenna array. This method of calculating far field pattern in phased array antennas by pattern multiplication leads to inaccurate design of phased array antennas because it neglects the coupling effect which exists between adjacent radiating elements. To mitigate mutual coupling in the proposed microstrip phased array antenna, defects are etched to the ground plane to reduce surface waves realizing DGS.

## 1.4 Problem Statement

The ambitious performance expected from 5G cellular communication network in order to accommodate variety of applications is enabled by different key technologies including millimeter wave frequency band. However, the millimeter wave band is accompanied by limitations of signal pathloss and propagation challenges due to small wavelengths. In Fifth generation (5G) network, phased array antennas are adopted to compensate for the propagation losses of the millimeter wave band by providing high directive gain and beamforming capabilities. Antenna elements used in phased arrays are compact and miniaturised in size. This leads to antenna elements being in close proximity to one another and giving rise to an undesirable problem of mutual coupling between the antenna elements. This problem is detrimental to the overall antenna array performance.

## 1.5 Research Aim and Objectives

The main aim of this thesis is to design and simulate a phased array antenna for 5G wireless applications which takes into consideration the effect of mutual coupling between the antenna elements. The specific objectives for the addressed research problem are listed below;

1. To compare the performance of different substrates under the model of a single patch antenna.
2. To design and simulate  $1 \times 4$  microstrip patch array antenna operating at 28 GHz.
3. To design and simulate an eight element phased array antenna operating at 28 GHz.
4. To incorporate a defected ground structure (DGS) to reduce mutual coupling effect in the designed eight element phased array antenna.

5. To compare the antenna performance of the phased array antenna with and without DGS.

## 1.6 Research Publications

The contribution of this thesis is mainly on the design and simulation of an eight element phased array antenna for 5G wireless applications. This contribution is supported by various local and international journal publications.

1. **R. Ramogomana**, K. Koodirle, G. A. Mapunda, L. Marata, B. Basutli, A. M. Zungeru, and J. M. Chuma "Review of Microstrip Patch Antenna Designs with Array Configurations," BIE 16th Biennial Conference, pp.1-10, Nov 2019.
2. **R. Ramogomana**, B. K. Ledimo, G. A. Mapunda, M. Mosalaosi, A. Yahya and B. Basutli, "A Survey on the State of the Art of Phased Array Antennas and Their Future Direction in Wireless Communication," submitted to Progress in Electromagnetics Research (under review).
3. G. A. Mapunda, **R. Ramogomana**, L. Marata, B. Basutli, A. S. Khan, and J. M. Chuma, "Indoor Visible Light Communication: A Tutorial and Survey," Wireless Communications and Mobile Computing, vol. 2020, pp. 1-46, Dec. 2020.
4. B.K. Ledimo, P. Moaro, **R. Ramogomana**, M. Mosalaosi, B. Basutli, "Design Procedure of a Frequency Reconfigurable Metasurface Antenna at mmWave Band" Telecom 2022, vol. 3, pp. 379-395.

## 1.7 Thesis Outline

The remaining part of this thesis is structured into four (4) chapters. Chapter 2 provides overview of antenna arrays. This includes different types of antenna arrays and their feeding networks. The chapter also entails the working principles of phased array antennas and how mutual coupling occurs in these antennas. Different methods and techniques used reduce mutual coupling are discussed. A study on microstrip patch antennas is presented. Furthermore, this chapter presents various parameters used to measure antenna performance, including gain, return loss, bandwidth etc.

Chapter 3 discusses the design of a single rectangular patch antenna operating at

28 GHz. The single rectangular patch antenna is designed using three different substrates and their performance is compared. Furthermore, this chapter compares the performance of the designed single patch antenna with existing single patch antennas operating at 28 GHz.

In Chapter 4, the focus is on the design of a suitable phased array antenna for 5G wireless applications. The design process starts with the design of a  $1 \times 4$  array antenna and then the design of eight element phased array antenna. A dumbbell shaped defected ground structure (DGS) is embedded on the designed phased array to mitigate mutual coupling effect existing in the antenna. Furthermore, this chapter compares the performance of the proposed phased array antenna without dumbbell DGS and the one with dumbbell DGS existing single patch antennas operating at 28 GHz.

Finally in Chapter 5, the findings and conclusion of the thesis are presented. Furthermore, the future works of the project are presented.

## Chapter 2

# Background on Antenna Arrays

This chapter presents the background theory of antenna arrays. The main focus is on different array configurations, feeding networks for antenna arrays, working principles of phased array antennas. Methods used to reduce mutual coupling in arrays are discussed. Antenna parameters which are used to measure the performance of phased array antenna are also presented.

### 2.1 Introduction to Antenna Arrays

An antenna array or array antenna is a system of multiple antenna elements arranged in a certain electrical or geometric configuration to achieve a directional radiation pattern [46–49]. Different antenna types can be used as antenna elements, for example microstrip antennas, dipole antennas, aperture and even horn antennas. An antenna array can be deployed on a small platform or over a large geographical area, for example; embedded systems or square kilometer array (SKA) [50]. In a single antenna element, the radiation pattern is characterized by low gain and low directivity [46]. The performance of a single antenna can be improved by size enlargement thus; resulting in more directive beams and high gain [46]. In practice, the approach of using large physical antennas is a disadvantage because it results in bulky antennas, which are often difficult to modify at a later stage. Antenna arrays offer an effective way of enlarging antenna dimensions without the need to increase the individual antenna size. For convenience and more practicality, the antenna elements in an array should be identical.

The total electromagnetic of an antenna array at a point away from its center is derived by summing the fields of each antenna element, merged appropriately both in magnitude and phase [46, 51, 52]. With the negligence of mutual coupling between these antenna elements, the assumption is that the current is the same in each element and isolated element, but this is not always the case even if the antenna elements are excited by the same phase and amplitude. In the provision of directive

patterns there is constructive and destructive interference of fields from individual antenna elements. With constructive interference, fields sum together to provide a maximum field in the desirable direction whereas for destructive interference, fields cancel out in the remaining space. To shape the overall radiation pattern of an antenna array with similar antenna elements the following can be adjusted;

1. The geometrical configuration of an antenna array
2. Relative pattern of the individual antennas
3. Relative displacement between antenna elements
4. Excitation amplitude
5. Excitation phase.

The overall radiation pattern of an antenna array is obtained as the product of the electric field of a single antenna located at the origin and the array factor. Array factor is a function that describes the position of the antenna elements in the array and the weights used. This factor differs for each antenna array. Mathematically, the total field of antenna array  $E_t$ , is given by:

$$E_t = [E_r \times \text{Array factor}] \quad (2.1)$$

where  $E_r$  is the field of a single antenna. There are different geometric configurations of antenna arrays and the commonly known ones being linear, planar and circular [46,53,54].

### 2.1.1 Linear Antenna Array

This is the most straight forward geometric configuration of an antenna array whereby antenna elements are arranged in a straight line with equal spacing between them [54–56] as shown in Figure 2.1. Linear antenna arrays can be classified into uniform and non-uniform arrays. In uniform linear array antenna, antenna elements are identical with equal current magnitude, uniform spacing and a progressive phase shift. With non-uniform linear array, there is non-uniform spacing between antenna elements and the elements are fed with different phases and amplitude [46].

The array factor of the linear antenna array shown in Figure 2.1 is described by [46]:

$$\begin{aligned} AF(\theta, \phi) &= 1 + e^{j\psi} + e^{j2\psi} + \dots + e^{j(N-1)\psi}, \\ &= \sum_{n=1}^{N-1} e^{j(N-1)\psi} \end{aligned} \quad (2.2)$$



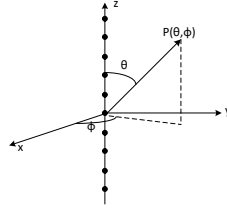


FIGURE 2.1: Linear array configuration with dots denoting the antenna elements [57]

where  $N$  is number of the antenna elements,  $\psi = kd \cos(\theta)$ ,  $d$  is the distance between antenna elements,  $\beta$  is the phase difference between antenna elements,  $k = 2\pi/\lambda$  and  $\lambda$  is the wavelength.

Multiplying equation (2.2) by  $e^{j\psi}$  and subtracting the resulting product from equation (2.2) yields

$$AF(\theta, \phi) = \frac{1 - e^{jN\psi}}{1 - e^{j\psi}} \quad (2.3)$$

Solving equation (2.3) results in

$$AF(\theta, \phi) = e^{j[(N-1)/2]\psi} \left[ \frac{\sin\left(\frac{N}{2}\psi\right)}{\sin\left(\frac{1}{2}\psi\right)} \right] \quad (2.4)$$

The array factor of a linear array may be normalized so that  $N$  is equal to unity. Therefore the normalized array is given by [46]:

$$AF(\theta, \phi) = \frac{\sin\left(\frac{N}{2}\psi\right)}{N \sin\left(\frac{\psi}{2}\right)}. \quad (2.5)$$

## 2.1.2 Planar Antenna Array

In planar array configuration antenna elements or individual antennas are arranged in one plane as shown in Figure 2.2. They are also called two dimensional (2D) arrays. This geometric configuration offers the advantage of beam steering occurring

in two planes, that is azimuth and elevation planes and its overall radiation pattern is characterised by reduced side lobe levels [58].

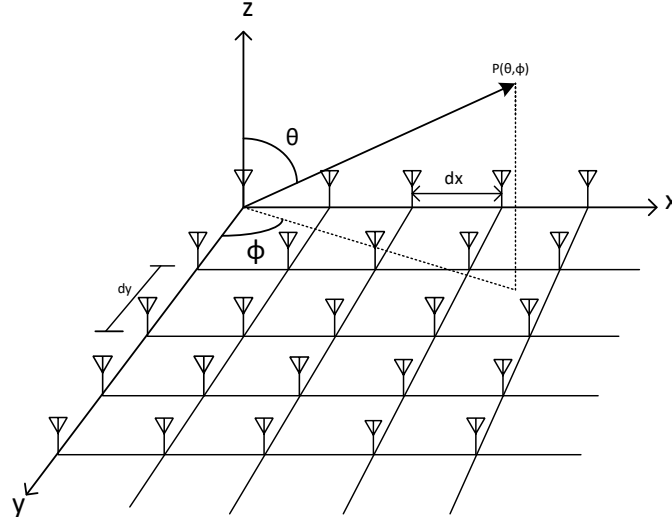


FIGURE 2.2: Planar array configuration with antenna elements in both x and y directions [46].

Planar array offers the design of complicated arrays hence there is an increase in complexity and cost [59]. In planar array configuration there are  $N_y$  antenna elements placed next to one another linearly in the  $y$  direction with equidistant of  $d_y$ . Another  $M_x$  antenna elements are aligned in the  $x$  direction with equidistant of  $d_x$  as illustrated in Figure 2.2. The array factor for this array is given by:

$$AF(\theta, \phi) = AF_x(\theta, \phi) \times AF_y(\theta, \phi) \quad (2.6)$$

where

$$AF_x(\theta, \phi) = \sum_{m=1}^M I_m e^{j(m-1)(kd_x \sin(\theta) \cos(\phi))} \quad (2.7)$$

and

$$AF_y(\theta, \phi) = \sum_{n=1}^M I_n e^{j(n-1)(kd_y \sin(\theta) \sin(\phi))} \quad (2.8)$$

Therefore

$$AF(\theta, \phi) = \sum_{n=1}^N I_n \left[ \sum_{m=1}^M I_m e^{j(m-1)(kd_x \sin(\theta) \cos(\phi))} \right] e^{j(n-1)kd_y \sin(\theta) \sin(\phi)} \quad (2.9)$$

For a uniform planar array,  $I_m = I_n = I_0$  then the above equation (2.9) is written as

$$AF(\theta, \phi) = I_0 \sum_{n=1}^N e^{j(n-1)kd_y \sin(\theta) \sin(\phi)} \sum_{m=1}^M e^{j(m-1)kd_x \sin(\theta) \cos(\phi)} \quad (2.10)$$

whereby  $I_m, I_n$  are the excitation amplitudes,  $I_0$  indicates amplitude excitation at the origin. The normalised array factor of uniform planar array is given by [46]:

$$AF_n(\theta, \phi) = \left\{ \frac{\sin\left(M\frac{\psi_x}{2}\right)}{M \sin\left(\frac{\psi_x}{2}\right)} \right\} \left\{ \frac{\sin\left(\frac{\psi_y}{2}\right)}{N \sin\left(\frac{N\psi_y}{2}\right)} \right\} \quad (2.11)$$

where  $\psi_y = kd_y \sin(\theta) \sin(\phi)$  and  $\psi_x = kd_x \sin(\theta) \cos(\phi)$ .

### 2.1.3 Circular Antenna Arrays

The geometric configuration of antenna elements in this array is a ring arrangement as illustrated in Fig. 2.3. This array type generate omnidirectional beams and there is uniform spacing of antenna elements and elements have identical amplitude and phase [46].

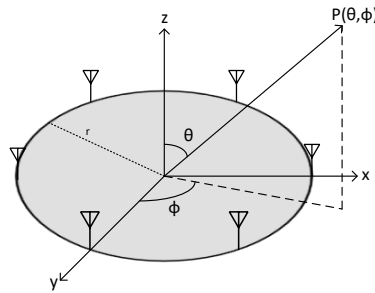


FIGURE 2.3: Circular array configuration with antenna elements [59].

The array factor for this array is described by [59]:

$$\begin{aligned}
 AF(\theta, \phi) &= \sum_{n=1}^N I_n e^{jkr \sin \phi (\cos \theta_n \cos \theta + \sin \theta_n \sin \theta)} \\
 &= \sum_{n=1}^N I_n e^{jkr \sin \phi \cos(\theta - \theta_n)}
 \end{aligned}
 \tag{2.12}$$

## 2.2 Feed Networks for Array Antennas

Antenna elements in an array configuration can be fed through a single line (series fed) or by multiple lines (corporate or parallel feeding).

### 2.2.1 Series Feed Network

In this feed network, a single line is used to feed the antenna or radiating elements and each antenna as shown in Figure 2.4. As shown by the figure, element feeds from the previous one. Any change which occur in any antenna element directly affects the performance of the other element. Advantages of this feed network include easy implementation and fabrication, reduced feed network losses and low sidelobe level of the array. However, this feed network is limited by providing a narrow bandwidth and being used in arrays with a fixed beam or arrays that use frequency scanning for beam scanning [46].

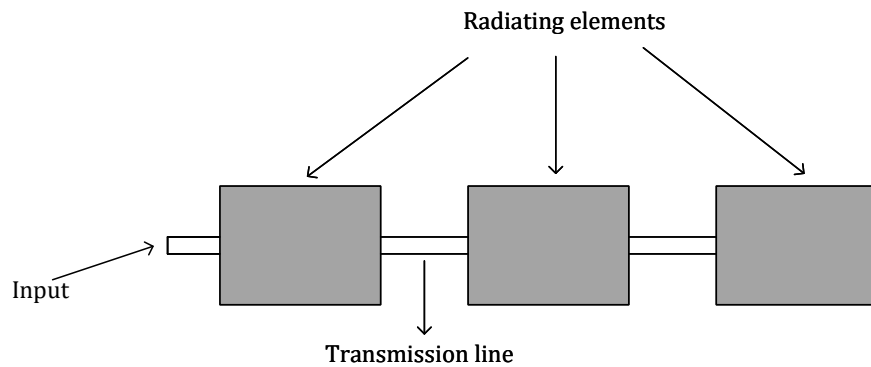


FIGURE 2.4: Series feed network.

### 2.2.2 Corporate Feed Network

In this feed network, multiple lines are used to feed the antenna elements as illustrated in Figure 2.5. From the figure, the power splits or feedlines of  $2^n$  (i.e.  $n = 2, 4, 8, 16, 32, 64$  etc) provided by corporate feed network are accomplished by using multiple section quarter wavelength impedance transformers or using tapered lines. Advantages of this feeding include equal power distribution to all antenna elements, ability to provide large bandwidths and have beam scanning properties. The limitation of this methods is high feed losses to due multiple lines [46].

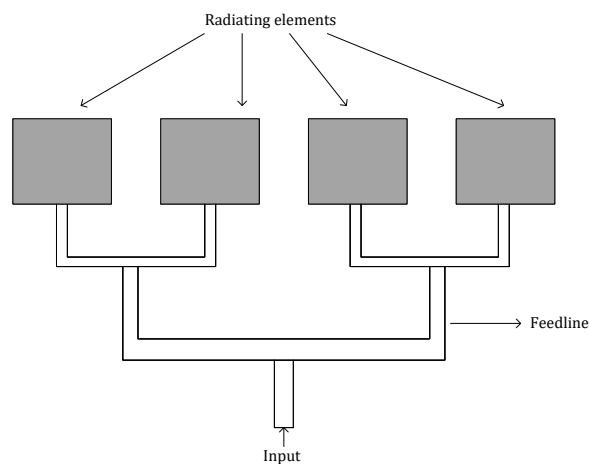


FIGURE 2.5: corporate feed network

## 2.3 Phased Array Antenna

Phased array antenna is a system of multiple antenna elements arranged in a certain electrical or geometric configuration each equipped with a specific time delay to steer electromagnetic beams in a desired direction [57, 60–64]. Fig.2.6 illustrates a schematic of a basic phased array antenna comprising of antenna elements, transmitter/receiver and phase shifters. Antenna elements such as dipole, slot and patch antenna are each equipped with phase shifters for the provision of phase shifting. Geometric configuration of these antenna elements can be linear, planar and circular [57]. The overall radiation pattern is obtained by the manipulation of the amplitude and phase of the signal emitted from individual antennas. There is constructive/destructive interference of signals to steer beams in desired directions which results in a combination of some signals forming one strong signal whereas others partially cancel out in unwanted direction [47, 65]. Phased array antennas have the

advantage to electronically steer beams in desired directions accurately and rapidly without regarding antenna size or weight thus obviating the need to reposition large antennas during beam steering [54]. In these systems, the path difference in free space is compensated by the introduction of time variation or phase delay in the signal emitted from each antenna [61].

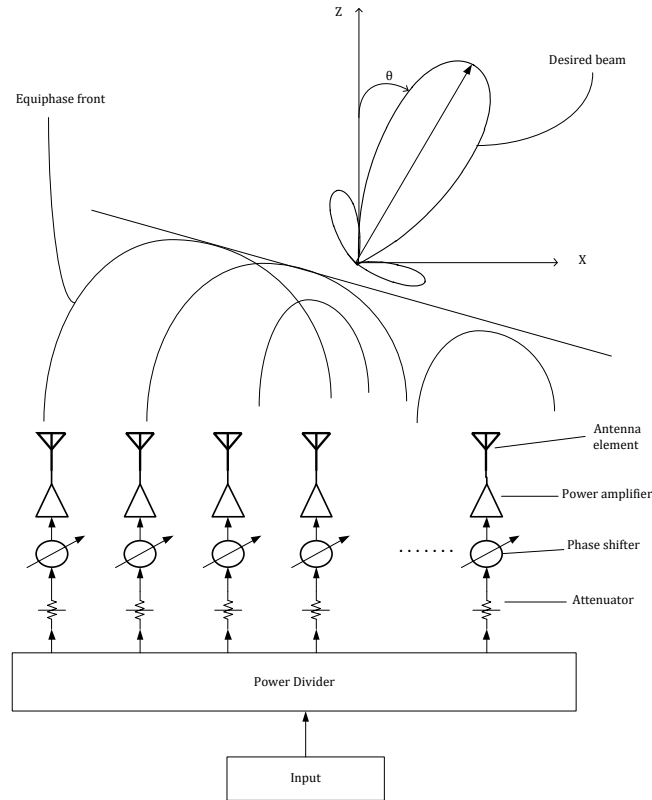


FIGURE 2.6: Phased array antenna in transmit mode [66]

Fig. 2.6 illustrates the block diagram of a phased array antenna in transmit mode with equally spaced " $N$ " antenna elements in transmitting mode. Each antenna element in PAA is equipped with a variable time delay to control the phases of the signals. In reception mode, the same concept is held because phased array antennas obey reciprocity. Due to the separation between antenna elements, the radiated beam will experience a time delay or phase shift given by:

$$\Delta\phi = \frac{2\pi d \sin(\theta)}{\lambda} \quad (2.13)$$

where  $d$  is spacing between antenna elements,  $\lambda$  is the wavelength of the signals and  $\theta$  is the boresight angle.

The geometric configuration of antenna elements in PAAs can also be either linear, circular or planar. For a linear PAA, antenna elements are identical, with current of equal magnitude, uniform amplitude, equal interspacing and a progressive phase shift. The array factor  $AF(\theta, \phi)$  in this geometry is proportional to the radiated field at a certain point in space and for antenna elements in the x-axis this is given by

$$F_a(\theta, \phi) = \sum_{n=0}^{N-1} I_n e^{jn(kd \cos \theta + \alpha)} \quad (2.14)$$

where  $I_n$  is the current magnitude of the  $n$ th element and  $d$  is the spacing between antenna elements.

If elements are in the z-axis,  $AF(\theta, \phi)$  is given by [57]:

$$F_a(\theta, \phi) = \sum_{n=0}^{N-1} I_n e^{jn(kd \cos \theta - \alpha)}. \quad (2.15)$$

The progressive phase between antenna elements enables the radiation pattern of PAA to be steered from broadside to the intended direction ( $\theta$ ) forming a beam scanning array. This further explains electronic beam scanning in PAAs. In practical implementation of PAAs, this is achieved by the use of phase shifters. If the array geometry is the z-axis, the progressive phase factor responsible for phase excitation between the antenna elements is given by

$$\alpha = kd \cos \theta \text{ or } \theta = \cos^{-1} \left( \frac{\alpha_z \lambda}{2\pi d} \right), \quad (2.16)$$

and the geometry of the array is on the x-axis, the above equation changes to

$$-\alpha = kd \cos \theta \text{ or } \theta = \cos^{-1} \left( \frac{-\alpha_x \lambda}{2\pi d} \right). \quad (2.17)$$

An optimized PAA design is achieved by having both the array factor and maxima of a single element antenna in the desired direction. Array factor is influenced by phase excitation and distance between antenna elements. If the distance between the antenna elements is larger than the wavelength, maximas of the main lobe called grating lobes will appear and this is not desirable for PAAs [57]. To prevent grating in PAA, interelement spacing  $d$  of the antenna elements must be chosen to fulfill the accompanying condition:

$$\frac{d}{\lambda} < \frac{1}{1 + |\cos \theta_0|}. \quad (2.18)$$

As such, the above equation indicate that the interspacing between antenna elements in a PAA should be one half-wavelength to prevent grating lobes during beam scanning.

The concept and principles of beam scanning in linear PAAs is extendable to planar PAAs. In this array geometry each row has identical current distributions but with different current levels. There is a uniform phase progression between the antenna elements in both the  $x$  and  $y$  direction due to the current distributions. The phase progression in the  $x$  direction is given by,  $\alpha_x = kd_x \sin \theta \cos \phi_0$  and in the  $y$  direction,  $\alpha_y = kd_y \sin \theta \sin \phi_0$ . The overall array factor of a planar phased array is given by

$$AF(\theta, \phi) = \left[ \sum_{m=1}^M I_m e^{j(m-1)(kd_x \sin \theta \cos \phi + \alpha_x)} \right] \left[ \sum_{n=1}^N I_n e^{j(n-1)kd_y \sin \theta \sin \phi + \alpha_y} \right] \quad (2.19)$$

## 2.4 Mutual Coupling in Phased Array Antennas

Modern wireless communication demands for the usage of compact and miniaturized antennas. Hence there is reduction in antenna size resulting in antenna elements being in close proximity to one another and giving rise to a problem called mutual coupling [39, 46]. This a phenomenon in antenna arrays whereby there is electromagnetic interaction between antenna elements [67]. It is an undesirable effect which describe energy transmitted by the transmitting antenna element being received by the adjacent one and vice versa because antennas obey reciprocity. Hence, this effect is detrimental to the overall performance of the antenna arrays because it affects antenna parameters such as gain, directivity, beam width and overall radiation. Furthermore, other parameters affected are antenna impedance, steering vector, interference suppression, direction of arrival (DOA), output signal-to-interference-plus noise ratio SINR [68]. Factors which mutual coupling depend on are spacing between antenna elements, antenna type used, number of antenna elements, geometric configuration of antenna elements, feed network components such as couplers and phase shifters. In relation to space between antenna elements, low inter-element space leads to decrease in of the array aperture thus reducing output SINR of the array. This is because mutual coupling affect the steering vector which is responsible for amplitude and phase manipulation. As a result this will cause undesirable effect to the desired signal vector and thus altering the array's radiation pattern [69]. Mutual coupling effect have driven researchers to research more into the effect including in adaptive arrays.



For explanation, consider two antenna elements  $A$  and  $B$  in an array as illustrated in Figure 2.7. In transmitting mode illustrated by Figure 2.7a, a source is attached to antenna element  $A$  and it generates energy. This energy travels towards the radiating element and gets radiated into free space. Part of this radiated energy is gets coupled by adjacent element, element  $B$ . A current flow is induced thus re-radiating the received energy into space whereas the other part of the energy is driven to the source. The energy gets imposed with the energy generated by antenna element  $B$ , causing a standing wave and changing the input impedance of the antenna. In Figure 2.7b, the antennas are in reception mode with an incident plane wave stroking them. The incident wave strikes antenna element  $A$  first and causes current induction. There will be radiation of energy into free space due to the induced current and the majority of the energy travels towards the load. Some the radiated energy is coupled by antenna element  $B$ . If there is impedance mismatch in antenna element  $A$ , some of the energy is reflected and radiated into space. Furthermore, there will current induced in antenna element  $B$  due to the energy from antenna element  $A$ . As in like antenna element  $A$ , there will be radiation of energy. This process will be same even if the incident wave strikes antenna element  $B$  first.

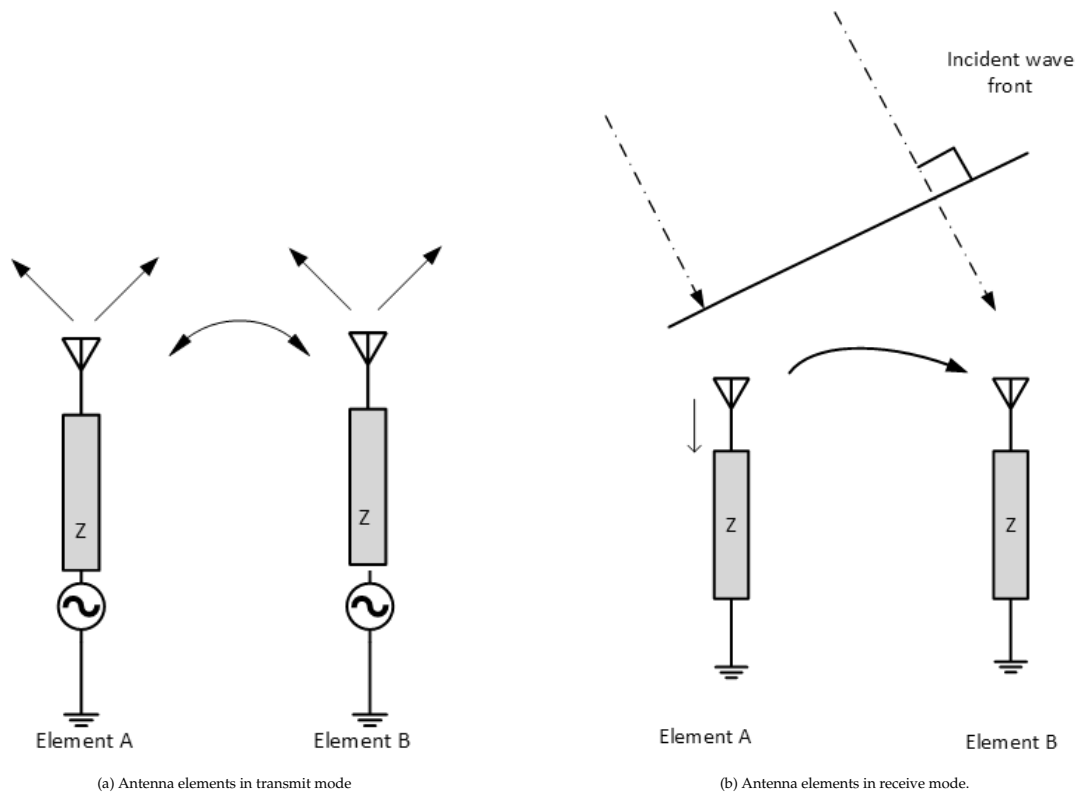


FIGURE 2.7: Mutual Coupling in transmit and reception mode.

There are different solutions proposed and implemented to reduce of mutual coupling effect in antenna arrays. One technique which has attracted a lot attraction is the usage of electromagnetic band gap (EBG) structures [39,40]. EBG have an extraordinary property of suppressing surface waves and accomplishing high seclusion characteristics of antenna array [70,71]. These antenna structures have the ability to block frequencies of a particular frequency band and have in-phase coefficient [72]. A huge number of basic EBG applications exists particularly at low mmWave and microwave frequency regions examples being electronic PAA, bluetooth, mobile telephony and global position systems (GPS) [73–75]. In antennas for mobile phones this technique has come in handy because it prevents undesired electromagnetic waves. Presence of surface wave suppression property in EBG enhance antenna array performance by incrementing antenna gain and reducing back radiation.

There are various designed and proposed EBG structures for mitigation of mutual coupling effect in antenna arrays. Authors in [72] designed a microstrip PAA with a novel mushroom like EBG structure for wireless local area network (WLAN) application with a resonance frequency of 5.8 GHz. The patch element had a size of  $14 \times 11.4 \text{ mm}^2$  using FR4 as its dielectric substrate with dielectric constant of 4.4 and a height of 1.6 mm. A  $2 \times 2$  array was embedded with a  $2 \times 5$  mushroom-like EBG structure between the radiating patch elements. The proposed antenna suppressed unwanted surface waves at frequency stop band between 4.8 GHz to 7 GHz catering for the resonance frequency. In comparison the antenna array without the EBG structure indicated a coupling of -21 dB and array with embedded EBG structure there was a 23 dB mutual coupling reduction. In [76], the authors designed and tested a microstrip antenna phased array with a uniplanar compact EGB substrate. The antenna was feed through probe feeding and characterized by an array element configuration of  $7 \times 5$  with an operating frequency of 5.75 GHz. From both the simulated and measured results, the proposed antenna successfully reduced mutual coupling effect between the antenna elements. Authors [77] proposed a microstrip array antenna for x-band application embedded with EBG structure operating at a resonant frequency of 10.2 GHz and fed through a coaxial feed. Unit cell of the EBG structure was designed into an array of  $21 \times 2$  configuration and it was embedded between the two patch elements separated by a distance of  $\lambda/6$ . The proposed antenna reduced mutual coupling between the elements by 4 dB.

Another way of reducing mutual coupling effect between antenna elements of an array is through the use of defected ground structures (DGS). DGS are an etched configuration embedded on a transmission line's ground plane [41,42]. This ground

plane deflection disarrange current distributions of the ground plane thus bringing a change to transmission line parameters such as line capacitance, resistance and inductance. Etched ground plane configuration can give effective inductance and capacitance of the antenna which are key parameters at resonant frequency [41, 78, 79]. Authors in [80] designed a four element MIMO antenna array with a defected ground structure operating at 5.8 GHz for WLAN application. Characteristics mode analysis was done to design a better DGS unit cell without affecting the radiation characteristics of the array antenna. In the analysis of measured results, the proposed antenna array produced a realized gain of 5.3 dB, total radiation efficiency of 84% and a bandwidth of 200 MHz. Finally the proposed array antenna produced mutual coupling of -32 dB between the antenna elements. A four element array antenna with a dumbbell shaped DGS to reduce mutual coupling effect between the radiating elements was designed and fabricated in [81]. The designed array antenna was analyzed using a finite integration technique (FIT) and it achieved mutual coupling reduction of 20 dB, antenna gain of 9.54 dB in both E and H planes and a radiation efficiency of 88%. In [82], authors proposed a coplanar linear polarized antenna array embedded with three U-shaped DGS at a center frequency of 3.6 GHz. The proposed array obtained a mutual reduction of 10 dB between antenna elements.

In recent years, metamaterials have emerged as one the methods to reduce mutual coupling effect in antenna arrays. Metamaterials are artificial structures in nature and exhibit either a negative permittivity or negative permeability [44, 45]. Metamaterials have the attribute of suppressing electromagnetic waves in certain frequency bands and as such they can suppress surface wave propagation thus reducing mutual coupling between antenna elements in the array [43]. A metamaterial super-substrate is proposed in [83] for mutual coupling suppression suitable for a planar phased array antenna. The metamaterial was Incorporated between the radiating patches of a  $2 \times 1$  patch array. From the simulation results, the proposed technique increased the antenna bandwidth by 160 MHz and reduced mutual coupling between the radiating patches by 5 dB. A slot combined complementary split ring resonator (SCCSRR) metamaterial structure is proposed to suppress mutual coupling in a densely packaged microstrip phased array in [84]. The SCCSRR metamaterial structure was placed between two radiating elements of microstrip phased array operating at 3.7 GHz on top side, bottom side, and on both side together. The proposed metamaterial structure achieved a significant mutual coupling reduction of 14.7 dB and total measured return loss of -26 dB. Authors in [85] proposed a slotted E-shaped metamaterial decoupling slab for densely packed MIMO antenna arrays.

The metamaterial decoupling slab was made up of two E-shaped slits and an inductive stub. The proposed metamaterial was located between the patch antenna elements. A prototype for this metamaterial was fabricated on a FR-4 substrate with a volume of  $67.41 \times 33.49 \times 1.6 \text{ mm}^3$ . The proposed metamaterial accomplished -43.7 dB mutual coupling reduction between the patch elements for 1.6 thick and 4.5 permittivity substrate.

Apart from metamaterials, DGS and EBG, there are various proposed techniques and methods in existing literature which are used to reduce mutual coupling in phased array antennas. The authors in [86] proposed a densely packed S-Band microstrip PAA with a mutual coupling based element. The mutual coupling based element was used to decrease the coupling effect in the antenna. Despite the radiating patches being closely placed, the proposed antenna achieved mutual coupling less than -25 dB. A novel wide-scan angle microstrip phased array antenna is proposed in [87]. The proposed antenna used two techniques to reduce mutual coupling between adjacent elements and these techniques are; parasitic decoupling walls and individual ground planes. The results of the proposed antenna indicates that the antennas has a scan angle of  $65^\circ$  in E-plane and  $60^\circ$  in H-plane and reduced mutual coupling to lower than -32 dB between adjacent elements. The proposed antenna had a VSWR less 2 over 20% operation bandwidth. A finite 544 element phased array prototype was fabricated from the proposed design and there was agreement between simulated and measured results over several scan angles. Mutual coupling between radiating elements can be reduced by a proper design of antenna elements or by orientating the polarization of antenna elements in the array [88]. The authors in [89] proposed to compensate for mutual coupling in conformal array antenna based on the active element pattern method. In the proposed method, the elements were classified based on the active element pattern and a total active pattern was achieved. The correction of mutual coupling in the array was done through excitation and active element pattern.

## 2.5 Microstrip Patch Antenna

There are various antenna types which are used as antenna elements in phased array antennas and these include dipole antenna, horn antenna, reflector antenna, microstrip antenna etc but for this thesis, microstrip patch antenna is used as an antenna element or radiating element for the proposed phased array antenna. The idea of microstrip patch antennas date back to 1953, with their first patent published in 1955 but these antennas received a lot attention in the 1970s due to the advancement

of the printed circuit board (PCB) technology. Since then, they have been broadly deployed in different fields of wireless communication.

### 2.5.1 Basic characteristics of Microstrip Patch Antenna

A conventional microstrip antenna is illustrated in Figure 2.8 and is made up of a dielectric substrate, radiating patch, ground plane and feedline [46, 90]. In the configuration shown by Figure 2.8, the patch is etched into the substrate and it is source for radiation. At this layer, electromagnetic energy fringes off at the edges, goes through dielectric substrate and gets reflected by the ground plane and pass through the substrate into the free space. There are different dielectric substrates which are used in the design of a microstrip antenna and their electric constants range from 2.2 to 12 [46].

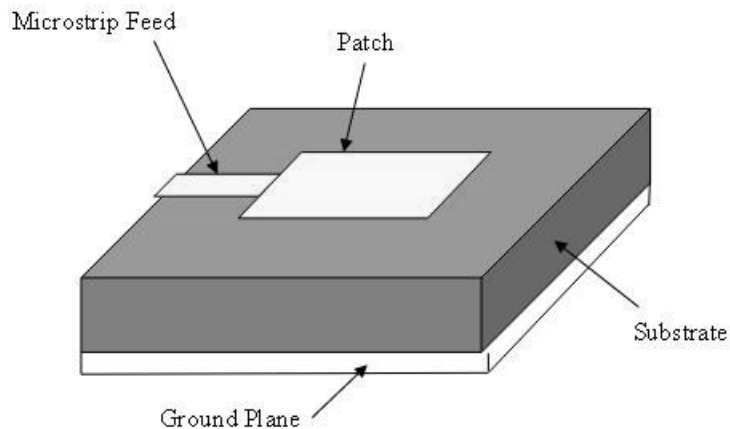


FIGURE 2.8: Microstrip patch antenna [91]

In practical applications, geometry of the radiating patch is either square, circular or rectangular but the rectangular and circular shapes are the commonly used because of their advantages such as easy fabrication, easy of analysis and attractive radiation characteristics. However different geometry are possible to be designed and some of the geometry is illustrated in Figure 2.9.

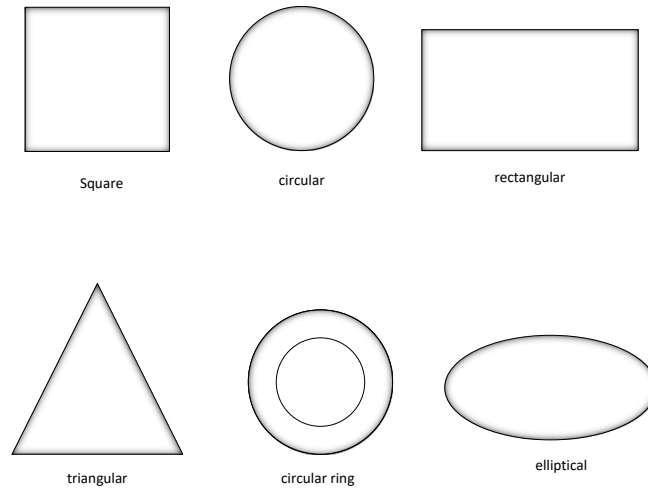


FIGURE 2.9: various geometry for patch antenna

For rectangular patch antenna, the dimensions of the antenna are calculated using the following steps [46]

1. Determine patch width ( $W$ ) for a good radiation efficiency

$$W = \frac{c}{2f_r} \sqrt{\frac{2}{\epsilon_r + 1}}, \quad (2.20)$$

**where,**

$c$  represents speed of light and

$f_r$  is the operating frequency

2. Determine the effective dielectric constant. Due to the finite dimensions (length and width) of the radiating patch, fields at the patch edges go through a fringing effect. This makes the microstrip patch appear electrically wider compared to its physical dimensions. In order to account for the fringing effect, an effective dielectric constant is introduced and it is calculated based on equation (2.21)

$$\epsilon_{\text{reff}} = \frac{\epsilon_r + 1}{2} + \frac{\epsilon_r - 1}{2} \left[ 1 + 12 \frac{h}{W} \right]^{-\frac{1}{2}}, \quad (2.21)$$

3. With the value of  $\epsilon_{\text{reff}}$ , the extended length  $\Delta L$  or fringing factor is calculated using equation (2.22)

$$\frac{\Delta L}{h} = 0.412 \frac{(\epsilon_{\text{reff}} + 0.3) \left( \frac{W}{h} + 0.264 \right)}{(\epsilon_{\text{reff}} - 0.258) \left( \frac{W}{h} + 0.8 \right)}, \quad (2.22)$$

4. Determine the length  $L$  of radiating patch

$$L = \frac{c}{2f_r \sqrt{\epsilon_{\text{reff}}}} - 2\Delta L. \quad (2.23)$$

5. Determine the ground plane dimensions, length ( $L_g$ ) and width ( $W_g$ ) are calculated as:

$$L_g = L + 6h \quad (2.24)$$

$$W_g = W + 6h \quad (2.25)$$

Microstrip antennas are broadly deployed in wireless communication because they exhibit numerous advantages over other antenna types. This advantages include; they are light in weight, small in size, have a lower cost of production, easy fabrication and are compatible with monolithic microwave integrated circuits [90, 92]. These antennas can also provide feed-line flexibility, frequency agility and dual frequency operations. Despite the abundance of patch antennas in modern wireless communication, their performance are still set back by some major disadvantages such as inherent narrow bandwidth, lower gain and low power handling capacity. Narrow bandwidth can be improved by increasing the height of the dielectric substrate, whereas array configuration is used to improve low gain and low power handling limitations [46].

### 2.5.2 Feeding Methods of Microstrip Patch Antennas

There are many ways to excite the radiating patch, but the commonly used are microstrip feedline, coaxial probe feeding, aperture and proximity coupling [46].

#### Microstrip feed line

This method is concerned with connecting a conducting strip to the radiating patch. The advantages of the microstrip feedline are ease of fabrication and simplified matching which is achieved by controlling inset position. However the tradeoff

which comes with this feeding method is the increment in surface waves and spurious feed radiation thus limiting the bandwidth [46,92,93].

### **Coaxial Probe feeding**

With this technique, the inner conductor of the coaxial is attached to the patch and the outer conductor is connected to the ground plane. The coaxial probe feed method offer advantages such as easy fabrication, easy impedance matching and low spurious radiation. The limitations of this method is that it still offers low bandwidth and it is difficult to model especially for thick substrates [46,92,93].

### **Aperture Coupling**

In aperture coupling feeding scheme, the ground plane separates two different substrates. The low substrate which is on the bottom part has a microstrip feedline which is used to couple energy to the patch through a slot on the ground plane. regarding substrates, the top substrate is characterized by a thick low dielectric constant whereas the bottom substrate is characterized by a high dielectric constant. Apart from separating substrates, the groundplane reduces polarazation purity and also minimises the formation of spurious radiation pattern. With this feeding scheme the feed mechanism element is fully optimized [46,92,93].

### **Proximity Coupling**

Proximity Coupling consists of two dielectric substrates with the feedline located between these substrates. Compared to other schemes, proximity coupling has a low bogus spurious radiation and offers much larger bandwidth. The shortfall which accompanys this scheme is difficulty in fabrication because due to the need of proper alignment of the substrate layers [46,92,93].

## **2.6 Antenna Parameters**

The antenna parameters explained below will be used throughout the thesis and some are used to measure the performance of phased array antenna. Each of the terms are briefly explained below.

### **2.6.1 Radiation Pattern**

Radiation pattern is a graphical representation of the radiation properties exhibited by an antenna as a spatial function [94]. Some of the radiation properties of



an antenna are polarization, directivity, field strength and radiation intensity [46]. Radiation patterns are most commonly represented in the far-field region and are subsequently plotted as a function of the directional coordinates. Far-field region also known as Fraunhofer region is a region where the radiation pattern does not change shape with distance from the source and electric (E) and magnetic (H) fields are orthogonal to one another and direction of propagation, as with the plane wave [46]. The radiation pattern describes the E and H field pattern of an antenna [95]. These patterns are represented in various ways with two dimensional (2D) and three dimensional (3D) being the common plots. For better visualization, the radiation pattern of antenna is normalized by its maximum value to produce a normalized field pattern [46]. In Figure 2.10, a radiation pattern of antenna is illustrated consisting of several lobes. These lobes are classified into main, minor, back and side lobes. Main lobe is the lobe with maximum field strength or radiation. A minor lobe is any radiation lobe except the main lobe. Side lobe is a radiation lobe which is any direction other than the main lobe and are the largest of the minor lobes. Side lobes are unwanted and should be minimized at all times. Back lobes are radiation lobes which are in opposite direction of the main lobe.

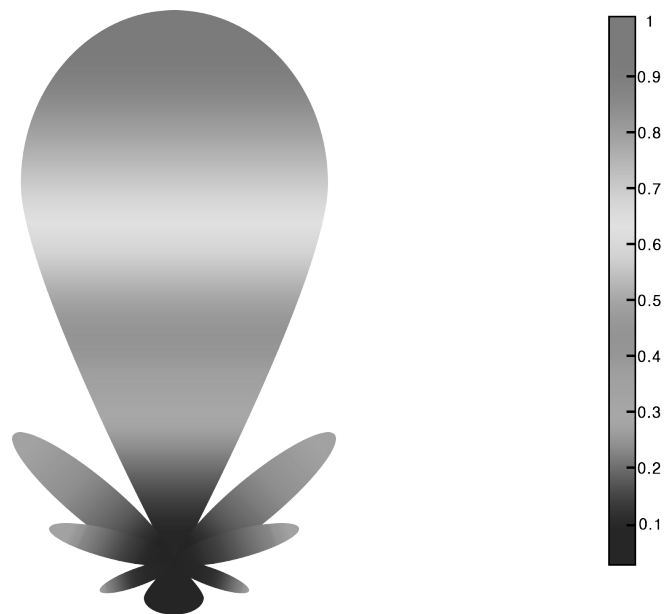


FIGURE 2.10: Radiation pattern of an antenna [46]

### 2.6.2 Beamwidth

Beamwidth which is associated with a radiation pattern of an antenna is defined as the separating two equivalent points on the opposite sides of the main lobe.

Beamwidth is measured at any point of the main lobe but common used beamwidths are halfpower beamwidth (HPBW) and first null beamwidth (FNBW). HPBW is measured where the radiation intensity of the mainlobe is half the maximum power (-3 dB) and FNBW is measured between the nulls of the antenna radiation pattern as illustrated in figure what what [46,96].

### 2.6.3 Directivity

Directivity of an antenna describes the ratio between radiation intensity of an antenna in a particular direction and averaged radiation intensity over all directions [46,97]. Directivity entails how well the antenna focuses the mainlobe. If a high value of directivity is obtained, this implies that there is a strong main lobe with very few minor lobes and vice versa. Directivity is dimensionless and in mathematical form is described as [46]:

$$D = \frac{U}{U_0} = \frac{4\pi U}{P_{rad}} \quad (2.26)$$

where  $U$  is the radiation intensity in a particular direction,  $U_0$  is the averaged radiation intensity and  $P_{rad}$  is the total radiated power.

### 2.6.4 Gain and Realized Gain

Gain is defined as the ratio of the radiation intensity in a particular to the radiation intensity of a reference antenna [98]. Reference antenna can be either be a isotropic or dipole antenna. Isotropic antenna is an antenna that radiates uniformly in all directions. Antenna gain which is referenced to an isotropic antenna, its units is expressed in dBi and if its referenced to a dipole antenna, its units is expressed in dBd. Gain indicates how strong the beam of an antenna can be send or received in a given. Furthermore, antenna gain does not take into account mismatch and reflection losses. Mathematically, antenna again is given by:

$$G = \frac{4\pi U}{P_{in}} \quad (2.27)$$

where  $U$  is the radiation intensity in a particular direction and  $P_{in}$  is the total input power.

Realized gain takes into consideration reflection and mismatch losses. According to IEEE standard for definitions of terms for antennas, realized gain is defined as "the gain of an antenna reduced by its impedance mismatch factor" [99].

### 2.6.5 Bandwidth

The bandwidth of an antenna is the range of frequencies where it operates with regards to certain characteristics or standards [46, 96]. According to the bandwidth definition, performance must be acceptable over a range of frequencies around the design center frequency. The range of frequencies are selected based on the intended use of the antenna. Bandwidth is measured using antenna and transmission line parameters such as return loss, antenna impedance or voltage standing wave ratio (VSWR) [46].

### 2.6.6 Active Reflection Coefficient

In practical application, antenna elements of the array are excited simultaneously. Evaluation of the reflection coefficient of each individual antenna element in the array does not give a good representation of the frequency response of the array due to mutual coupling, hence, active reflection coefficient is adopted. Active reflection coefficient describes the reflection coefficient of a single antenna element present in the array in the presence of mutual coupling and it also assesses impedance matching performance of the array [60, 100, 101]. The active reflection coefficient of antenna element in an array with  $N$  and  $M$  elements is given [100, 101]:

$$\Gamma_m = \sum_{n=1}^{N-1} S_{mn} \frac{a_n}{a_m}, \quad (2.28)$$

where  $S_{mn}$  is the transmission coefficient,  $a_n$  and  $a_m$  are the excitation coefficients for  $n$ th and  $m$ th element. During beam scanning, the transmission coefficient remains constant whereas excitation coefficients will change [100]. This may result in having a high active reflection coefficient indicating impedance mismatch.

### 2.6.7 Beam Scanning

The practice of beam scanning involves steering a beam of radiation in desirable directions and phased arrays have the ability to rapidly and accurately scan beams from the broadside to the desired angle [58]. There are various techniques used for beam scanning namely; phase scanning, frequency scanning and time delay scanning. Phase scanning is achieved through the use of phase shifters incorporated in each antenna element of the array. Frequency scanning is used to exploit the frequency sensitive characteristics of phase scanning because at one particular frequency, all antenna elements will be in phase [102]. Using the schematic of linear

phased arrays, the phase across the aperture tilts linearly and there is beam scanning. Time-delay scanning is the employment of time delays in order to achieve a desired phased relationship between antenna elements. This is done by inserting variable delay networks in front of radiating elements and varying the inter-element  $\Delta t$  because delay lines are used instead of phase shifters [103]. Broadband operations use time delay scanning because main beam direction does not vary with frequency [104].

## 2.7 Transmission Line Parameters

Transmission lines are used to transmit signals from the source to the antenna and have different parameters which are critical for measuring antenna performance. These parameters are briefly explained below.

### 2.7.1 Voltage Standing Wave Ratio

Voltage standing wave ratio (VSWR) also known as standing wave ratio indicates the amount of mismatch between transmission line and antenna [46]. It is also defined as the ratio of the maximum voltage to the minimum voltage in a standing wave pattern [46]. If there is an impedance mismatch between a transmission line, some of the energy is absorbed by the antenna as losses and some is reflected back to the source [105]. As such, increasing reflection magnitude ( $\Gamma$ ) and the ratio of the maximum voltage to the minimum voltage increases. Value of VSWR ranges between 1 and infinity, where 1 indicates a matched load. Equation (2.29) shows VSWR as a function of reflection coefficient and voltages.

$$\text{VSWR} = \frac{V_{max}}{V_{min}} = \frac{1 + \Gamma}{1 - \Gamma} \quad (2.29)$$

### 2.7.2 Impedance Matching

Impedance matching is the process of designing the input impedance so as it correctly corresponds to its signal source ensuring maximizing power transfer and minimizing reflections [105]. Common impedance matching techniques are quarter wave transformer and stub matching [46,105].

### 2.7.3 Return Loss

Return loss compares the power reflected by an antenna and the power transmitted into the antenna [46,105]. It is expressed as a logarithmic ratio measured in decibels

(dB) A small return loss is an indication of poor performance because less power is transmitted into the antenna. Return loss is measured as follows [105]:

$$\text{RL}[\text{dB}] = -10 \log \left( \frac{P_r}{P_{in}} \right) = -20 \log(|\Gamma_{in}|) \quad (2.30)$$

where  $P_r$  is the reflected power,  $P_{in}$  is the incident power and  $\Gamma_{in}$  is the reflection coefficient at the input of the transmission line.

## 2.8 Conclusion

This chapter presented fundamentals required for the rest of the thesis. It covered array theory, working principle of phased array antennas, how mutual coupling occurs, different methods used to reduce mutual coupling, theory of microstrip antennas as a radiating element for an array antenna. Finally, parameters used to measure antenna performance were discussed. In Chapter 3 of this thesis, basic theory of microstrip antennas and the presented antenna parameters are used to design and measure the performance of a single rectangular patch antenna. In Chapter 4, array theory is used to design a  $1 \times 4$  array antenna and subsequently, an eight element phased array antenna.

## Chapter 3

# Microstrip Patch Antenna Design

Microstrip patch antennas are widely used as radiating elements for phased array antennas in various wireless applications due to their numerous advantages over other antenna types. This chapter presents the design of a single rectangular patch antenna operating at 28 GHz. The selection of a dielectric substrate is an important aspect in the design of a microstrip patch antenna, therefore, a single rectangular patch antenna is designed based on three different dielectric substrates with varying dielectric constants and heights. The single rectangular patch antenna uses a quarter wave transformer for impedance matching between the transmission line and radiating patch. Furthermore, simulation results of the designed single patch antenna and how it compares with existing single patch antennas designed for 5G wireless applications is presented in this chapter. The simulation results are obtained using computer simulation technology (CST) studio suite software.

### 3.1 Introduction

Microstrip patch antennas have become prominent in modern wireless communications due to their various advantages such as realization in a compact form, low fabrication cost thus mass production, low profile and light weight, support circular and linear polarization, and capability to support dual and triple band frequency operations [46, 106]. Despite their many advantages, patch antennas have limitations such as narrow bandwidth, low gain and are sensitive to temperature and humidity [46, 106]. Different approaches have been developed over the years to curb drawbacks of these antennas. For example, bandwidth enhancement can be achieved by either increasing the height of the dielectric substrate or decreasing the dielectric constant of the substrate. Moreover, low gain of this antenna type can be improved through array configuration [90]. This indicates that microstrip patch antennas can be used as radiating elements in antenna arrays including phased array antennas. Microstrip patch antennas are used in numerous applications such as radar, mobile and satellite communications, MIMO, GPS, telemedicine, bluetooth, WiMAX

etc [46,92,107]. Gradually, the improvement of printed circuit board (PCB) technology have made microstrip patch antennas a very viable option for millimeter wave communications. Recently, there is a growing interest in applying microstrip patch antennas for 5G wireless applications, especially around 28 and 39 GHz frequency bands. Furthermore, patch antennas are envisaged to play a role in the sixth generation (6G) of mobile generation which is predicted to be commercialized in early 2028 by transmitting and receiving terahertz (THz) waves [108,109].

The selection of a dielectric substrate of a patch antenna is a very important aspect in the design of a microstrip patch antenna because it influences its overall antenna performance. In this chapter, a single rectangular patch antenna is designed based on three different dielectric substrates with varying dielectric constants and heights. The three dielectric substrates are RT/Duroid 5880, FR-4 and RO 3003. The main objective is to carry a comparative analysis and therefore choose the antenna with the best performance to be used as a radiating element for the proposed phased array antenna.

### 3.1.1 Related Works

Different works have been carried out to perform a comparative analysis regarding the impact of different dielectric substrates on the performance of microstrip patch antennas. The authors in [110] designed and fabricated five triangular patch antennas using five different substrates namely RT Duroid 5870, Taconic TLC, RO4003, Bakelite and FR4 Glass Epoxy. The antennas operated at a frequency of 28 GHz and used coaxial probe feeding for the excitation of the radiating patches. From the simulation results, the antenna designed using RT Duroid 5870 presented better antenna performance as compared to the other antennas. A staircase shaped microstrip patch antenna is designed and analyzed using four different substrates in [111]. The dielectric substrates used are RT Duroid, FR4 Glass Epoxy, Bakelite and Ceramic. Moreover the antenna was used for Ku-band applications and operated at a frequency of 15 GHz. From the simulation results, the antenna designed using RT Duroid yielded the best antenna performance. In [112], the authors designed and analyzed a rectangular microstrip patch antenna based on six different substrates. The used dielectric substrates are glass Pyrex, Styrofoam, Quartz, Ceramic, Polystyrene and FR-4. These antennas are excited with a strip line feed at a resonant frequency of 3 GHz. Furthermore, the simulation results of the antenna designed with Polystyrene indicated a good performance as compared to the antennas designed using different substrates. An analysis of the impact of dielectric substrates

on the performance of 28 GHz antenna for 5G wireless applications was conducted by the authors in [21]. A  $2 \times 2$  microstrip antenna array was modelled, simulated and analysed on five different dielectric substrates namely; Rogers RO4350B, Epoxy Mold Compound (Mold), FR402, Astra MT77 and Megtron 6. The authors used coaxial probe for the excitation of the radiating elements. Moreover, inset fed and a quarter wave transformer were adopted for impedance matching. From the simulation results, the antenna array designed using Megtron 6 yielded the best antenna performance.

### 3.1.2 Contributions

This chapter provides the following contributions:

- Design and simulation of a single rectangular patch antenna at 28 GHz applicable for 5G wireless applications.
- A comparative analysis of a 5G microstrip patch antenna based on three different dielectric substrates.

## 3.2 Design Model

The design of the proposed phased antenna for 5G wireless applications is initiated by the design of a single rectangular patch antenna. The design procedure for a single patch antenna involves specifying the dielectric substrate of the antenna, dielectric constant of the substrate ( $\epsilon_r$ ) height of the substrate ( $t$ ) and the resonant or operating frequency. From these specified parameters, the dimensions of the antenna such as the patch length and width can be determined. In this chapter, a single rectangular patch antenna is designed using three different dielectric substrates with varying dielectric constants and heights. The designs are further evaluated to inform the selection of the best antenna which can be used as a radiating element for the proposed phased array antenna. In the millimeter wave band it becomes complex to select substrate due to high conductor loss experienced by substrates as such a substrate with a low loss tangent becomes very desirable at this band [113]. For this chapter, the three dielectric substrates under consideration for the proposed patch antenna are RT-5880, FR-4 and RO 3003. These are the commonly used dielectric substrates for the microstrip antennas designed for millimeter wave band and 5G wireless applications [114]. Different researchers have proposed microstrip patch antennas operating at frequency 28 GHz using the three named dielectric substrates. In [115–119], the authors used RT/Duroid 5880 as a dielectric substrate for



their proposed patch antennas. The authors in [120–124] used FR-4 as a dielectric substrate and furthermore the authors in [125–128] used RO3003 as dielectric substrate in their designs.

The proposed single rectangular patch antenna in this chapter is illustrated in Figure 3.1. The antenna is made up of rectangular radiating patch, a quarter wave transformer and  $50\ \Omega$  feedline.  $50\ \Omega$  is used because it is the most popular in transmission lines order to minimize reflection and return loss [46]. In this design, the radiating patch of the single patch antenna is made using copper with a thickness of 0.035 mm. Copper is also used as a conducting material for the ground plane and transmission line of the antenna. Furthermore, the operating frequency for this proposed single rectangular patch antenna is 28 GHz.

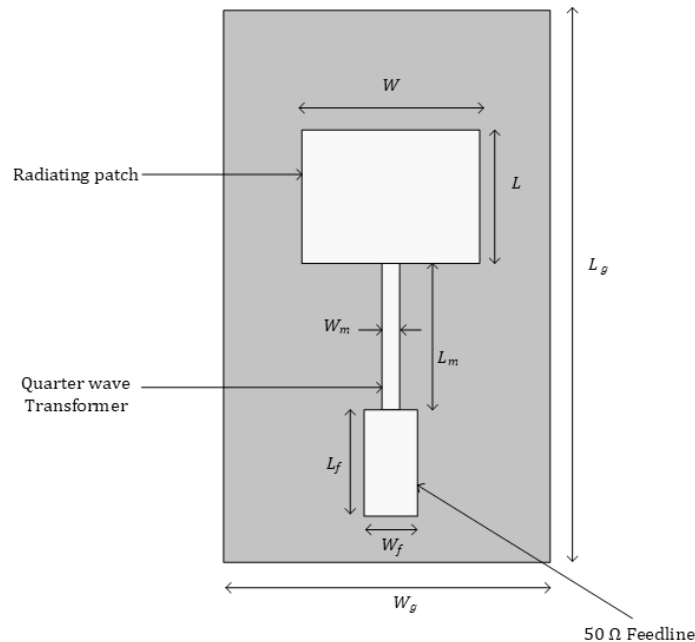


FIGURE 3.1: The proposed single element antenna.

### 3.2.1 Design Process

The design process for the proposed microstrip follows the design of a rectangular patch antenna described in Chapter 2 under subsection 2.5.1. RT-5880 substrate is used in the first design with a dielectric constant of 2.2 and a height of 0.5 mm. FR-4 is used in the second design with a dielectric constant of 4.3 and a height of 1.6 mm. Finally, RO 3003 is used in the final design with a dielectric constant of 3.0 and a height of 0.76 mm.

### Design using RT/Duroid 5880 Substrate

For the calculations of the first design which use Roger RT/Duroid 5880 dielectric substrate, the dimensions are calculated using equations (2.20) to (2.25) as described in Chapter 2. The calculation of the patch width ( $W$ ), effective dielectric constant ( $\epsilon_{\text{reff}}$ ), extension length of the patch ( $\Delta L$ ), the actual length ( $L$ ) of the patch and ground plane dimensions are indicated below.. Calculations begin with the width of the patch using equation (2.20).

$$W = \frac{3 \times 10^8}{2(28 \times 10^9)} \sqrt{\frac{2}{2.2 + 1}} = 4.232 \text{ mm.}$$

The effective dielectric constant is calculated using equation (2.21) as:

$$\epsilon_{\text{reff}} = \frac{2.2 + 1}{2} + \frac{2.2 - 1}{2} \left[ 1 + 12 \frac{0.5}{4.232} \right]^{-\frac{1}{2}} = 1.95 \text{ mm.}$$

The extension length of the patch using equation (2.22) as:

$$\Delta L = 0.412(0.5) \frac{(2.3 + 0.3) \left( \frac{W}{h} + 0.264 \right)}{(2.3 - 0.258) \left( \frac{4.232}{0.5} + 0.8 \right)} = 0.74 \text{ mm.}$$

The actual length of radiating patch is calculated using equation (2.23) as:

$$L = \frac{3 \times 10^8}{2(28 \times 10^9) \sqrt{2.3}} - 2(0.74) = 3.28 \text{ mm.}$$

Once the size of the radiating patch is determined, the size of the ground plane is also determined. The dimensions of the ground plane are calculated by equations (2.24) and (2.25) as:

$$L_g = 3.28 + 6(0.5) = 6.28 \text{ mm,}$$

$$W_g = 4.232 + 6(0.5) = 7.232 \text{ mm.}$$

For the excitation of the radiating patch, the single rectangular patch antenna uses a microstrip feedline to transmit power from the source to the patch due to its simplicity and easy analysis. For a given characteristic impedance  $Z_0$  of the feedline, where  $h$  is substrate height, the width of the microstrip feedline is computed based on equation 3.1 and is given as [46]:

$$W_f = \begin{cases} \frac{8e^A h}{e^{2A} - 2} & \text{for } \frac{W}{h} < 2 \\ \frac{2}{\pi} \left[ B - 1 - \ln(2B - 1) + \frac{\epsilon_r - 1}{2\epsilon_r} \left( \ln(B - 1) + 0.39 - \frac{0.61}{\epsilon_r} \right) \right] h, & \text{for } \frac{W}{h} > 2 \end{cases} \quad (3.1)$$

where

$$A = \frac{Z_0}{60} \sqrt{\frac{\epsilon_r + 1}{2}} + \frac{\epsilon_r - 1}{\epsilon_r + 1} \left( 0.23 + \frac{0.11}{\epsilon_r} \right),$$

$$B = \frac{377\pi}{2Z_0\sqrt{\epsilon_r}}.$$

The single rectangular patch antenna is excited using a microstrip feed line which is connected to an input port source with a characteristic impedance of 50  $\Omega$ . With this given characteristic impedance, the width of the feedline of the single patch antenna using RT Duroid substrate is calculated using equation (3.1). By using  $w/h > 2$  condition, auxiliary variable  $B$  is determined as:

$$B = \frac{377\pi}{2(50)\sqrt{2.2}} = 7.9851.$$

The width is determined from the following relationship as:

$$W_f = \frac{2}{\pi} \left[ 7.9851 - 1 - \ln(2(7.9851) - 1) + \frac{2.2 - 1}{4.4} \left( \ln(7.9851 - 1) + 0.39 - \frac{0.61}{2.2} \right) \right] 0.5 = 1.64 \text{ mm.}$$

The length is determined from the following relationship:

$$L_f = 3(0.5) = 1.5 \text{ mm.}$$

To match the impedance between the transmission line and the radiating patch, the proposed single patch antenna use a quarter wave transformer for impedance matching. Transmission line sections for a quarter wave transformer have a length of a quarter of the guided wavelength ( $\lambda_g/4$ ) to match a transmission line to a certain load. The impedance of a quarter wave transformer is given as:

$$Z_{\text{qwt}} = \sqrt{Z_a Z_0}, \quad (3.2)$$

where  $Z_a$  is the impedance of the patch and is given by:

$$Z_a = 90 \frac{\epsilon_r^2}{\epsilon_r - 1} \left( \frac{L}{W} \right)^2. \quad (3.3)$$

The width and length of a quarter wave transformer are given by equations 3.4 and 3.5 respectively.

$$Z_{\text{qwt}} = \frac{60}{\sqrt{\epsilon_{\text{reff}}}} \ln \left( \frac{8h}{W_m} + \frac{W_m}{4h} \right). \quad (3.4)$$

The length of the quarter wave transformer is given as:

$$L_m = \frac{\lambda}{4\sqrt{\epsilon_{\text{reff}}}}, \quad (3.5)$$

where  $\lambda$  is the free space wavelength.

For the single patch antenna designed with RT/Duroid 5880 substrate, the impedance of the quarter wave transformer is calculated using equation 3.2, where  $Z_0 = 50 \Omega$ . This is initiated by the calculation of  $Z_a$  and this is given as:

$$Z_a = 90 \frac{2.2^2}{2.2 - 1} \left( \frac{3.05}{4.232} \right)^2 = 205.68 \Omega. \quad (3.6)$$

Therefore the impedance of the quarter wave transformer is

$$Z_{\text{qwt}} = \sqrt{50(205.68)} = 101.41 \Omega.$$

The calculated values of  $W_m$  and  $L_m$  are 0.304 mm and 1.917 mm respectively. Furthermore, the above calculations have resulted in the design dimensions of the single rectangular patch using a RT/Duroid 5880 substrate and summarized in Table 3.1.

Table 3.1: Dimensions of the single patch antenna using RT/Duroid 5880 substrate.

Parameter	Symbol	Dimension (mm)
Patch length	$L$	3.28
Patch width	$W$	4.232
Width of transmission line	$W_f$	1.64
Length of transmission line	$L_f$	1.5
Width of QWT	$W_m$	0.304
Length of QWT	$L_m$	1.917
Ground plane length	$L_g$	6.28
Ground plane width	$W_g$	7.232

### Summary on the designs using FR-4 and RO3003 substrates

The designs of single rectangular patch antennas using FR-4 and RO3003 as dielectric substrates follow the same design procedure used in the design of a rectangular patch antenna with a RT Duroid substrate and their geometry is also similar to the one illustrated by Figure 3.1. The calculated design dimensions of a single rectangular patch antenna using FR-4 and RO 3003 as dielectric substrates are presented in Table , respectively.

Table 3.2: Dimensions of the single patch antenna using RT Duroid and FR-4 substrates.

Parameter (mm)	Symbol	Dielectric Substrate	
		FR-4	RO 3003
Patch length	$L$	2.228	2.9927
Patch width	$W$	3.2909	3.7881
Width of transmission line	$W_f$	1.34	1.11
Length of transmission line	$L_f$	1.76	1.32
Width of QWT	$W_m$	0.33	0.201
Length of QWT	$L_m$	1.81	1.783
Ground plane length	$W_g$	7.0228	4.4927
Length of QWT	$L_g$	8.0909	5.2881

## 3.3 Simulation Results of the Single Patch Antenna

Simulations below are carried out using CST microwave studio. CST studio suite is a high-performance three dimensional (3D) electromagnetic (EM) analysis software for designing, simulating and optimizing electromagnetic systems.

### 3.3.1 Reflection Coefficient

The reflection coefficient of an antenna is indicated by the scattering parameter (S-Parameter) in this case  $S_{11}$ . This is the relation between the source and antenna during the operation of an antenna in a single-port circuit. As such, the reflection coefficient of the single rectangular patch antenna is measured from base value of -10 dB, which indicates that 10 % of the incident power is reflected and 90 % of the power is delivered to the antenna. Figure 3.2 illustrates reflection coefficients of the designed antennas using different substrates. As indicated by Figure 3.2, the rectangular patch antenna designed using FR-4 substrate has a reflection coefficient of -31.85 dB at frequency of 28.248 GHz and for the desired frequency (28 GHz), it has a reflection coefficient of -18.78 dB. For the R03003 patch, it illustrates a reflection coefficient of -15.66 dB at frequency of 28.592 GHz and for the desired frequency (28

GHz), it has a reflection coefficient of -10.9061 dB. The rectangular single patch antenna using RT/Duroid 5880 substrate has a reflection coefficient of -30.76 dB at 28 GHz. These results indicate that antenna designed using RT 5880 substrate operates at the desired frequency of 28 GHz whereas the other antennas designed using FR-4 and R03003 do not operate at the desired frequency.

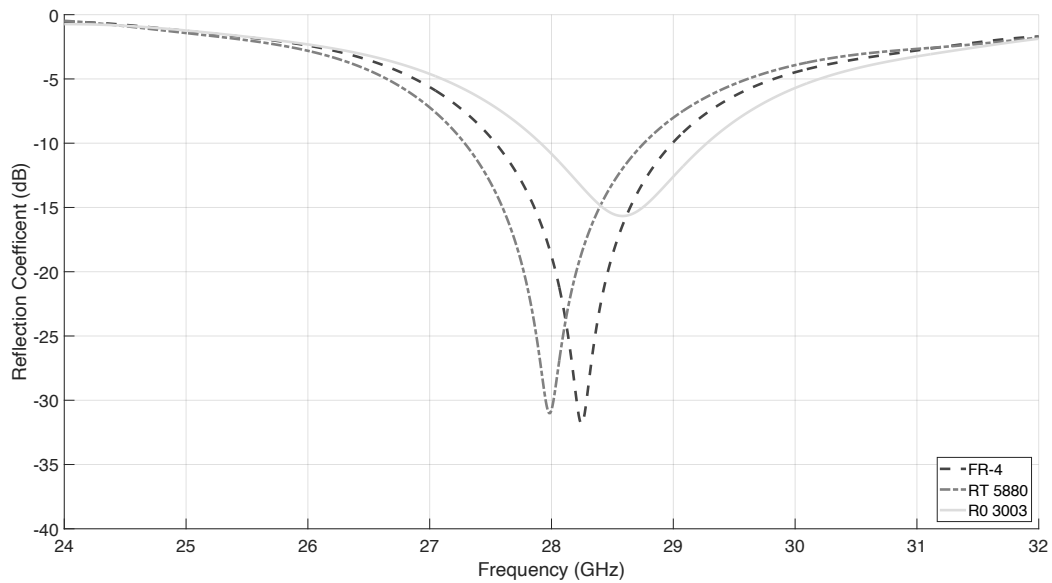


FIGURE 3.2: Comparison of reflection coefficient for antennas designed with different dielectric substrates.

From figure 3.2, the base value of -10 dB is used to calculate the bandwidth of the designed single rectangular patch antenna, which is obtained as the difference between highest frequency and lowest frequency at -10 dB. At -10 dB, the rectangular patch antenna designed using FR-4 substrate has a highest frequency of 28.99 GHz and lowest frequency of 27.52 GHz thus the antenna has a bandwidth of 1.44 GHz. For the rectangular patch antenna designed using RO3003 substrate, at -10 dB, it has a highest frequency of 29.272 GHz and lowest frequency of 27.912 GHz as such a bandwidth of 1.36 GHz. Finally, the rectangular single patch antenna designed using RT/Duroid 5880 substrate has a highest frequency of 28.748 GHz and lowest frequency of 27.289 GHz thus the antenna has a bandwidth 1.459 GHz

### 3.3.2 Voltage Standing Wave Ratio

In the case of a microstrip patch antenna, the voltage standing wave ratio (VSWR) should be less than 2 to indicate impedance matching between the patch and transmission line. The voltage standing wave ratio for the designed single patch antennas as a function of frequency is shown in Figure 3.3. As illustrated in Figure 3.3, the VSWR value obtained for a single patch antenna designed using RT/Duroid 5880 substrate equals 1.05968 at a resonance frequency of 28.00 GHz. For the R03003 single patch antenna, VSWR equals 1.8068. The rectangular single patch antenna using FR-4 substrate has a VSWR of 1.67612 at a resonance frequency of 28.00 GHz.

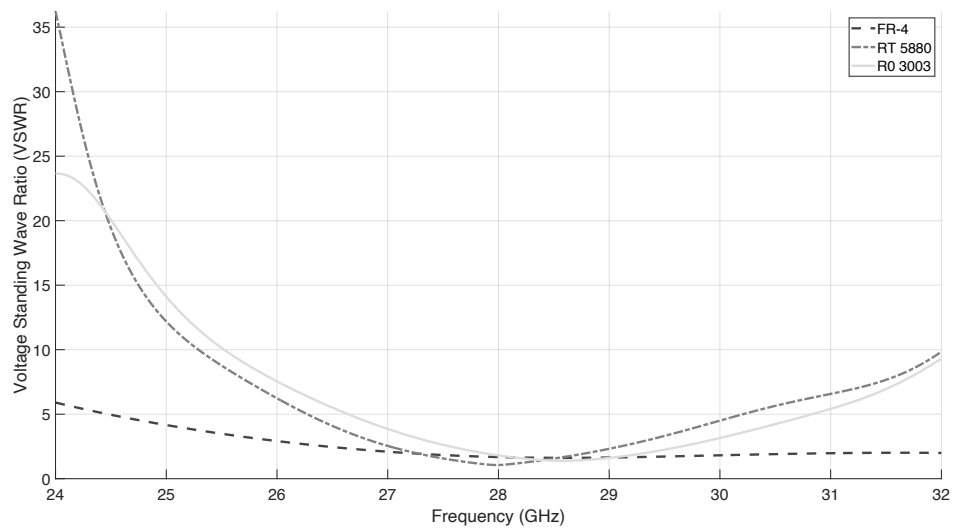
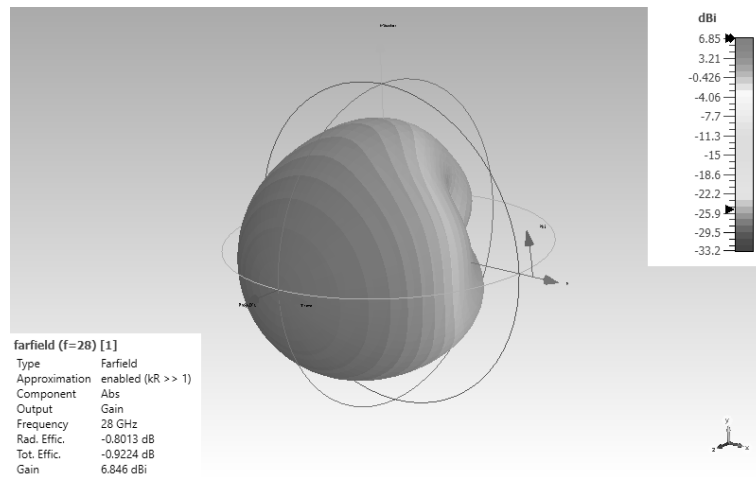


FIGURE 3.3: Comparison of VSWR for antennas designed with different dielectric substrates.

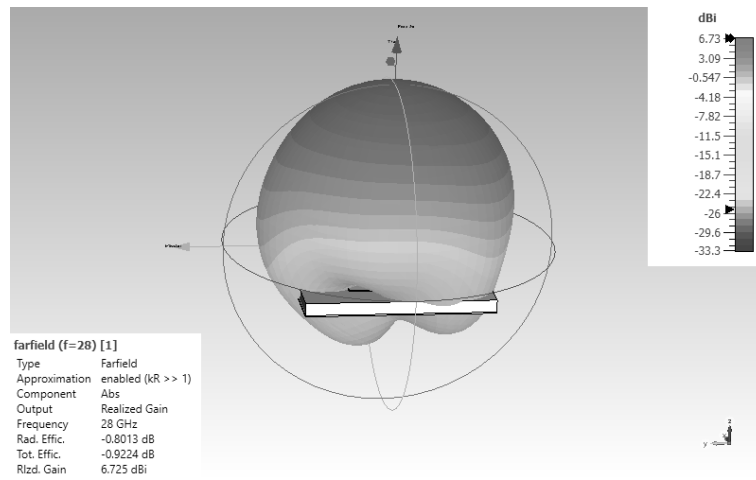
### 3.3.3 Far Field Pattern

The far field or radiation pattern of antenna represents a standardized distribution of the electric field, or the relative distribution of surface power density. Figure 3.4 to Figure 3.6 illustrates the far field plots of the designed rectangular patch antennas based on three different substrates. The far field plots of the patch antenna designed using a RT/Duroid 5880 are illustrated in Figure 3.4 both in one dimensional (1D) and three dimensional (3D). The Figure shows that the antenna has a gain of 6.846 dBi as illustrated by Figure 3.4a in 3D and realized gain of 6.74 dBi illustrated by 3.4b also in 3D. Furthermore, Figure 3.4c in 1D indicates that the antenna has a angular beam-width of  $78.1^\circ$  and side lobe level (SLL) of -11.5 dB. The far field plots of the patch antenna designed using a R0 3003 are illustrated in Figure 3.5 both in 1D and 3D. The Figure shows that the antenna has a gain of 6.252 dBi as illustrated by figure 3.5a in 3D and realized gain of 5.877 dBi illustrated by 3.5b also in 3D. Furthermore, Figure 3.5c in 1D indicates that the antenna has a angular beam-width of  $103.3^\circ$  and side lobe level (SLL) of -10.7 dB. Finally, the far field plots of the antenna designed using FR-4 are illustrated in Figure 3.6. The antenna has a gain of 3.275 dBi as illustrated by Figure 3.6a in 3D and realized gain of 2.47 dBi illustrated by Figure 3.6b also in 3D. The Figure indicates that the antenna has a angular beam-width of  $68.7^\circ$  and SLL of -7.6 dB. The gains of the designed antennas are referenced to an isotropic antenna and hence their units are expressed in dBi.

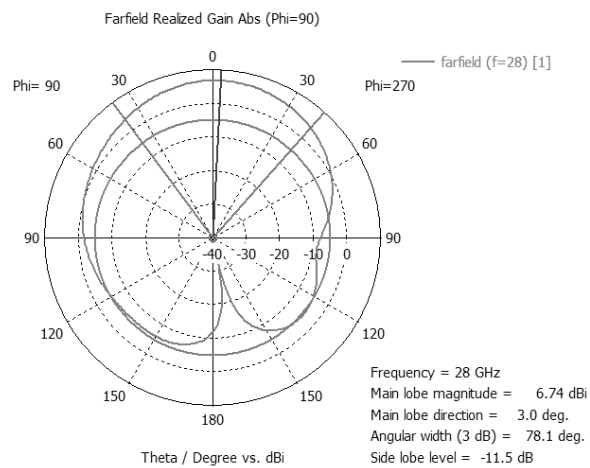




(a) Far field plot showing gain in 3D.

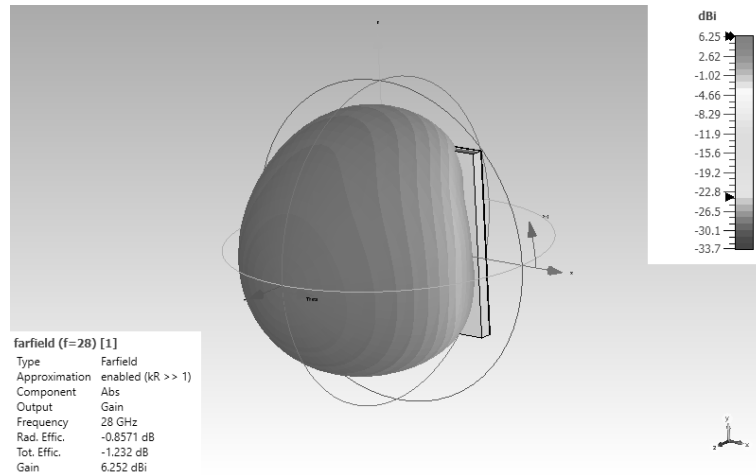


(b) Far field plot showing realized gain in 3D.

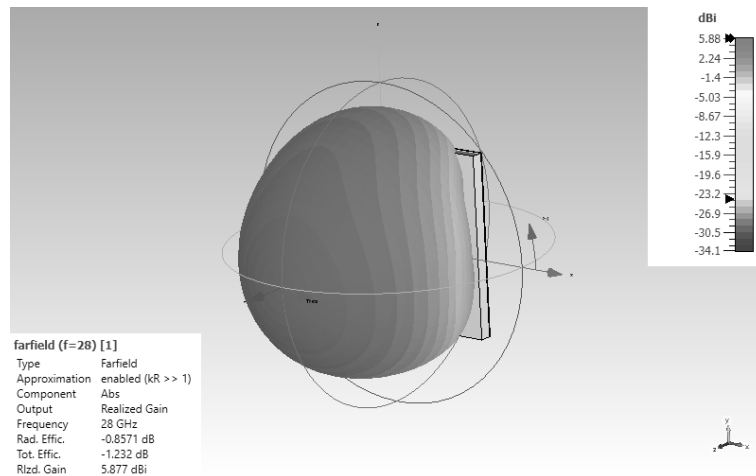


(c) Far field plot in 1D polar form.

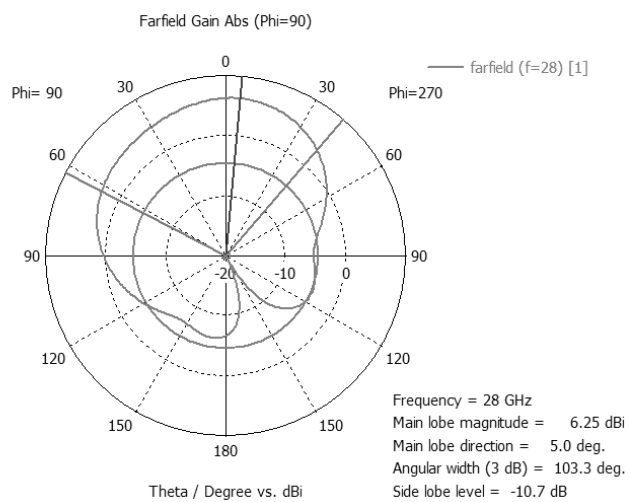
FIGURE 3.4: Far field plots of a single patch antenna using RT/Duroid 5880.



(a) Far field plot showing gain in 3D.

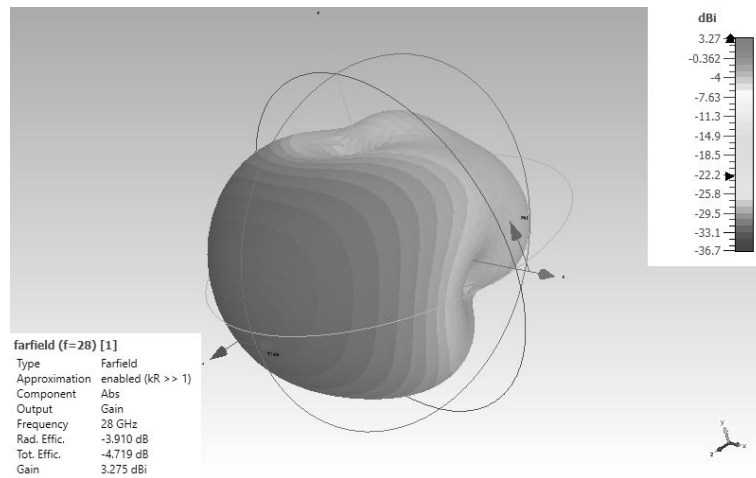


(b) Far field plot showing realized gain in 3D.

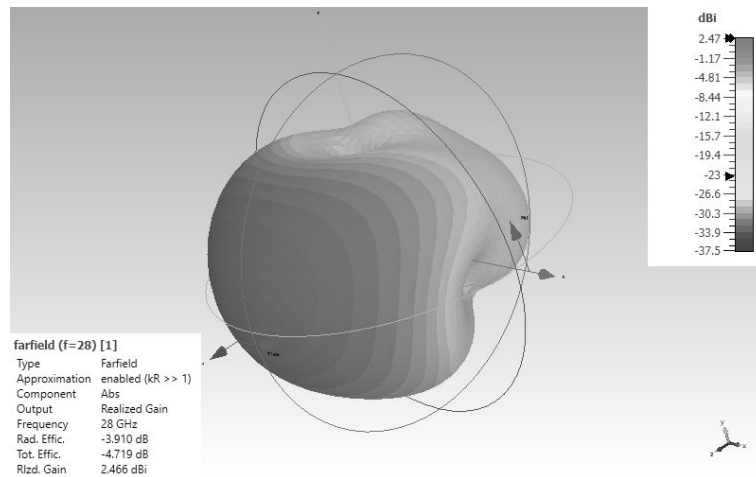


(c) Far field plot in 1D polar form.

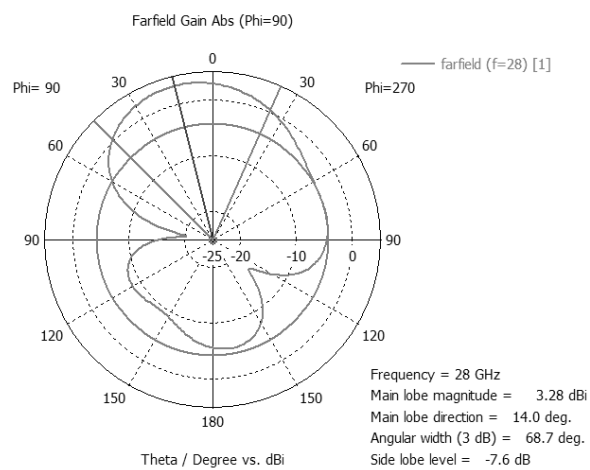
FIGURE 3.5: Far field plots of a single patch antenna using R0 3003 substrate.



(a) Far field plot showing gain in 3D.



(b) Far field plot showing realized gain in 3D.



(c) Far field plot in 1D polar form.

FIGURE 3.6: Far field plots of a single patch antenna using FR-4 substrate.

The above simulation results of the designed single rectangular patch antennas using three different substrates are presented in Table 3.3, summarizing the performance comparison of three designed antennas. From the results, the single patch antenna designed with RT 5880 substrate offers better antenna performance as compared to other designs hence it is chosen as the radiating element for the proposed phased array.

Table 3.3: Performance comparison for the three different dielectric substrates.

Parameter	Dielectric Substrate		
	RT/Duroid 5880	RO 3003	FR-4
Operating Frequency (GHz)	28.00	28.592	28.248
VSWR	1.05968	1.8068	1.67612
Gain (dB)	6.846	6.252	3.275
Realized Gain (dB)	6.74	5.877	2.466
Reflection Coefficient (dB)	-30.76	-10.9061	-15.664
Bandwidth (GHz)	1.459	1.36	1.44

The proposed single rectangular patch antenna is compared with existing single patch antennas for 5G applications. A comparative summary of the proposed antenna with the antennas described in literature is presented in Table 3.4. It shows that the proposed microstrip antenna in this work resonates well and it has good performance when compared to other published works.

Table 3.4: Comparison between the proposed single patch antenna with existing literature.

Ref	$S_{11}$ (dB)	Gain (dBi)	VSWR	Bandwidth (GHz)
[129]	-15.5	6.9	1.3	1.94
[120]	-39.3682	6.37	1.02	2.48
[116]	-22.51	5.06	1.162	5.57
[130]	-42	9.82	1	1.29
[131]	-17.4	6.72	1.2785	1.074
This work	-30.76	6.846	1.05968	1.459

### 3.4 Conclusion

This chapter presented the design and simulation of a single rectangular patch antenna operating at 28 GHz. The antenna was designed and analyzed based on three different dielectric substrates. From the simulations, the single patch antenna designed with RT/Duroid 5880 substrate offers better antenna performance as compared to other designs because it offered better VSWR, gain, reflection coefficient and bandwidth. As such, it was chosen as the radiating element for the proposed phased array.

## Chapter 4

# Phased Array Antenna Design

In the previous chapter, three single patch antennas were designed using three dielectric substrates. After antenna performance comparison, the single patch antenna designed using RT 5880 dielectric substrate was chosen as the radiating element for the proposed microstrip phased array antenna due to its n better performance . In this chapter, the framework for the design and performance of the proposed eight element microstrip phased array antenna for 5G wireless applications is presented. Firstly, a  $1 \times 4$  microstrip array antenna is designed and then, this array is used to design an eight element phased array antenna. To realize a phased array antenna, phase shifting concept is introduced at the excitation ports and beam steering is achieved. Finally, a dumbbell shaped defected ground structure (DGS) is introduced to the array for the reduction of mutual coupling effect in the array.

### 4.1 Introduction

Due to the rapid advances in wireless mobile communication technologies, services demanding high data rates have increased over the years. As such, the fifth generation (5G) of mobile communication has been launched to meet these demands and is currently receiving considerable attention. This mobile generation is envisioned to provide high data rates of gigabits per second, high cell edge rates of gigabits per second and reduced latency [11, 132]. One of the key technologies that enables the services of 5G systems is the use of millimeter wave frequency band [13]. The 3rd Generation Partnership Project (3GPP) 5G specification have arranged frequency bands in the millimeter wave band for 5G applications and these include 26 GHz, 28 GHz and 39 GHz bands [133]. However these bands are accompanied by limitations of signal path loss and propagation challenges [15, 21, 22]. Consequently, antenna arrays with high antenna gain are used to mitigate losses in the millimeter wave band without consuming any more power and cost [25–27]. The high antenna gain provided by antenna arrays provides a narrow radiation beam thus limiting the angular coverage. Therefore, phased array antennas are adopted due to their

electronic beam steering capability in desired directions [33].

Phased array antennas are used in various applications such radar, radio astronomy, internet of things (IoT), medical applications, mobile and satellite communications etc. Gradually, the advancements of component technology especially silicon over the years have made phased array antennas a very viable option for millimeter wave communications. Recently, there is a growing interest in applying phased array antennas for 5G wireless applications due to their electronic beam steering, high gain and beamforming capabilities. In this chapter, an eight element phased array antenna for 5G wireless applications operating at 28 GHz is designed. Initially a  $1 \times 4$  microstrip array antenna is designed and it is used to design the proposed eight element microstrip phased array antenna by duplicating it into another  $1 \times 4$  array. To realise a phased array antenna, these two  $1 \times 4$  array antennas are simultaneously feed by two excitation ports and phase shifting is introduced at these ports to achieve beam steering. A dumbbell shaped DGS is incorporated to the proposed phased array antenna to reduce mutual coupling between the radiating arrays. Finally, the simulation results of the proposed eight element phased array antenna are compared with the simulations of other works and a conclusion is presented.

### 4.1.1 Related Works

There are different designs of phased array antennas proposed for 5G wireless applications [134–144]. In [134] the authors proposed a millimeter wave beam steerable planar array for 5G mobile terminal applications. The array consisted of eight slot antenna units and fed by eight  $50 \Omega$  discrete ports. In simulation results analysis, the array gave  $S_{11}$  parameter less than -10 dB in the frequency range of 24.2-32 GHz and 37- 42.2 GHz. A millimeter wave phased array antenna with a switchable three dimensional (3D) coverage for 5G handset terminal application is presented in [138]. The antenna considered the effect of mutual coupling and was reduced. The 3D coverage was realized by having three subarrays of microstrip patch antennas along the upper edges of the mobile phone printed circuit board (PCB). The antenna elements present in each subarray were at distance of  $\lambda/2$  between one another and operated at a frequency of 28 GHz. For mutual coupling reduction between adjacent elements, notches between antenna elements were introduced on the ground plane and each element of the handset array was rotated by  $45^\circ$  along its axis. The proposed phased array was validated by simulation results which showed that mutual coupling was less -30 dB.

Cheng *et al.* in [136] presented the design of a low cost series feed beam steerable millimeter wave antenna for 5G mobile terminal operating at millimeter wave band. The geometry of the proposed array is a sandwich like structure with two layers of substrates. Ten uniformly distributed array elements were placed on the top layer and microstrip transmission feed line on the bottom layer. The proposed array did not use phase shifters nor power divider, rather switches located along the microstrip transmission feed line were utilised. The array achieved gain variation of 3 dB and steerable angle of  $121^\circ$ . In mobile terminals the diversity gain is improved by the use of multi-polarized antenna arrays to scrub the shortfall of polarization mismatch. The study in [145], proposed the design of a compact phased planar inverted-e antenna (PIEA) array with four antenna elements operating at a frequency of 6 GHz for 5G applications. The proposed array took into consideration mutual coupling effect and deployed three different mutual coupling techniques. These are dual shorting pins, which is modified planar inverted-f antenna (PIFA), making slots in the ground plane between array elements and making two slits in each of these etched slots. The proposed design reduced mutual coupling between antenna elements by -19 dB, produced a peak antenna gain of 8.36 dBi and maximum scan angle of  $\pm 70^\circ$ .

In [142], Nigam *et al.* proposed a four element phased array microstrip antenna for 5G applications operating in the 27-28 GHz frequency band. Initially a single antenna element was designed with a quarter wave transformer used for impedance matching. The proposed array composed of 8 ports to create more phase variations at the input enabling the creation of multiple beams in different directions. After simulation, the proposed array operated with an antenna gain of 13.7 dB and half power beamwidth (HPBW) of  $23.4^\circ$ . Authors in [140] proposed the design of a multi-polarized antenna array applicable for 5G mobile terminals. The phased array composed of 16 elements and was designed by alternatively deploying the two antenna elements along the edge of the mobile terminals. The proposed array was capable of providing real time configuration and polarization of antenna elements to achieve maximum quality of service (QoS).

### 4.1.2 Contributions

Some of the discussed designs in the previous subsection, for example [135–137] do not account for mutual coupling effect in their operation. This thesis proposes an eight element phased array antenna for 5G wireless applications operating at 28 GHz. This work is motivated by [135]. Unlike the work in [135], this work uses

corporate feed network for feeding the radiating patches and considers mutual coupling effect between the radiating arrays. This chapter presents the following contributions:

- Design and simulation of an eight element phased array antenna operating at 28 GHz with dum bell shaped DGS to reduce mutual coupling between the radiating arrays.

## 4.2 Four Elements Array Design

The overall performance of a single antenna can be improved by duplicating into an array configuration. In this thesis, the designed single patch antenna using RT Duroid 5880 substrate is arranged into  $1 \times 4$  array antenna as illustrated by Figure 4.1 to increase its gain and overall performance. The  $1 \times 4$  array configuration uses corporate feeding network due to its advantages over series feed network to feed the radiating patches and as such, new design parameter such as the space between the radiating patches is considered. Furthermore, the parameters used in the design of a single rectangular patch antenna such as the size of radiating patch, dielectric substrate and its height and impedance matching technique remain unchanged. The proposed  $1 \times 4$  microstrip array is excited by symmetrical 1D corporate feeding network with a quarter wave transformer for impedance matching between the feed lines. The microstrip feed line is connected to a  $50 \Omega$  input port source and therefore has characteristic impedance of  $50 \Omega$  ( $Z_0 = 50 \Omega$ ). At the T-junction, the  $50 \Omega$  microstrip line splits into two microstrip lines as illustrated by Figure 4.1. As a result, the resulting characteristic impedance's of the two lines are given as follows:

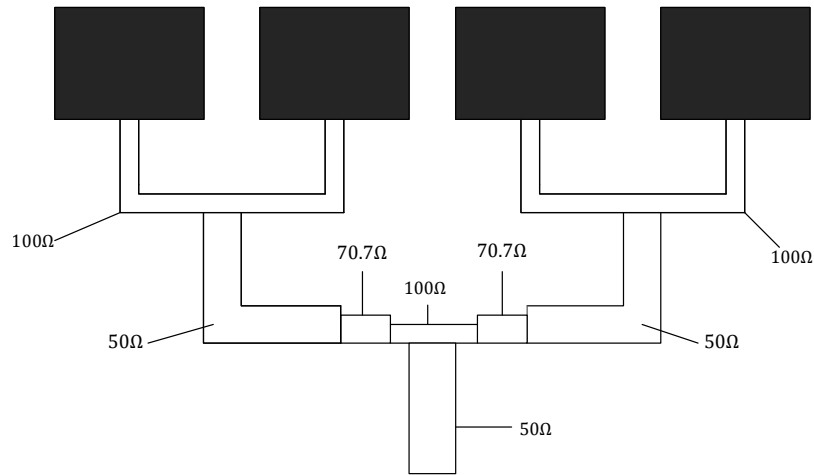
$$Z_1 = 50n \quad (4.1)$$

where the factor  $n$  is the number of microstrip transmission lines at the T-junction. This results in the two lines having a characteristic impedance of  $100 \Omega$ . Furthermore, the distance between the radiating patches is kept at  $0.5\lambda$ . The dimensions of feed-lines of the array are calculated in the same way as in chapter 3 of this thesis and are presented in table 4.1 .



Table 4.1: Dimensions of the  $1 \times 4$  array antenna.

Parameter	Symbol	Dimension (mm)
Patch length	$L$	3.28
Patch width	$W$	4.232
Width of $50 \Omega$ transmission line	$W_{50\Omega}$	1.64
Length of $50 \Omega$ transmission line	$L_{50\Omega}$	3.0
Width of $100 \Omega$ transmission line	$W_{100\Omega}$	0.50
Length of $100 \Omega$ transmission line	$L_{100\Omega}$	0.438
Width of $70.7 \Omega$ line (Quarter wave transformer)	$W_m$	0.98
Length of $70.7 \Omega$ line (Quarter wave transformer)	$L_m$	1.805
Ground plane length	$L_g$	6.28
Ground plane width	$W_g$	7.232

FIGURE 4.1: The designed  $4 \times 1$  array antenna.

### 4.2.1 Simulation Results of Four Elements Array Antenna

The simulation results of  $1 \times 4$  microstrip array antenna are also carried out using CST microwave studio suite and the results of the array are shown in Figure 4.2 to Figure 4.5.

#### Reflection Coefficient

The reflection coefficient of the antenna array is measured the same way as in a single patch antenna. The designed  $1 \times 4$  array antenna operates at a frequency of 28.25 GHz with a reflection coefficient value  $S_{11}$  of -31.85 dB as illustrated in Figure 4.2. The base value of -10 dB is used to calculate the bandwidth of the proposed

antenna, which is obtained as the difference between highest frequency and lowest frequency at -10 dB. For this designed array antenna, the obtained bandwidth is 1.47 GHz. This result is an increment since the single patch antenna has a bandwidth of 1.46 GHz. Furthermore, this proves that the impedance is well matched by the quarter wave transformer and thus the power is divided equally at the junctions.

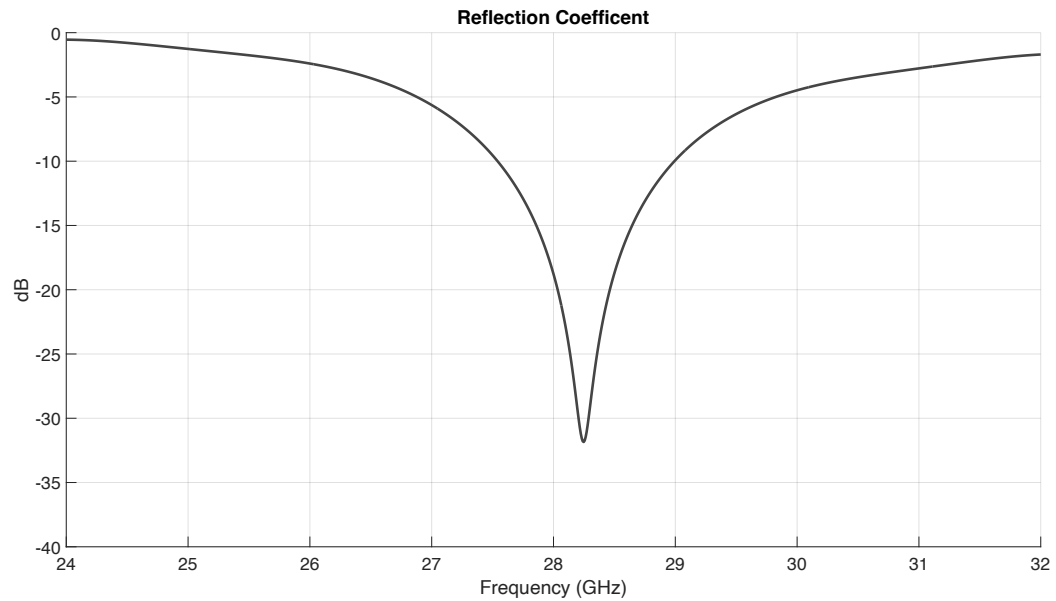


FIGURE 4.2: Reflection coefficient of the four element array antenna.

## VSWR

The simulated VSWR of the  $1 \times 4$  array antenna is shown in Figure 4.3, and VSWR is observed at an operating frequency of 28 GHz, the array has a VSWR of 1.26.

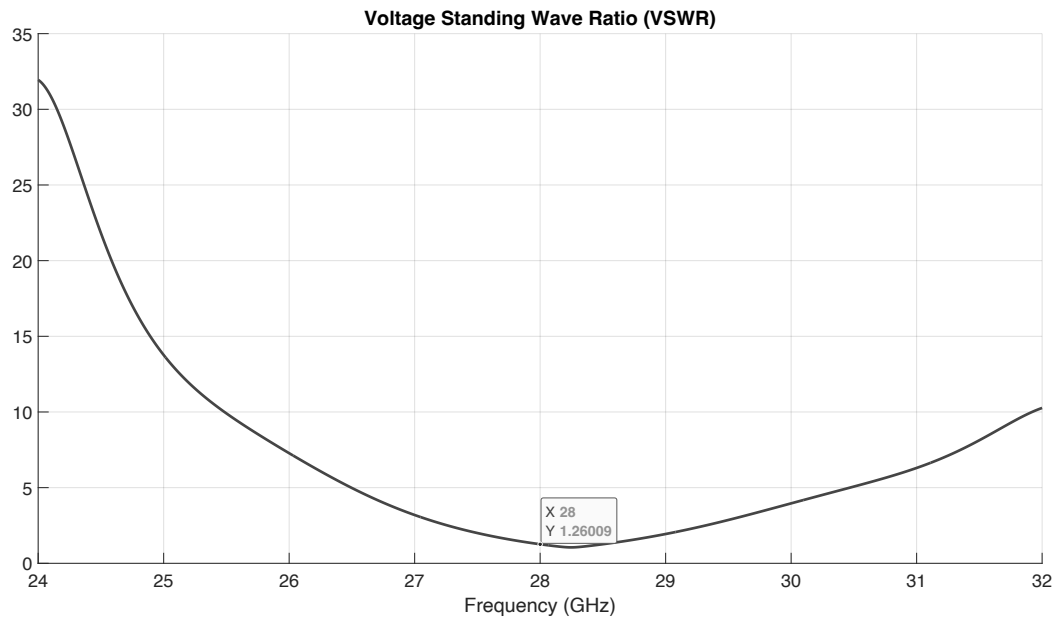


FIGURE 4.3: VSWR of the four element array antenna.

## FarField

The far field plots of the designed  $1 \times 4$  array antenna are illustrated in Figure 4.5 both in 1D and 3D indicating that the array antenna has a directive radiation pattern. The figure shows that the array antenna has a gain of 10.8 dBi as illustrated by Figure 4.5a in 3D and realized gain of 6.68 dBi illustrated by 4.5b also in 3D. Also, Figure 4.5c in 1D indicates that the antenna has a angular beam-width of  $18.7^\circ$  and side lobe level of -1.4 dB. Furthermore, radiation pattern plot illustrated in 4.4 indicates that the designed antenna has directivity of 11.5 dBi

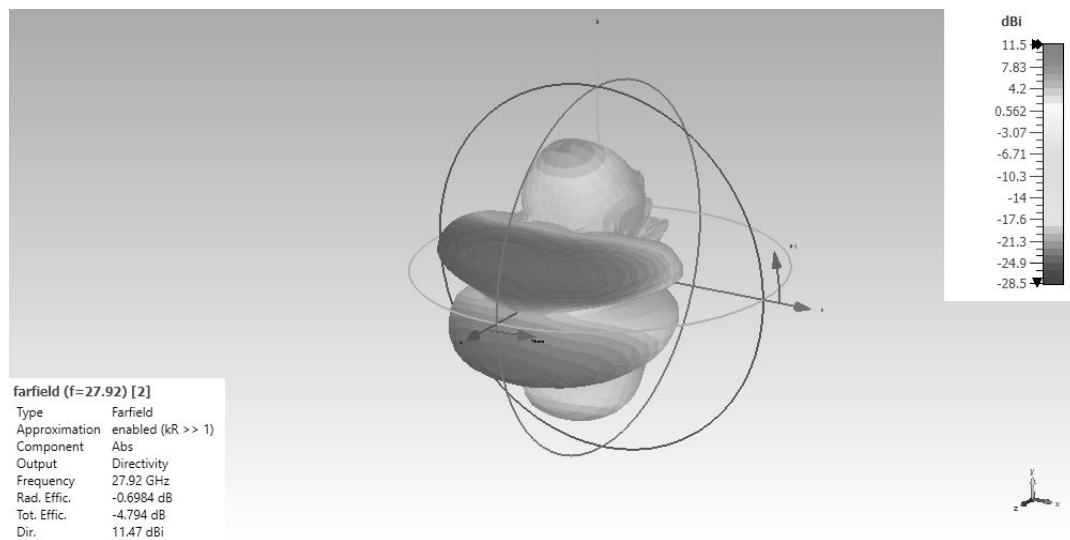
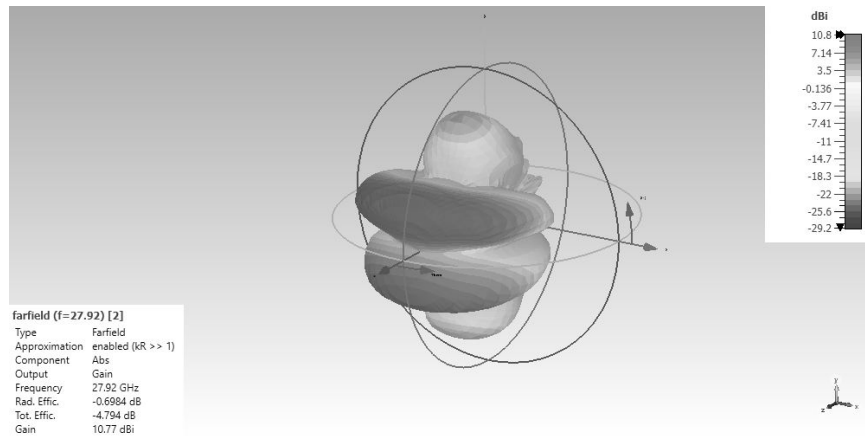
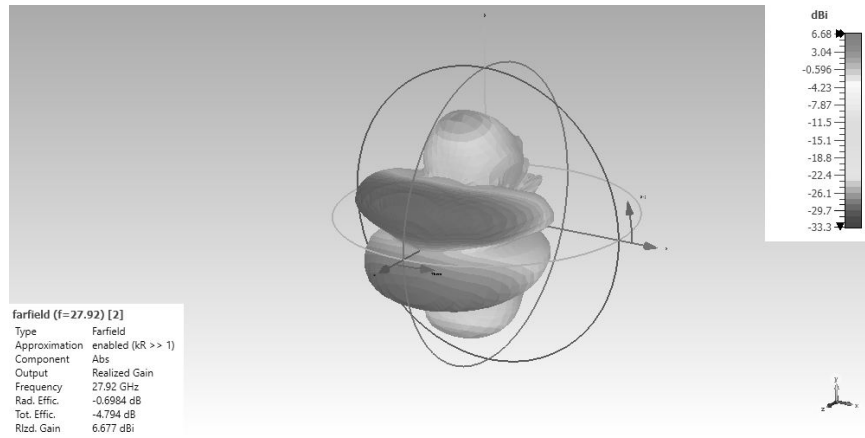


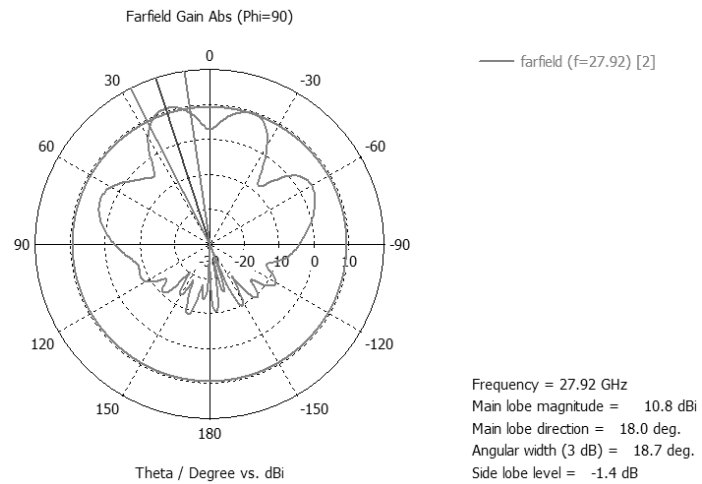
FIGURE 4.4: Directivity of the antenna array in 1D.



(a) Far field plot showing gain in 3D.



(b) Far field plot showing realized gain in 3D.



(c) Far field plot in 1D polar form.

FIGURE 4.5: Far field plots of  $1 \times 4$  array antenna.

### 4.3 Eight Elements Phased Array Antenna Design

In this section, the design process and simulation results of an eight element phased array antenna are presented. Figure 4.6 illustrates the antenna array configuration with eight radiating patches. As shown in the figure, the array uses two identical  $1 \times 4$  antenna arrays with two simultaneous feeding ports. These ports are used to achieve beam steering and measure mutual coupling of the antenna array. In this array, all design parameters used in the design of  $1 \times 4$  antenna array remain unchanged.

#### 4.3.1 Results Analysis of the Designed Antenna

The simulation results of eight element phased array antenna are also carried out using CST microwave studio suite. Figure 4.6 illustrates the designed array on the CST software layout and the results of the array are shown below.

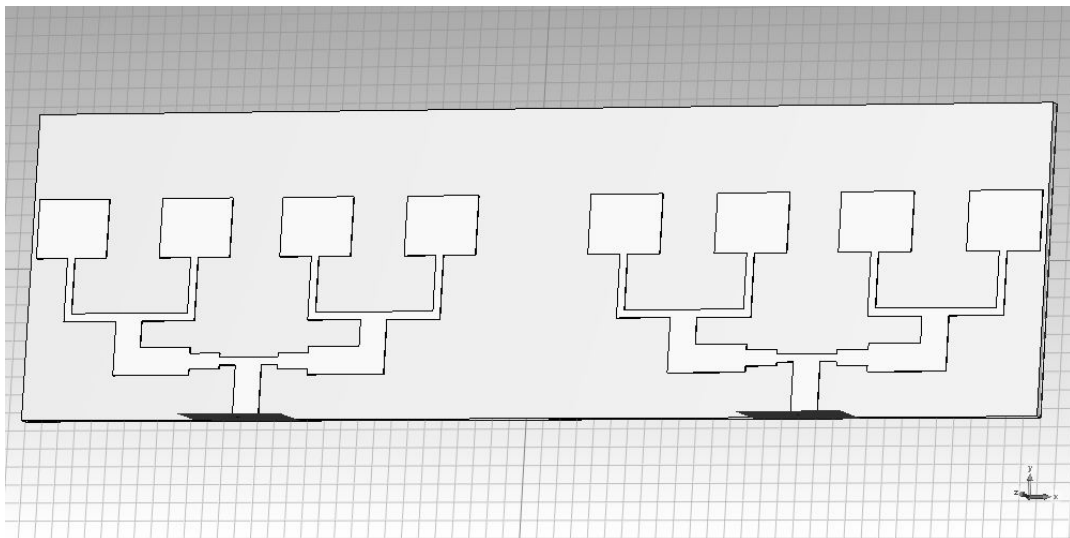


FIGURE 4.6: The simulated eight element phased array antenna in a CST software layout.

### Reflection Coefficient

The S-parameters of the proposed phased array antenna are measured as in  $1 \times 4$  array and are illustrated in Figure 4.7. On the contrary, this array has two excitation ports which work simultaneously to feed the radiating patches thus results in the array having four S-parameters. These are  $S_{11}$ ,  $S_{22}$ ,  $S_{12}$  and  $S_{21}$ .  $S_{11}$  and  $S_{22}$  indicate the reflection coefficient of the array whereas  $S_{12}$  and  $S_{21}$  indicate the relation between the two arrays (mutual coupling). As shown by Figure 4.7,  $S_{11}$  is equal to  $S_{22}$  shown by a magenta dashed line in the figure, this indicates that there is simultaneously feeding of the array. Moreover,  $S_{12}$  is equal to  $S_{21}$  to indicate the existence of mutual coupling between the two  $1 \times 4$  antenna arrays as shown by the blue solid line in the figure. The proposed antenna array indicates reflection coefficient of -40.19 dB at 28.28 GHz. The mutual coupling observed between the arrays is -27.97 dB at 28 GHz. Furthermore, the proposed phased array antenna offers below -10 dB impedance bandwidth between 27.51 GHz and 29.02 GHz with an overall bandwidth of 1.51 GHz.

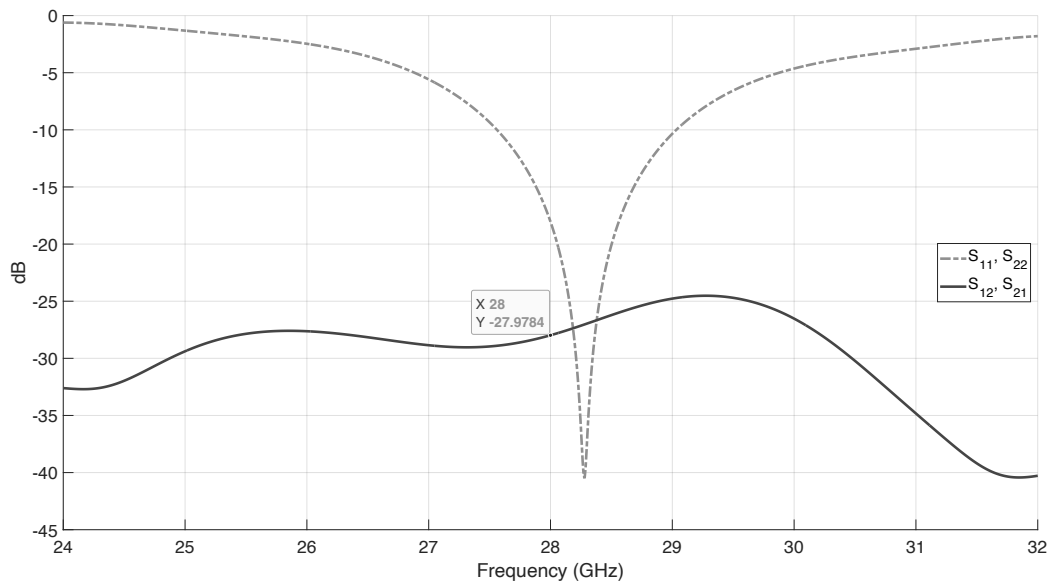


FIGURE 4.7: Reflection coefficient and mutual coupling of the proposed antenna.

### VSWR

VSWR of the eight element phased array antenna is shown in Figure 4.8. As depicted in Figure 4.8, at an operating frequency of 28 GHz, the proposed phased array has a VSWR of 1.38.

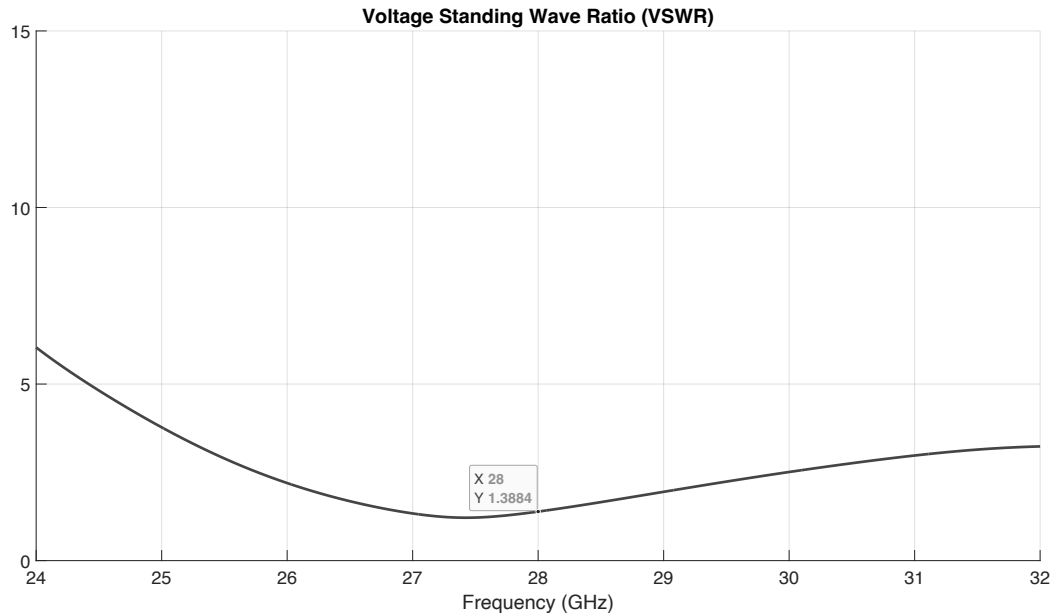
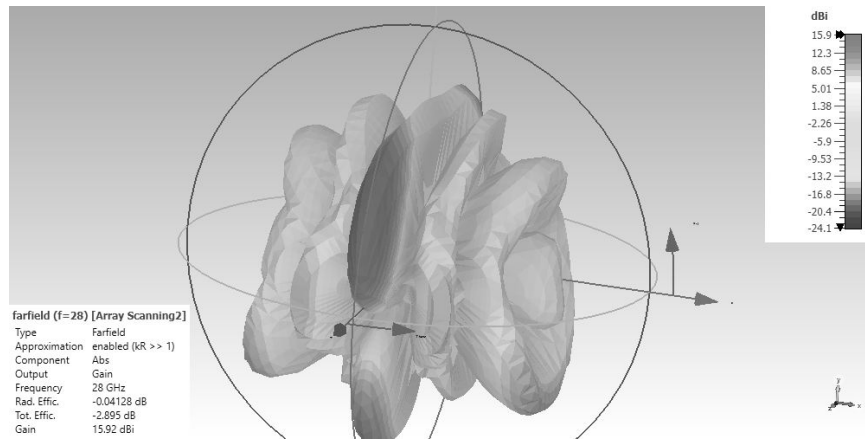


FIGURE 4.8: VSWR of the phased array antenna.

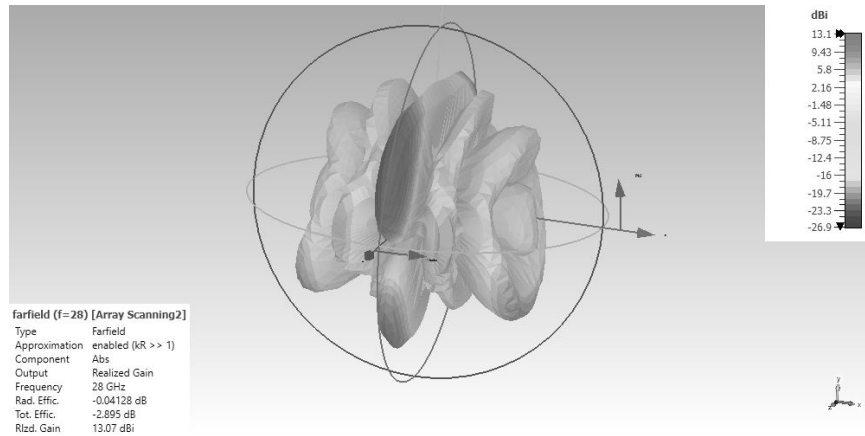
### FarField

The radiation pattern of the proposed phased array antenna is illustrated in Figure 4.9. Before determining the scan angle of the phased array antenna or before beam steering is carried out, the main lobe is not maximum at  $\theta = 0^\circ$  rather the main lobe is shifted to the left side (y-axis) by a few degrees. As shown in the figure, the phased array antenna has a gain of 15.92 dBi as illustrated by Figure 4.9a in 3D and realized gain of 13.07 dBi illustrated by Figure 4.9b also in 3D. There is a significant increase on the antenna gain due to many radiating elements as compared to the  $1 \times 4$  array antenna. Also, Figure 4.5c in 1D indicates that the antenna has a angular beam-width of  $23.0^\circ$  and side lobe level of -3.3 dB. As shown in the figure, the antenna has big side and back lobes. This is caused by the coupling effect which exist in array enhanced by the presence of surface waves. Furthermore, radiation pattern plot illustrated in Figure 4.10 indicates that the designed antenna has directivity of 16 dBi.

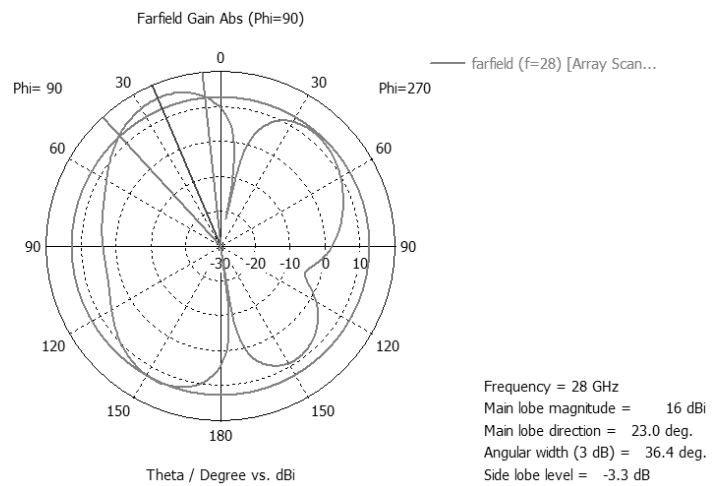




(a) Far field plot showing gain in 3D.



(b) Far field plot showing realized gain in 3D.



(c) Far field plot in 1D polar form.

FIGURE 4.9: Far field plots of the phased array antenna before beam steering.

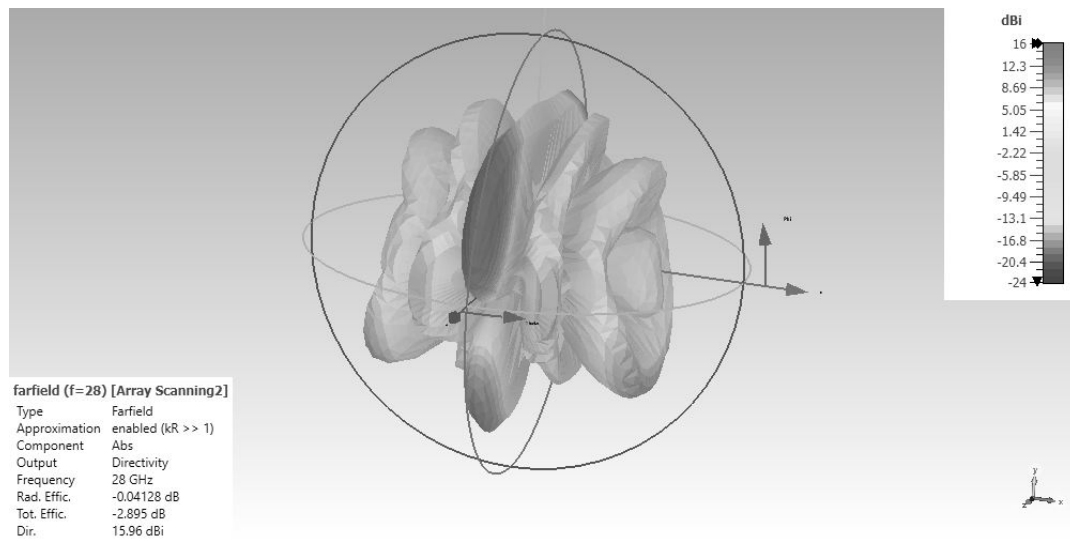


FIGURE 4.10: Directivity of the phased antenna array in 3D.

### Beam Steering

Over the years there has been broad deployment of phased array antennas in modern wireless applications due to their advantages which include the ability to rapidly and accurately scan beams from the broadside to the desired direction. In practical applications, phase shifting in phased array antennas is achieved through the use of digital phase shifters to steer the main beam in desirable directions. In this chapter, phase shifting is carried out at the excitation ports by manipulating the phase of the ports. The proposed phased array antenna use a uniform excitation distribution with excitation amplitudes to each radiating are constant with an average power of 0.5 W. In order to investigate the scanning performance and determine the scan angle of the proposed phased array antenna, the main beam is steered as illustrated in Figure 4.11 with a range from  $0^\circ$  to  $180^\circ$ . As shown by the figure, the gain (dB) is plotted versus theta (degrees) in Cartesian plane. The antenna achieved a scan angle of  $\pm 41^\circ$  with a scan loss of 3.3 dB as it is scanned from  $15^\circ$  to  $90^\circ$ . As the antenna is scanning, there is a decrease in antenna gain due to the increase of side-lobes and appearance of nulls at some angles. In conclusion, this proposed phased array antenna has a very limited scan angle meaning that it is not able to steer the radiation beam to certain directions.

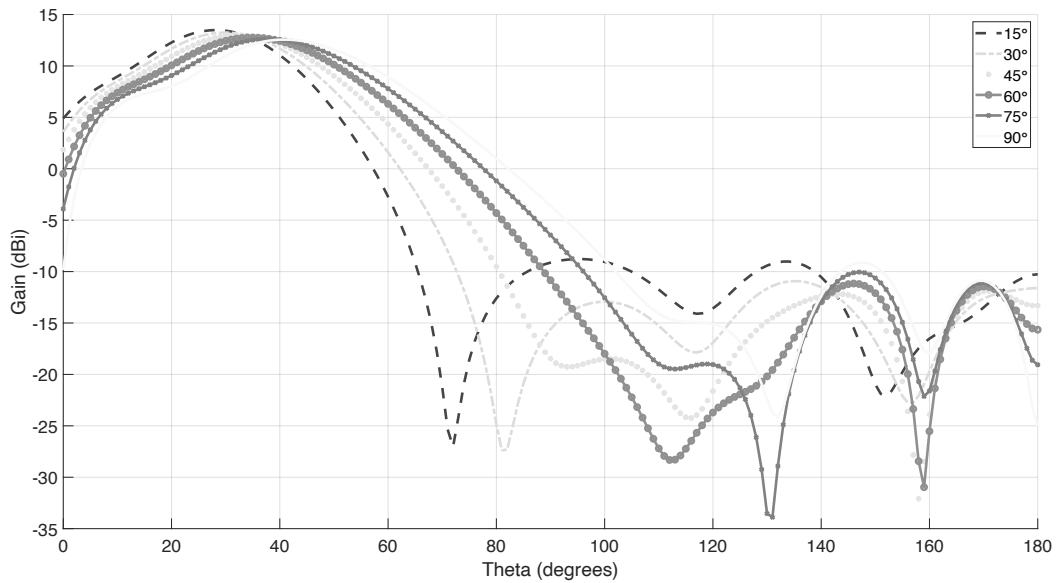


FIGURE 4.11: Beam steering performance of the antenna without DGS.

### 4.3.2 Mutual Coupling Reduction

Mutual coupling in antenna arrays is an undesirable phenomenon because it distorts the radiating behaviour of the elements in the array thus negatively affecting the overall array performance. Mutual coupling between array elements occurs due to space and surface waves. In antenna arrays which use microstrip patch antennas as elements, mutual coupling is increased mostly by the existence of surface waves. This is because microstrip patch antennas use thick dielectric substrates and this excites surface waves reflecting off the ground plane. Mutual coupling causes scan blindness and reduces scan range in phased array antennas. Over the years, many methods have been developed to reduce mutual effects between array elements. This includes, usage of electromagnetic band gap (EBG) [72, 76, 77, 146–149], parallel coupled-line resonators [150], metamaterials [83–85, 151], frequency selective surface (FSS) [152], active element pattern method [89], defected ground structures (DGS) [80–82, 153–155] and many different methods.

Some of the aforementioned methods for reducing mutual coupling are considered costly and impractical to implement particularly when dealing with surface waves. Therefore, in this chapter, a dumbbell shaped DGS is used to reduce mutual coupling effect between radiating elements. This is because DGSs are comparably easy to design and fabricate and their equivalent

circuits are easy to realize [41]. The proposed dumbbell shaped DGS for the eight element phased array antenna is illustrated in Figure 4.12. It consists of a slot width ( $g$ ), dumbbell head ( $a$ ) and slot length between the dumbbell ( $d$ ). The dumbbell DGS is placed between the two adjacent  $1 \times 4$  arrays of the proposed phased array antenna to suppress the pronounced mutual coupling. The overall dimensions of the DGS are  $a = 2$  mm,  $d = 1.64$  mm,  $s = 0.4$  mm and  $g = 2$  mm. The dimension of the designed dumbbell shaped DGS are derived from trial and error method. This because there is no clear analytical procedure to derive DGS dimensions in the millimeter wave band. The authors in [156] proposed an analytical procedure to derive dimensions of dumbbell shaped DGS used in a microstrip antenna arrays based on a genetic algorithm. The authors presented a mathematical formula to calculate the slot head ( $a$ ). The limitation with this proposed formula is that, it beneficial for low frequencies (sub 6 GHz) but for this proposed work, the formulas are not favourable because the designed phased array antenna operates at 28 GHz hence the calculated value of ( $a$ ) is very small and hence not usable. Therefore a trial and error method was adopted. The value of  $d$  is equal to the width of the microstrip feedline,  $g$  was selected between 0.2 - 0.5 mm and  $a$  is equal to  $b$ .

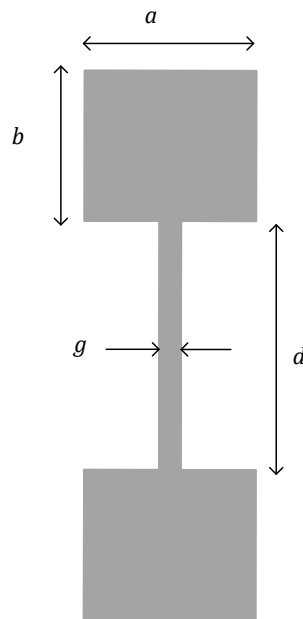


FIGURE 4.12: Dumbbell shaped DGS.

### 4.3.3 Simulation of Phased Array Antenna with DGS.

#### Reflection Coefficient

The magnitude of S-parameters ( $S_{11}$ ,  $S_{22}$ ,  $S_{12}$  and  $S_{21}$  in dB) versus frequency (GHz) of the the proposed eight element phased array antenna with a dumbbell shaped DGS is illustrated in Figure 4.13. The figure indicates that the insertion of a dumbbell shaped DGS between the two arrays reduces mutual coupling by 6.27 dB, that is a reduction from -27.97 dB to -34.24 dB at 28 GHz. There is a frequency shift in the operating frequency as compared to the phased array antenna without dumbbell shaped DGS. This is due to the slow-wave effects of dumbbell shaped DGS. As shown in the figure, the antenna has a reflection coefficient of -27.22 dB at a frequency of 28.37 GHz. Furthermore, the proposed phased array antenna offers below -10 dB impedance bandwidth between 27.6 GHz and 29.21 GHz with an overall bandwidth of 1.61 GHz. This indicates that there is an increment of antenna bandwidth. An increment in bandwidth, indicates that range of frequencies over which the antenna can operate correctly has improved thus an improvement in the overall system.

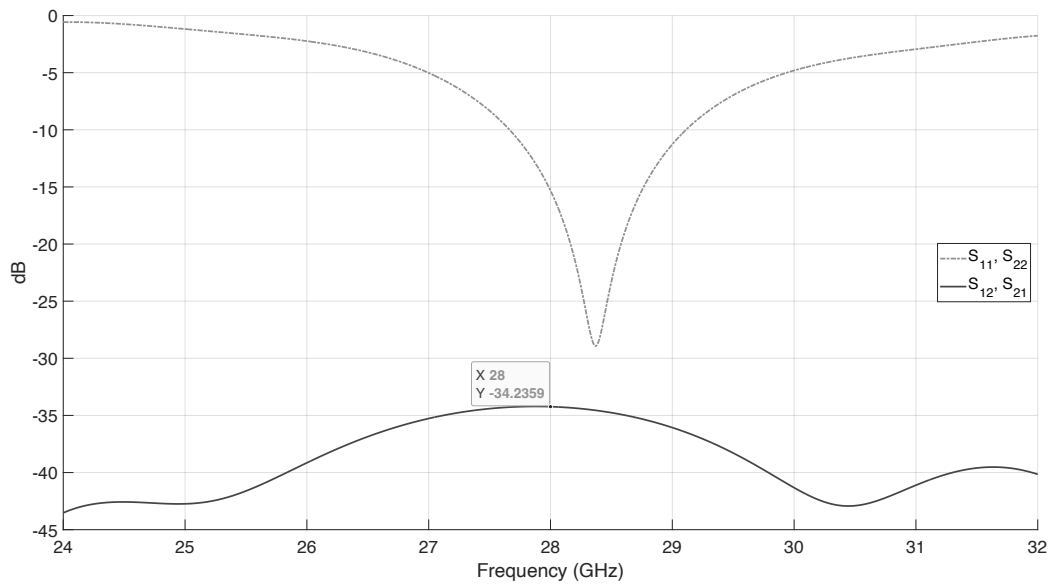


FIGURE 4.13: Reflection coefficient and mutual coupling of the phased array antenna with dumbbell DGS.

## VSWR

The simulated VSWR of phased array antenna with a dumbbell shaped DGS is shown in Figure 4.8. The figure illustrates that, at an operating frequency of 28 GHz, phased array has a VSWR of 2.1. This indicates that there is a loss occurring in the antenna due to the defects made to the antenna configuration. Furthermore, the losses are enhanced by changing the boundary setting of the ground plane (Z minimum) to be open instead of closed in the CST software. Therefore the dumbbell DGS becomes a radiator and bring more losses to the antenna.

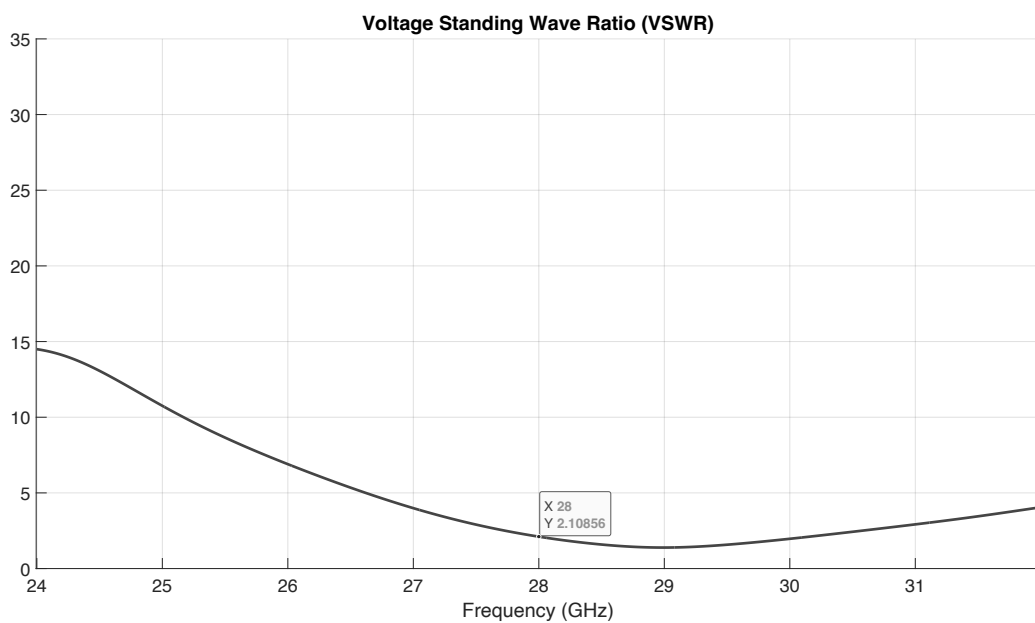


FIGURE 4.14: VSWR of the phased array antenna with dumbbell shaped DGS.

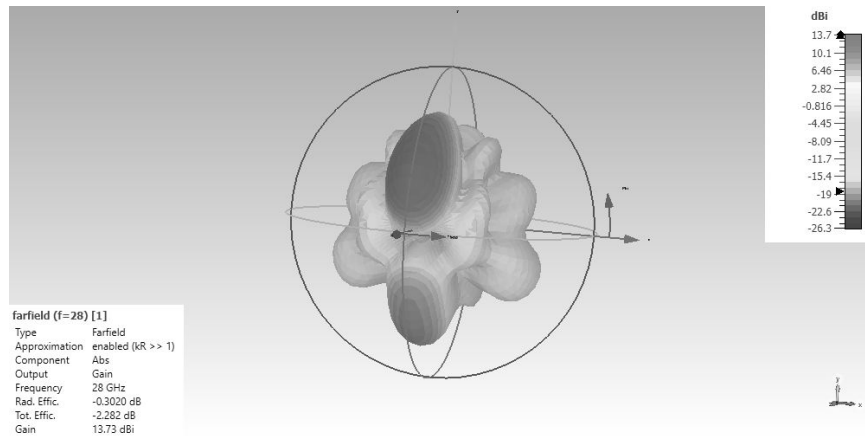
## FarField

The farfield patterns of the proposed phased array antenna with a dumbbell shaped DGS is illustrated in Figure 4.15. Before determining the scan angle of the phased array antenna or before beam steering is carried out, the phased array antenna has a gain of 13.73 dBi as illustrated by Figure 4.9a in 3D and realized gain of 11.75 dBi illustrated by Figure 4.9b also in 3D. There is a significant decrease in the antenna gain due to the increased back lobes. This a setback because a reduction in antenna gain indicates a decrease in antenna coverage. Also, Figure 4.5c in 1D indicates that the antenna has a angular beam-width of  $35.4^\circ$  and side lobe level of -4.0 dB. As

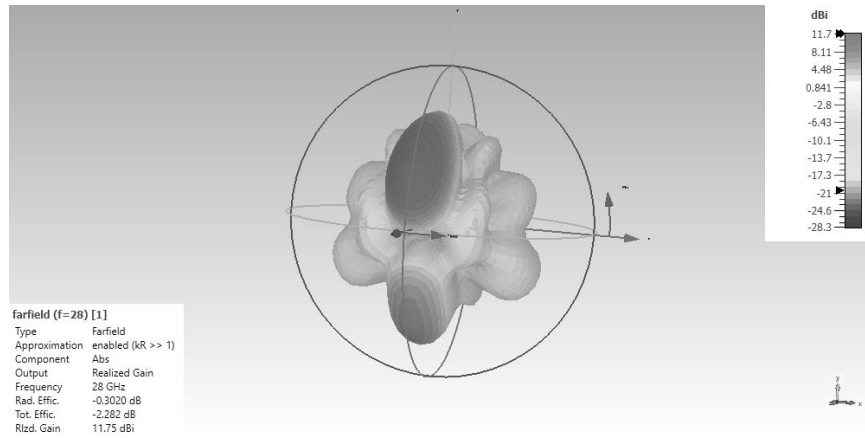
shown in the figure, the antenna has big side and back lobes. Furthermore, radiation pattern plot illustrated in Figure 4.10 indicates that the designed antenna has directivity of 14 dBi.

### **Beam Steering**

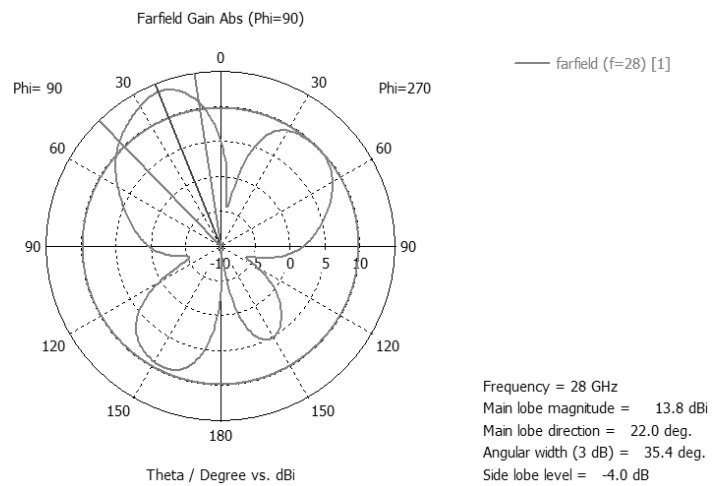
The scanning performance of the proposed phased array antenna with dumbbell shaped DGS is illustrated with a range from  $0^\circ$  to  $180^\circ$  in Figure 4.17. As shown by the figure, the gain (dB) is plotted versus theta (degrees) in Cartesian plane. From the figure, the antenna achieved a scan angle of  $\pm 35^\circ$  with a scan loss of 0.5 dB. This is a decrease in beam scanning performance as compared to the antenna without DGS. This antenna also has a very limited scan angle. As the antenna is scanning, there is a decrease in antenna gain due to the increase of grating lobes and appearance of nulls at some angles. Grating lobes are unwanted lobes because they have larger amplitudes which almost equal to the one of main lobe. Based on the results, simulations it is illustrated that insertion of dumbbell DGS did not bring merits to far-zone radiation patterns related parameters.



(a) Far field plot showing gain in 3D.



(b) Far field plot showing realized gain in 3D.



(c) Far field plot in 1D polar form.

FIGURE 4.15: Far field plots of the phased array antenna before beam steering.



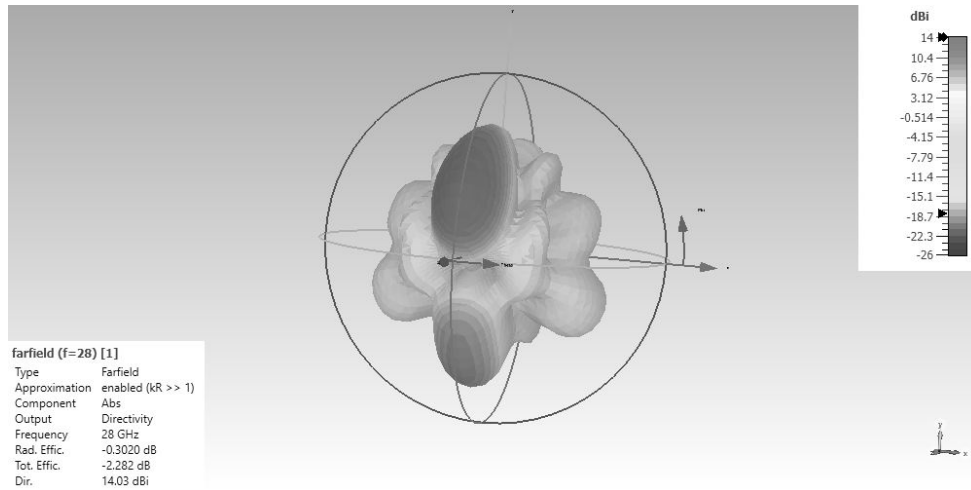


FIGURE 4.16: Directivity of the phased antenna array in 3D.

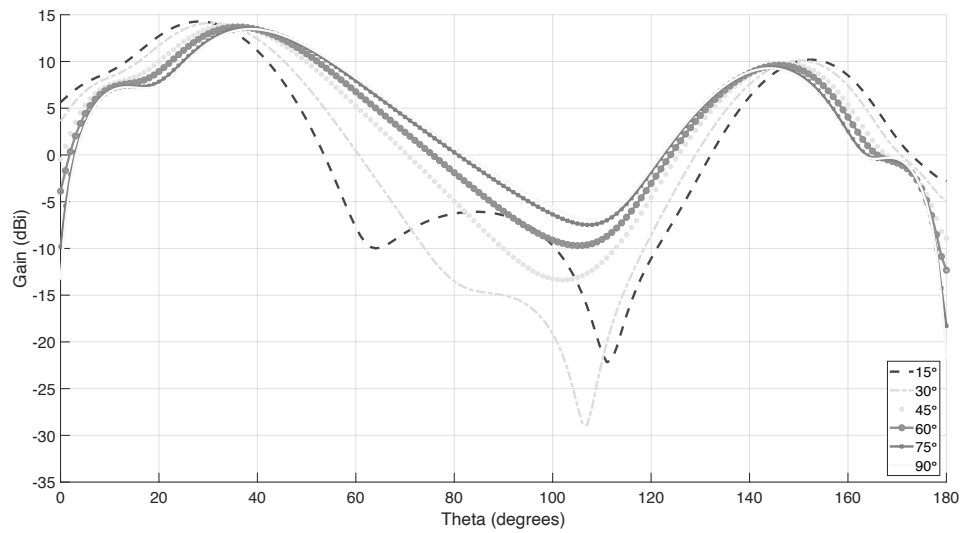


FIGURE 4.17: Beam steering performance of the phased array antenna with DGS.

In the overall analysis of the proposed phased array antenna, the insertion of a dumbbell shaped DGS came with both benefits and shortfalls in the overall antenna performance. The insertion of a dumbbell shaped DGS increased the bandwidth of the antenna and reduced mutual coupling between antenna elements. However, there is a decrease in antenna gain. During beam steering, the phased array antenna without DGS experienced a high scan loss as compared to the one with DGS. Moreover, the phased array antenna without DGS achieved a scan angle of  $\pm 41^\circ$  whereas the one with DGS achieved a scan angle of  $\pm 35^\circ$ . The simulation results of the designed phased array antenna (with and without DGS) are presented in Table 4.2, summarizing the performance comparison of two designed antennas.

Table 4.2: Performance comparison of the phased array antenna with and without DGS.

Parameter	Units	Phased Array Antenna	
		Without DGS	With DGS
Reflection Coefficient	dB	-40.19	-27.22
Bandwidth	GHz	1.51	1.61
Mutual Coupling	dB	-27.97	-34.24
VSWR	-	1.38	2.1
Gain	dBi	15.92	13.73
Realized Gain	dBi	13.07	11.75
Directivity	dB	15.96	14.03
Scan Angle	o	$\pm 41$	$\pm 35$

The proposed phased array antenna is compared with existing phased array antennas for 5G wireless applications. A comparative summary of the proposed antenna with the antennas described in literature is presented in Table 4.3.

Table 4.3: Comparison of the designed phased array antenna with existing works.

Ref	$S_{11}$ (dB)	Bandwidth (GHz)	Gain (dBi)	Scan Angle (o)
[136]	-	-	10	121
[142]	-38	-	13.7	$\pm 22$
[141]	-32	4.2	11.59	40
[143]	-30	1	8	$\pm 45$
[145]	$< -15$	0.7	8.36	$\pm 70$
This work (Without DGS)	-40.19	1.51	15.92	$\pm 41$
This work (with DGS)	-27.22	1.61	13.73	$\pm 35$

## 4.4 Conclusion

This chapter presented the design and simulation of an eight element phased array antenna operating at 28 GHz. Initially, a  $1 \times 4$  array antenna is designed and analyzed. From the simulation results, the  $1 \times 4$  array antenna has a reflection coefficient of -31.85 dB, bandwidth of 1.47 GHz, VSWR of 1.28, gain of 10.8 dBi, realized gain of 6.68 dBi, angular beam width of  $18.7^\circ$  and directivity of 11.5 dBi. The designed  $1 \times 4$  array antenna was used to design eight element phased array antenna. The simulation results indicated that, the designed phased array antenna has a reflection coefficient of -40.19 dB, bandwidth of 1.51 GHz, VSWR of 1.38, antenna gain of 15.92 dBi, realized gain of 13.07 dBi, angular beam-width of  $23.0^\circ$ , directivity of 16 dBi, scan angle of  $\pm 41^\circ$  and mutual coupling of -27.97 dB. To reduce mutual coupling effect, a dumbbell shaped DGS was inserted in the array and reduced mutual coupling by 6.27 dB. Furthermore, the phased array antenna with DGS has a reflection coefficient of -27.22 dB, bandwidth of 1.61 GHz, VSWR of 2.1, antenna gain of 13.73 dBi, realized gain of 11.75 dBi, angular beam-width of  $35.4^\circ$ , directivity of 14.03 dBi, scan angle of  $\pm 35^\circ$ . However, the insertion of a dumbbell shaped DGS came with both benefits and shortfalls in the overall antenna performance.

## Chapter 5

# Conclusions

### 5.1 Conclusion

The proliferation of data traffic in wireless communication have resulted in a shift towards millimeter wave frequency band and the launch of 5G networks. Millimeter wave band provide high bandwidth which results in achieving high data rates but this frequency band come with a cost of propagation challenges. Antenna arrays with high antenna gain are used to compensate these challenges. Antenna arrays have a shortfall of having a limited angular coverage due to narrow beams. As such, phased array antennas are adopted to provide electronic beam steering in desirable directions. In this thesis, an eight element phased array antenna is designed and simulated, operating at a frequency of 28 GHz for 5G wireless applications. The designed phased array antenna uses a rectangular patch antenna as antenna element and corporate feed as a feeding network. Furthermore, the mutual coupling effect which exists in the designed phased array antenna is reduced by inserting a dumbbell shaped DGS between radiating elements. The main findings of this thesis are as follows:

- In Chapter 3, a single rectangular patch antenna operating at 28 GHz is designed and analyzed based on three different dielectric substrates. From the simulations, the single patch antenna designed with RT/Duroid 5880 substrate offers better antenna performance as compared to other designs hence it is chosen as the antenna element for the proposed eight element phased array antenna.
- Chapter 4 proposes an eight element phased array antenna operating at 28 GHz for 5G wireless applications. Initially, a  $1 \times 4$  microstrip array antenna was designed and then, the array was used to design the proposed phased array antenna. The array was fed with two simultaneous feeding ports, which were

also used to achieve beam steering and measure mutual coupling of the antenna array. The designed eight element phased array antenna used a dumbbell shaped DGS to reduce mutual coupling and a mutual coupling reduction of 6.27 dB was achieved. However, the insertion of a dumbbell shaped DGS came with both benefits and shortfalls in the overall antenna performance. The insertion of a dumbbell shaped DGS increased the bandwidth of the antenna and reduced mutual coupling between antenna elements. However, there was a decrease in antenna gain and directivity.

## 5.2 Future Works

Phased array antennas are considered key enablers for the next generation networks due to their characteristics such as electronic beam steering high antenna and beam-forming capabilities. In the pursuit of achieving the objectives of this thesis, additional challenges and ideas that deserve further investigation popped up. The challenges and the ideas are listed below.

- Fabricate the designed phased array antenna to compare simulation and measurement results.
- Develop a framework for deriving dimensions of a dumbbell shaped DGS in the millimeter wave frequency instead of using the trial and error method like in this thesis.
- Design a phased array antenna which use both series and feed (hybrid) networks with re-configurable antenna elements to achieve a wide beam scan angle. This is because the proposed phased in this thesis has limited scan angle.

## References

- [1] T. Mshvidobadze, "Evolution mobile wireless communication and lte networks," in *2012 6th International Conference on Application of Information and Communication Technologies (AICT)*, 2012, pp. 1–7.
- [2] A. Al-Salihy, M. Madi, and S. Alomari, "A survey in mobile generations and their mobility management," *European Journal of Scientific Research*, vol. 58, pp. 88–102, 08 2011.
- [3] D. Goodman, "Second generation wireless information networks," *IEEE Transactions on Vehicular Technology*, vol. 40, no. 2, pp. 366–374, 1991.
- [4] S. Ohmori, Y. Yamao, and N. Nakajima, "The future generations of mobile communications based on broadband access technologies," *IEEE Communications Magazine*, vol. 38, no. 12, pp. 134–142, 2000.
- [5] J. L. Burbank, J. Andrusenko, J. S. Everett, and W. T. Kasch, *Second-Generation (2G) Cellular Communications*. Wiley-IEEE Press, 2013, pp. 250–365.
- [6] N. Chandran and M. Valenti, "Three generations of cellular wireless systems," *IEEE Potentials*, vol. 20, no. 1, pp. 32–35, 2001.
- [7] S. Behrad, E. Bertin, and N. Crespi, "Securing authentication for mobile networks, a survey on 4G issues and 5G answers," in *2018 21st Conference on Innovation in Clouds, Internet and Networks and Workshops (ICIN)*, 2018, pp. 1–8.
- [8] J. A. del Peral-Rosado, R. Raulefs, J. A. López-Salcedo, and G. Seco-Granados, "Survey of cellular mobile radio localization methods: From 1G to 5G," *IEEE Communications Surveys Tutorials*, vol. 20, no. 2, pp. 1124–1148, 2018.
- [9] B. Clerckx, A. Costanzo, A. Georgiadis, and N. Borges Carvalho, "Toward 1 G mobile power networks: Rf, signal, and system designs to make smart objects autonomous," *IEEE Microwave Magazine*, vol. 19, no. 6, pp. 69–82, 2018.
- [10] Q. K. Ud Din Arshad, A. U. Kashif, and I. M. Quershi, "A review on the evolution of cellular technologies," in *2019 16th International Bhurban Conference on Applied Sciences and Technology (IBCAST)*, 2019, pp. 989–993.
- [11] T. Alexander, W. Mazurczyk, A. Mishra, and A. Perotti, "Mobile communications and networks," *IEEE Communications Magazine*, vol. 57, no. 1, pp. 42–42, 2019.
- [12] A. M. Niknejad, S. Thyagarajan, E. Alon, Y. Wang, and C. Hull, "A circuit designer's guide to 5g mm-wave," in *2015 IEEE Custom Integrated Circuits Conference (CICC)*, 2015, pp. 1–8.

- [13] L. Wan, Z. Guo, Y. Wu, W. Bi, J. Yuan, M. ElKashlan, and L. Hanzo, "4G/5G spectrum sharing: Efficient 5g deployment to serve enhanced mobile broadband and internet of things applications," *IEEE Vehicular Technology Magazine*, vol. 13, no. 4, pp. 28–39, 2018.
- [14] P. Gandotra and R. K. Jha, "Next generation cellular networks and green communication," in *2018 10th International Conference on Communication Systems Networks (COMSNETS)*, 2018, pp. 522–524.
- [15] S. Kutty and D. Sen, "Beamforming for Millimeter Wave Communications: An Inclusive Survey," *IEEE Communications Surveys and Tutorials*, vol. 18, no. 2, pp. 949–973, 2016.
- [16] R. T. Prabu, M. Benisha, V. T. Bai, and V. Yokesh, "Millimeter wave for 5G mobile communication application," *Proceeding of IEEE - 2nd International Conference on Advances in Electrical, Electronics, Information, Communication and Bio-Informatics, IEEE - AEEICB 2016*, pp. 236–240, 2016.
- [17] F. Boccardi, R. Heath, A. Lozano, T. L. Marzetta, and P. Popovski, "Five disruptive technology directions for 5G," *IEEE Communications Magazine*, vol. 52, no. 2, pp. 74–80, 2014.
- [18] T. E. Bogale and L. B. Le, "Massive MIMO and mmWave for 5G Wireless HetNet: Potential Benefits and Challenges," *IEEE Vehicular Technology Magazine*, vol. 11, no. 1, pp. 64–75, 2016.
- [19] O. E. Ayach, S. Rajagopal, S. Abu-Surra, Z. Pi, and R. W. Heath, "Spatially sparse precoding in millimeter wave mimo systems," *IEEE Transactions on Wireless Communications*, vol. 13, no. 3, pp. 1499–1513, 2014.
- [20] Q. C. Li, H. Niu, A. T. Papathanassiou, and G. Wu, "5G network capacity: Key elements and technologies," *IEEE Vehicular Technology Magazine*, vol. 9, no. 1, pp. 71–78, 2014.
- [21] I. Ndip, T. H. Le, O. Schwanitz, and K. D. Lang, "A comparative analysis of 5G mmWave antenna arrays on different substrate technologies," *MIKON 2018 - 22nd International Microwave and Radar Conference*, pp. 222–225, 2018.
- [22] R. R. Turjo, S. M. Real, and M. H. Sagor, "Phased Array Antenna with Key Shaped Elements for 60 GHz mmWave Communications," *2019 International Workshop on Antenna Technology (iWAT)*, pp. 178–181, 2019.
- [23] M. Shafi, A. F. Molisch, P. J. Smith, T. Haustein, P. Zhu, P. De Silva, F. Tufvesson, A. Benjebbour, and G. Wunder, "5G: A tutorial overview of standards, trials, challenges, deployment, and practice," *IEEE Journal on Selected Areas in Communications*, vol. 35, no. 6, pp. 1201–1221, 2017.
- [24] S. Dang, O. Amin, B. Shihada, and M.-S. Alouini, "What should 6G be?" *Nature Electronics*, vol. 3, no. 1, pp. 20–29, 2020.
- [25] J. Helander, K. Zhao, Z. Ying, and D. Sjöberg, "Performance analysis of millimeter-wave phased array antennas in cellular handsets," *IEEE Antennas and Wireless Propagation Letters*, vol. 15, pp. 504–507, 2016.

- [26] A. Shaikh and M. J. Kaur, "Comprehensive survey of massive mimo for 5G communications," in *2019 Advances in Science and Engineering Technology International Conferences (ASET)*, 2019, pp. 1–5.
- [27] Y. Niu, Y. Li, D. Jin, L. Su, and A. V. Vasilakos, "A survey of millimeter wave communications (mmwave) for 5G: opportunities and challenges," *Wireless networks*, vol. 21, no. 8, pp. 2657–2676, 2015.
- [28] S. Hur, T. Kim, D. J. Love, J. V. Krogmeier, T. A. Thomas, and A. Ghosh, "Millimeter wave beamforming for wireless backhaul and access in small cell networks," *IEEE Transactions on Communications*, vol. 61, no. 10, pp. 4391–4403, 2013.
- [29] S. Rajagopal, S. Abu-Surra, Z. Pi, and F. Khan, "Antenna array design for multi-gbps mmwave mobile broadband communication," in *IEEE Global Telecommunications Conference - GLOBECOM 2011*, 2011, pp. 1–6.
- [30] S. Han, C. I, Z. Xu, and C. Rowell, "Large-scale antenna systems with hybrid analog and digital beamforming for millimeter wave 5G," *IEEE Communications Magazine*, vol. 53, no. 1, pp. 186–194, 2015.
- [31] T. S. Rappaport, F. Gutierrez, E. Ben-Dor, J. N. Murdock, Y. Qiao, and J. I. Tamir, "Broadband millimeter-wave propagation measurements and models using adaptive-beam antennas for outdoor urban cellular communications," *IEEE Transactions on Antennas and Propagation*, vol. 61, no. 4, pp. 1850–1859, 2013.
- [32] W. Roh, J.-Y. Seol, J. Park, B. Lee, J. Lee, Y. Kim, J. Cho, K. Cheun, and F. Aryanfar, "Millimeter-wave beamforming as an enabling technology for 5G cellular communications: theoretical feasibility and prototype results," *IEEE Communications Magazine*, vol. 52, no. 2, pp. 106–113, 2014.
- [33] R. Valkonen, "Compact 28-GHz phased array antenna for 5G access," *IEEE MTT-S International Microwave Symposium Digest*, pp. 1334–1337, 2018.
- [34] X. Ge, R. Zi, X. Xiong, Q. Li, and L. Wang, "Millimeter wave communications with oam-sm scheme for future mobile networks," *IEEE Journal on Selected Areas in Communications*, vol. 35, no. 9, pp. 2163–2177, 2017.
- [35] A. N. Uwaechia and N. M. Mahyuddin, "A comprehensive survey on millimeter wave communications for fifth-generation wireless networks: Feasibility and challenges," *IEEE Access*, vol. 8, pp. 62 367–62 414, 2020.
- [36] F. Khan and Z. Pi, "mmwave mobile broadband (mmb): Unleashing the 3–300ghz spectrum," in *34th IEEE Sarnoff Symposium*, 2011, pp. 1–6.
- [37] X. Wang, L. Kong, F. Kong, F. Qiu, M. Xia, S. Arnon, and G. Chen, "Millimeter wave communication: A comprehensive survey," *IEEE Communications Surveys and Tutorials*, vol. 20, no. 3, pp. 1616–1653, 2018.
- [38] W. Hong, Z. H. Jiang, S. He, J. Zhou, P. Chen, Z. Yu, J. Chen, L. Tian, C. Yu, J. Zhai, N. Zhang, and G. Yang, "Limitations of phased arrays for 5G wireless communications," *2017 IEEE International Symposium on Antennas and Propagation USNC/URSI National Radio Science Meeting*, pp. 1467–1468, 2017.



- [39] H. S. Farahani, M. Veysi, M. Kamyab, and A. Tadjalli, "Mutual coupling reduction in patch antenna arrays using a UC-EBG superstrate," *IEEE Antennas and Wireless Propagation Letters*, vol. 9, pp. 57–59, 2010.
- [40] A. Y. Ashyap, S. H. B. Dahlan, Z. Zainal Abidin, M. I. Abbasi, M. R. Kamarudin, H. A. Majid, M. H. Dahri, M. H. Jamaluddin, and A. Alomainy, "An overview of electromagnetic band-gap integrated wearable antennas," *IEEE Access*, vol. 8, pp. 7641–7658, 2020.
- [41] M. K. Khandelwal, B. K. Kanaujia, and S. Kumar, "Defected ground structure: Fundamentals, analysis, and applications in modern wireless trends," *International Journal of Antennas and Propagation*, vol. 2017, p. 22, 2017.
- [42] L. H. Weng, Y. C. Guo, X. W. Shi, and X. Q. Chen, "An overview on defected ground structure," *Progress In Electromagnetics Research B*, vol. 7, pp. 173–189, 2008.
- [43] A. Kumar, A. Q. Ansari, B. K. Kanaujia, J. Kishor, and L. Matekovits, "A review on different techniques of mutual coupling reduction between elements of any mimo antenna. part 2: Metamaterials and many more," *Radio Science*, vol. 56, no. 3, pp. 1–22, 2021.
- [44] V. M. Jayakrishnan and M. L. Liya, "A survey of electromagnetic waves based metamaterials and applications in various domains," in *2020 Third International Conference on Smart Systems and Inventive Technology (ICSSIT)*, 2020, pp. 662–666.
- [45] A. Valipour, M. H. Kargozarfard, M. Rakhshi, A. Yaghootian, and H. M. Sedighi, "Metamaterials and their applications: an overview," *Proceedings of the Institution of Mechanical Engineers, Part L: Journal of Materials: Design and Applications*, 2021.
- [46] C. A. Balanis, *Antenna theory: analysis and design*, 4th ed. New jersey: John wiley & sons, 2016.
- [47] H. J. Visser, *Array and Phased Array Antenna Basics*, 1st ed. Wiley, 2005.
- [48] L. C. Godara, "Applications of Antenna Arrays to Mobile Communications , Part I : Performance Improvement , Feasibility , and System Considerations," *Proceedings of the IEEE*, vol. 85, no. 7, pp. 1031–1060, 1997.
- [49] R. Kohno, "Spatial and Temporal Communication Theory Using Adaptive Antenna Araray," *IEEE Personal Communications*, vol. 5, no. 1, pp. 28–35, 1998.
- [50] S. Rao, N. Llombart, S. J. Wijnholds, W. A. Van Cappellen, J. G. Bij De Vaate, and A. Van Ardenne, "Antenna applications corner: Phased-array antenna system development for radio-astronomy applications," *IEEE Antennas and Propagation Magazine*, vol. 55, no. 6, pp. 293–308, 2013.
- [51] T. A. Milligan, *Modern Antenna Design*, 2nd ed. New Jersey: John Wiley & Sons, Inc., Hoboken, New Jersey, 2005.
- [52] I. Systems, R. Energy, and A. S. Fez, "Comparative study of the radiation performance between uniform and non-uniform excitation of linear patch antenna array for UWB radar applications," *Wseas Books: Mathematical and Computational Methods in Electrical Engineering*, pp. 89–95, 2015.

- [53] W. H. Kummer, "Basic Array Theory," *Proceedings of the IEEE*, vol. 80, no. 1, pp. 127–140, 1992.
- [54] Z. N. Chen, *Handbook of Antenna Technologies*, D. Liu, H. Nakano, X. Qing, and T. Zwick, Eds. Singapore, Singapore: Springer Verlag, Singapore, 2016.
- [55] R. C. Hansen, "Microwave Scanning Antennas, Volume II: Array Theory and Practice," in *Microwave Scanning Antennas, Volume II: Array Theory and Practice*. Academic Press, 1966, ch. 1,4, p. 400.
- [56] R. J. Mailloux, *Phased Array Antenna Handbook*, 2nd ed. Norwood, Massachusetts: Artech House, 2005.
- [57] D. Parker and D. C. Zimmermann, "Phased arrays - Part I: Theory and architectures," *IEEE Transactions on Microwave Theory and Techniques*, vol. 50, no. 3, pp. 678–687, 2002.
- [58] S. Ghosh and D. Sen, "An Inclusive Survey on Array Antenna Design for Millimeter-Wave Communications," *IEEE Access*, vol. 7, pp. 83 137–83 161, 2019.
- [59] N. H. Noordin, V. Zuniga, A. O. El-Rayis, N. Haridas, A. T. Erdogan, and T. Arslan, "Uniform circular arrays for phased array antenna," in *2011 Loughborough Antennas & Propagation Conference*, 2011, pp. 1–4.
- [60] R. C. Hansen, *Phased Array Antennas*. New York, United States: John Wiley & Sons Ltd, 1998.
- [61] A. H. Naqvi and S. Lim, "Review of recent phased arrays for millimeter-wave wireless communication," *Sensors (Switzerland)*, vol. 18, no. 10, p. 3194, 2018.
- [62] E. Carpentieri, U. F. D'Elia, E. De Stefano, L. Di Guida, and R. Vitiello, "Millimeter-wave phased-array antennas," in *2008 IEEE Radar Conference*, 2008, pp. 1–5.
- [63] B. A. Kopp, C. R. Moore, and R. V. Coffman, "Transmit/receive module packaging: electrical design issues," *Johns Hopkins APL Technical Digest (Applied Physics Laboratory)*, vol. 20, no. 1, pp. 70–80, 1999.
- [64] W.-Q. Wang and H. Shao, "A flexible phased-mimo array antenna with transmit beamforming," *International Journal of Antennas and Propagation*, vol. 2012, 2012.
- [65] R. Sturdivant, C. Quan, and E. Chang, *Systems Engineering of Phased Arrays*. Artech House, 2019.
- [66] A. J. Fenn, D. H. Temme, W. P. Delaney, and W. E. Courtney, "The Development of Phased-Array Radar Technology," *Lincoln laboratory journal*, vol. 12, no. 2, pp. 321–340, 2000.
- [67] C. Craeye and D. González-Ovejero, "A review on array mutual coupling analysis," *Radio Science*, vol. 46, no. 2, pp. 1–25, 2011.
- [68] H. Singh, H. L. Sneha, and R. M. Jha, "Mutual coupling in phased arrays: A review," *International Journal of Antennas and Propagation*, vol. 2013, no. Ddd, 2013.
- [69] L. Babu Saraswathi Kavitha and I. Jacob Raglend, "A wide-scan phased array antenna for a small Active Electronically Scanned Array: A review," *Proceedings of IEEE International Conference on Circuit, Power and Computing Technologies (ICCPCT)*, pp. 1008–1016, 2013.

- [70] M. T. Islam and M. S. Alam, "Compact EBG structure for alleviating mutual coupling between patch antenna array elements," *Progress in Electromagnetics Research*, vol. 137, pp. 425–438, 2013.
- [71] B. Mohamadzade and M. Afsahi, "Mutual coupling reduction and gain enhancement in patch array antenna using a planar compact electromagnetic bandgap structure," *IET Microwaves, Antennas and Propagation*, vol. 11, no. 12, pp. 1719–1725, 2017.
- [72] A. Kaabal, M. E. Halaoui, S. Ahyoud, and A. Asselman, "A Low Mutual Coupling Design for Array Microstrip Antennas Integrated with Electromagnetic Band-Gap Structures," *Procedia Technology*, vol. 22, no. October 2015, pp. 549–555, 2016.
- [73] M. S. Alam, N. Misran, B. Yatim, and M. T. Islam, "Development of electromagnetic band gap structures in the perspective of microstrip antenna design," *International Journal of Antennas and Propagation*, vol. 2013, 2013.
- [74] M. S. Alam, M. Islam, and N. Misran, "Design analysis of an electromagnetic band gap microstrip antenna," *American Journal of Applied Sciences*, vol. 8, pp. 1374–1377, 12 2011.
- [75] P. De Maagt, R. Gonzalo, Y. C. Vardaxoglou, and J. M. Baracco, "Electromagnetic Bandgap Antennas and Components for Microwave and (Sub)Millimeter Wave Applications," *IEEE Transactions on Antennas and Propagation*, vol. 51, no. 10 I, pp. 2667–2677, 2003.
- [76] Z. Iluz, R. Shavit, and R. Bauer, "Microstrip antenna phase array with electromagnetic bandgap substrate," *IEEE Transactions on Antennas and Propagation*, vol. 52, no. 6, pp. 1446–1453, 2004.
- [77] A. Arora and N. Kumar, "To reduce mutual coupling in microstrip patch antenna arrays elements using electromagnetic band gap structures for X-band," *2017 International Conference On Nextgen Electronic Technologies: Silicon to Software, ICNETS2 2017*, pp. 228–230, 2017.
- [78] M. Kumar and V. Nath, "Analysis of low mutual coupling compact multi-band microstrip patch antenna and its array using defected ground structure," *Engineering Science and Technology, an International Journal*, vol. 19, no. 2, pp. 866–874, 2016.
- [79] M. Salehi, A. Motevasselian, A. Tavakoli, and T. Heidari, "Mutual coupling reduction of microstrip antennas using defected ground structure," *2006 IEEE Singapore International Conference on Communication Systems*, pp. 1–5, 2006.
- [80] E. Fritz-Andrade, A. Perez-Miguel, R. Gomez-Villanueva, and H. Jardon-Aguilar, "Characteristic mode analysis applied to reduce the mutual coupling of a four-element patch MIMO antenna using a defected ground structure," *IET Microwaves, Antennas and Propagation*, vol. 14, no. 2, pp. 215–226, 2020.
- [81] M. I. Ahmed, A. Sebak, E. A. Abdallah, and H. Elhennawy, "Mutual coupling reduction using defected ground structure (DGS) for array applications," *2012 15th International Symposium on Antenna Technology and Applied Electromagnetics*, pp. 2–6, 2012.
- [82] K. Wei, J. Y. Li, L. Wang, Z. J. Xing, and R. Xu, "Mutual coupling reduction of microstrip antenna array by periodic defected ground structures," *APCAP 2016 - 2016 IEEE 5th Asia-Pacific Conference on Antennas and Propagation*, pp. 389–390, 2017.

- [83] M. Alibakhshikenari, A. Salvucci, G. Polli, B. S. Virdee, C. H. See, R. Abd-Alhameed, F. Falcone, A. Andújar, J. Anguera, and E. Limiti, "Mutual coupling reduction using metamaterial supersubstrate for high performance amp; densely packed planar phased arrays," in *2018 22nd International Microwave and Radar Conference (MIKON)*, 2018, pp. 675–678.
- [84] M. F. Shafique, Z. Qamar, L. Riaz, R. Saleem, and S. A. Khan, "Coupling suppression in densely packed microstrip arrays using metamaterial structure," *Microwave and Optical Technology Letters*, vol. 57, no. 3, pp. 759–763, 2015.
- [85] K. H. Moussa, A. S. I. Amar, M. Mabrouk, and H. G. Mohamed, "Slotted e-shaped meta-material decoupling slab for densely packed mimo antenna arrays," *Micromachines*, vol. 12, no. 8, 2021.
- [86] M. SalarRahimi and G. A. E. Vandenbosch, "Decreasing mutual coupling in a phased array using a mutual coupling based element," in *2019 IEEE Asia-Pacific Microwave Conference (APMC)*, 2019, pp. 1098–1100.
- [87] B. Abbasi Arand, A. Bazrkar, and A. Zahedi, "Design of a phased array in triangular grid with an efficient matching network and reduced mutual coupling for wide-angle scanning," *IEEE Transactions on Antennas and Propagation*, vol. 65, no. 6, pp. 2983–2991, 2017.
- [88] X. Chen, M. Abdullah, Q. Li, J. Li, A. Zhang, and T. Svensson, "Characterizations of mutual coupling effects on switch-based phased array antennas for 5G millimeter-wave mobile communications," *IEEE Access*, vol. 7, pp. 31 376–31 384, 2019.
- [89] Z. Li, Y. Wang, and Z. Wang, "Mutual coupling compensation of the conformal array antenna based on the active element pattern method," in *Proceedings of the 2015 International Conference on Electrical, Computer Engineering and Electronics*. Atlantis Press, 2015/06, pp. 835–839.
- [90] R. Waterhouse, *Microstrip Patch Antennas: A Designer's Guide*, 1st ed. New York: Springer Science & Business Media, 2003.
- [91] R. Dakir, J. Zbitou, A. Mouhsen, A. Tribak, A. M. Sanchez, and M. Latrach, "Rectangular planar antenna using u-slot for bandwidth improvement," *Electrical and Electronic Engineering*, vol. 3, no. 4, pp. 118–121, 2013.
- [92] F. Kuroki and H. Ohta, "L-shaped monopole array for terrestrial broadcasting reception in the UHF band," *Proceedings of the 37th European Microwave Conference, EUMC*, vol. 2, no. 5, pp. 1070–1073, 2007.
- [93] S. Srivastava, A. Khandelwal, and S. Sharma, "Microstrip Patch Antenna: A Survey," *IOSR Journal of Electrical and Electronics Engineering Ver. II*, vol. 9, no. 4, pp. 2278–1676, 2014.
- [94] D. B. Miron, "Chapter 2 - antenna fundamentals i," in *Small Antenna Design*, D. B. Miron, Ed. Burlington: Newnes, 2006, pp. 9–41.
- [95] G. Monser, *Antenna Design: A Practical Guide*. McGraw-Hill, 1996.
- [96] W. Stutzman and G. Thiele, *Antenna theory and design*, 2nd ed. John Wiley & Sons, 1998.

- [97] S. Noghianian and S. K. Sharma, *Radiation Pattern Reconfigurable Antennas*. Wiley, 2021, pp. 67–121.
- [98] T. S. Bird, *Arrays of Aperture Antennas*. Wiley, 2015, pp. 219–305.
- [99] “Ieee standard for definitions of terms for antennas,” *IEEE Std 145-2013 (Revision of IEEE Std 145-1993)*, pp. 1–50, 2014.
- [100] Y. Li, S. Xiao, and J. Guo, “A Review of Wideband Wide-Angle Scanning 2-D Phased Array and Its Applications in Satellite Communication,” *Journal of Communications and Information Networks*, vol. 3, no. 1, pp. 21–30, 2018.
- [101] R. Mailloux, *Phased Array Antenna Handbook*, ser. Antennas and Propagation Library. Artech House, 2005.
- [102] N. Boskovic, B. Jakanovic, and V. Markovic, “Frequency scanning antenna arrays with metamaterial based phased shifters,” *FACTA UNIVERSITATIS Series Electronics and Energetics*, vol. 32, pp. 449–461, 09 2019.
- [103] M. Skolnik, *Radar Handbook, Third Edition*, ser. Electronics electrical engineering. McGraw-Hill Education, 2008.
- [104] R. C. Hansen, *Scanning Antennas*. American Cancer Society, 1999.
- [105] D. Pozar, *Microwave Engineering, 4th Edition*. Wiley, 2011.
- [106] R. J. James and P. Hall, *Handbook of Microstrip Antennas, Volume 1*, Volume 1, Ed. London: Peter Peregrinus Ltd., 1989.
- [107] K. B. a. B. U.A. Bakshi, *Antennas And Wave Propagation*, 14th ed. New Delhi: Oxford University Press, 2009.
- [108] W. Jiang, B. Han, M. A. Habibi, and H. D. Schotten, “The road towards 6g: A comprehensive survey,” *IEEE Open Journal of the Communications Society*, vol. 2, pp. 334–366, 2021.
- [109] S. N. Hafizah Sa’don, M. R. Kamarudin, M. H. Dahri, A. Y. I. Ashyap, F. C. Seman, M. I. Abbasi, and Z. Z. Abidin, “The review and analysis of antenna for sixth generation (6g) applications,” in *2020 IEEE International RF and Microwave Conference (RFM)*, 2020, pp. 1–5.
- [110] A. Khan and R. K. Nema, “Analysis of five different dielectric substrates on microstrip patch antenna,” *International Journal of Computer Applications*, vol. 55, pp. 40–47, 2012.
- [111] R. Dalvi and A. Dessai, “Effects of different substrates on staircase shaped microstrip patch antenna for ku band,” in *2018 IEEE International Conference on Computational Intelligence and Computing Research (ICIC)*, 2018, pp. 1–6.
- [112] S. D. Mahamine, R. S. Parbat, S. H. Bodake, and M. P. Aher, “Effects of different substrates on rectangular microstrip patch antenna for s-band,” in *2016 International Conference on Automatic Control and Dynamic Optimization Techniques (ICACDOT)*, 2016, pp. 1142–1145.
- [113] A. Chang. Challenges when selecting the right substrate board material to make a 5G mmwave antenna.

- [114] P. Y. J. Su, Y. P. Wang, Y. C. Pai, Y. W. Lu, T. Shih, A. Kang, D. Lai, and D. S. Jiang, "Material impact with package solution for 5G rf application," in *Proceedings of the ASME 2020 International Technical Conference and Exhibition on Packaging and Integration of Electronic and Photonic Microsystems. ASME 2020 International Technical Conference and Exhibition on Packaging and Integration of Electronic and Photonic Microsystems.*, Virtual, Online. October 27–29, 2020., pp. 1–6.
- [115] J. Colaco and R. Lohani, "Design and implementation of microstrip patch antenna for 5G applications," in *2020 5th International Conference on Communication and Electronics Systems (ICCES)*, 2020, pp. 682–685.
- [116] R. Przesmycki, M. Bugaj, and L. Nowosielski, "Broadband microstrip antenna for 5G wireless systems operating at 28 ghz," *Electronics*, vol. 10, no. 1, 2021.
- [117] J. Colaco and R. Lohani, "Design and implementation of microstrip circular patch antenna for 5G applications," in *2020 International Conference on Electrical, Communication, and Computer Engineering (ICECCE)*, 2020, pp. 1–4.
- [118] J. Saini and S. K. Agarwal, "Design a single band microstrip patch antenna at 60 ghz millimeter wave for 5G application," in *2017 International Conference on Computer, Communications and Electronics (Comptelix)*, 2017, pp. 227–230.
- [119] M. F. Rafdzi, S. Y. Mohamad, A. A. Ruslan, N. F. A. Malek, M. R. Islam, and A. H. A. Hashim, "Study for microstrip patch antenna for 5G networks," in *2020 IEEE Student Conference on Research and Development (SCORED)*, 2020, pp. 524–528.
- [120] A. F. Kaeib, N. M. Shebani, and A. R. Zarek, "Design and analysis of a slotted microstrip antenna for 5G communication networks at 28 ghz," in *2019 19th International Conference on Sciences and Techniques of Automatic Control and Computer Engineering (STA)*, 2019, pp. 648–653.
- [121] Y. Ghazaoui, A. E. Alami, M. E. Ghzaoui, S. Das, D. Barad, and S. Mohapatra, "Millimeter wave antenna with enhanced bandwidth for 5G wireless application," *Journal of Instrumentation*, vol. 15, no. 01, pp. T01 003–T01 003, jan 2020.
- [122] S. K. Noor, N. Ramli, N. M. Sahar, and T. Khalifa, "Compact and wide bandwidth microstrip patch antenna for 5G millimeter wave technology: Design and analysis," *Journal of Physics: Conference Series*, vol. 1878, no. 1, p. 012008, may 2021.
- [123] S. Verma, L. Mahajan, R. Kumar, H. S. Saini, and N. Kumar, "A small microstrip patch antenna for future 5G applications," in *2016 5th International Conference on Reliability, Infocom Technologies and Optimization (Trends and Future Directions) (ICRITO)*, 2016, pp. 460–463.
- [124] R. R. N. N, A. A. Jugale, and M. R. Ahmed, "Microstrip patch antenna design for fixed mobile and satellite 5G communications," *Procedia Computer Science*, vol. 171, pp. 2073–2079, 2020, third International Conference on Computing and Network Communications (CoCoNet'19).
- [125] A. K. Gondi, A. D. Jaiswal, S. J. Vignesh, and D. Yadav, "High directivity and high gain microstrip patch antenna for 5G application with defective and suspended ground plane," in *2021 5th International Conference on Electronics, Materials Engineering Nano-Technology (IEMENTech)*, 2021, pp. 1–5.

- [126] M. AboEl-Hassan, A. E. Farahat, and K. F. Hussein, "Compact-size quad-band patch antenna for 5G mobile communications," *Microwave and Optical Technology Letters*, vol. 63, no. 12, pp. 3067–3071, 2021.
- [127] J. Kornprobst, K. Wang, G. Hamberger, and T. F. Eibert, "A mm-wave patch antenna with broad bandwidth and a wide angular range," *IEEE Transactions on Antennas and Propagation*, vol. 65, no. 8, pp. 4293–4298, 2017.
- [128] A. Abdalaziz and E. Hamad, "Design of a compact high gain microstrip patch antenna for tri-band 5G wireless communication," *Frequenz -Berlin-*, vol. 73, pp. 45–52, 01 2019.
- [129] D. Imran, M. M. Farooqi, M. I. Khattak, Z. Ullah, M. I. Khan, M. A. Khattak, and H. Dar, "Millimeter wave microstrip patch antenna for 5G mobile communication," in *2018 International Conference on Engineering and Emerging Technologies (ICEET)*, 2018, pp. 1–6.
- [130] M. M. Amir Faisal, M. Nabil, and M. Kamruzzaman, "Design and simulation of a single element high gain microstrip patch antenna for 5G wireless communication," in *2018 International Conference on Innovations in Science, Engineering and Technology (ICISSET)*, 2018, pp. 290–293.
- [131] R. K. Goyal and U. Shankar Modani, "A compact microstrip patch antenna at 28 ghz for 5G wireless applications," in *2018 3rd International Conference and Workshops on Recent Advances and Innovations in Engineering (ICRAIE)*, 2018, pp. 1–2.
- [132] T. S. Rappaport, S. Sun, R. Mayzus, H. Zhao, Y. Azar, K. Wang, G. N. Wong, J. K. Schulz, M. Samimi, and F. Gutierrez, "Millimeter wave mobile communications for 5G cellular: It will work!" *IEEE Access*, vol. 1, pp. 335–349, 2013.
- [133] D. Garcia-Roger, E. E. González, D. Martín-Sacristán, and J. F. Monserrat, "V2x support in 3GPP specifications: From 4G to 5G and beyond," *IEEE Access*, vol. 8, pp. 190 946–190 963, 2020.
- [134] Y. Liu and L. Zhang, "A planar mm-wave beam-steerable array antenna for 5G mobile terminal applications," in *2019 Cross Strait Quad-Regional Radio Science and Wireless Technology Conference (CSQRWC)*, 2019, pp. 1–3.
- [135] M. Khalily, R. Tafazolli, T. A. Rahman, and M. R. Kamarudin, "Design of phased arrays of series-fed patch antennas with reduced number of the controllers for 28-ghz mm-wave applications," *IEEE Antennas and Wireless Propagation Letters*, vol. 15, pp. 1305–1308, 2016.
- [136] C. Deng, D. Liu, B. Yektakhah, and K. Sarabandi, "Series-fed beam-steerable millimeter-wave antenna design with wide spatial coverage for 5G mobile terminals," *IEEE Transactions on Antennas and Propagation*, vol. 68, no. 5, pp. 3366–3376, 2020.
- [137] J. Zhang, S. Zhang, Z. Ying, A. S. Morris, and G. F. Pedersen, "Radiation-pattern reconfigurable phased array with p-i-n diodes controlled for 5g mobile terminals," *IEEE Transactions on Microwave Theory and Techniques*, vol. 68, no. 3, pp. 1103–1117, 2020.
- [138] M. Abdullah, X. Chen, Q. Li, and T. A. Khan, "A 28 ghz switchable 3-d coverage millimeter-wave phased array antenna for 5g handset terminals," in *2019 European Microwave Conference in Central Europe (EuMCE)*, 2019, pp. 423–426.

- [139] N. O. Parchin, R. A. Abd-Alhameed, and M. Shen, "A beam-steerable antenna array with radiation beam reconfigurability for 5g smartphones," in *2020 14th European Conference on Antennas and Propagation (EuCAP)*, 2020, pp. 1–4.
- [140] W. Hong, S. Ko, Y. Lee, and K. Baek, "Multi-polarized antenna array configuration for mmwave 5g mobile terminals," in *2015 International Workshop on Antenna Technology (iWAT)*, 2015, pp. 60–61.
- [141] J. Qi, H. Zheng, M. Wang, R. Liu, C. Tang, and E. Li, "A phased array composed of dipole with semicircular ring for 5G," in *2019 International Conference on Microwave and Millimeter Wave Technology (ICMMT)*, 2019, pp. 1–3.
- [142] H. Nigam, M. Mathur, M. Arora, and R. Singh, "Enhancing gain with multiple beams for four element phased array microstrip antenna using rogers substrate material for 5G applications," *Materials Today: Proceedings*, vol. 30, pp. 203–209, 2020, international Conference on Advancement in Nanoelectronics and Communication Technologies (ICANCT-2020).
- [143] K. Y. Kapusuz and U. Oguz, "Millimeter wave phased array antenna for modern wireless communication systems," *2016 10th European Conference on Antennas and Propagation, EuCAP 2016*, no. 1, pp. 1–4, 2016.
- [144] S. Danesh, A. Araghi, M. Khalily, P. Xiao, and R. Tafazolli, "Millimeter wave phased array antenna synthesis using a machine learning technique for different 5G applications," in *2020 International Symposium on Networks, Computers and Communications (ISNCC)*, 2020, pp. 1–5.
- [145] M. K. Ishfaq, T. Abd Rahman, M. Himdi, H. T. Chattha, Y. Saleem, B. A. Khawaja, and F. Masud, "Compact four-element phased antenna array for 5g applications," *IEEE Access*, vol. 7, pp. 161 103–161 111, 2019.
- [146] E. Adas, F. De Flaviis, and N. G. Alexopoulos, "Mode-free radiating electromagnetic bandgap materials as phased array antenna elements," *2017 IEEE Antennas and Propagation Society International Symposium*, pp. 1661–1662, 2017.
- [147] X. Li, M. Chen, Z. H. Wu, and Q. Cheng, "A low-profile wideband phased array antenna using ebg structures in p-band," in *2019 IEEE International Conference on Computational Electromagnetics (ICCEM)*, 2019, pp. 1–3.
- [148] A. S. Alqadami, N. Nguyen-Trong, K. Bialkowski, and A. Abbosh, "Mutual coupling reduction in wideband electromagnetic medical imaging antenna array using compact electromagnetic band gap," *2019 IEEE International Symposium on Antennas and Propagation and USNC-URSI Radio Science Meeting (APSURSI)*, pp. 999–1000, 2019.
- [149] T. Jiang, T. Jiao, and Y. Li, "Array Mutual Coupling Reduction Using L-Loading E-Shaped Electromagnetic Band Gap Structures," *International Journal of Antennas and Propagation*, vol. 2016, 2016.
- [150] K. S. Vishvakshenan, K. Mithra, R. Kalaiarasan, and K. S. Raj, "Mutual coupling reduction in microstrip patch antenna arrays using parallel coupled-line resonators," *IEEE Antennas and Wireless Propagation Letters*, vol. 16, pp. 2146–2149, 2017.



- 
- [151] K. Yu, X. Liu, and Y. Li, "Mutual coupling reduction of microstrip patch antenna array using modified split ring resonator metamaterial structures," in *2017 IEEE International Symposium on Antennas and Propagation USNC/URSI National Radio Science Meeting*, 2017, pp. 2287–2288.
- [152] M. Ghaderi and N. C. Karmakar, "Frequency selective surface for reducing mutual coupling in antenna arrays," in *Asia-Pacific Microwave Conference 2011*, 2011, pp. 1877–1880.
- [153] D. Gao, F. Di, S. Fu, X. Quan, and Z. Cao, "A Defected Ground Structure (DGS) for Reducing the Mutual Coupling of Dual Polarized Microstrip Antennas," *2018 International Conference on Microwave and Millimeter Wave Technology*, pp. 1–3, 2018.
- [154] Y. Yu, L. Yi, X. Liu, and Z. Gu, "Mutual coupling reduction of dual-frequency patch antenna arrays," *Applied Computational Electromagnetics Society Journal*, vol. 31, no. 9, pp. 1092–1099, 2016.
- [155] K. Wei, J. Y. Li, J. Su, M. L. Tao, and J. Xie, "Defected ground structures for mutual coupling suppression and XP level improvement," *2017 International Applied Computational Electromagnetics Society Symposium in China*, no. 1, pp. 1–2, 2017.
- [156] H. Moghadas and A. Tavakoli, "A design procedure for defected ground structure in antenna arrays based on genetic algorithm," in *Proceedings of the 2012 IEEE International Symposium on Antennas and Propagation*, 2012, pp. 1–2.